Spring 2021

# Stability analysis of microgrids using Markov jump linear systems

Gilles Mpembele



Department: Electrical and Computer Engineering

# STABILITY ANALYSIS OF MICROGRIDS USING MARKOV JUMP LINEAR SYSTEMS

by

GILLES MPEMBELE

A DISSERTATION

Presented to the Graduate Faculty of the

MISSOURI UNIVERSITY OF SCIENCE AND TECHNOLOGY

In Partial Fulfillment of the Requirements for the Degree

DOCTOR OF PHILOSOPHY

in

ELECTRICAL ENGINEERING

2021

Approved by:

Jonathan Kimball, Advisor
Mariesa Crow
Mehdi Ferdowsi
Bruce McMillin
Pourya Shamsi

## PUBLICATION DISSERTATION OPTION

This dissertation consists of the following three articles, formatted in the style used by the Missouri University of Science and Technology.

Paper I: Pages 12–43 have been submitted as *Markov Jump Linear System Analysis of a Microgrid Operating in Islanded and Grid-Tied Modes* to IEEE Transactions on Smart Grid.

Paper II: Pages 44–79 have been submitted as *Jump-Diffusion Modeling of a Markov Jump Linear System with Applications in Microgrids* to IEEE Transactions on Smart Grid.

Paper III: Pages 80–107 are intended for submission as *Mean-square stability of a microgrid's jump-diffusion model* to IEEE Transactions on Smart Grid.

# ABSTRACT

This research discusses stochastic models for a microgrid operating between standalone and grid-tied modes. The transitions between different modes are modeled as a continuous-time Markov chain (CTMC). In each operating mode, the system is modeled using conventional differential algebraic equations (DAEs), linearized around some equilibrium point.

In Topic-I, a model is developed using the Stochastic Hybrid Systems (SHSs) formulation. The microgrid is modeled as a Markov jump linear system (MJLS), which is a type of SHS in which the discrete events evolve according to a Continuous Time Markov Chain (CTMC). The model allows for the derivation of Ordinary Differential Equations that represent the evolution of the conditional moments of the stochastic system, and subsequently the derivation of a matrix representation of these ODEs. The validation of the model relies on comparing numerical results obtained from the simulation of the IEEE 37-bus microgrid system to the conventional averaged Monte Carlo simulation.

The jumps in Topic-I are impulsive and large overshoots can occur. In Topic-II, a jump-diffusion model is developed based on a stochastic differential equation with jumps. The Jump component is modeled as a compound Poisson process, and the resulting conditional moments converge with greater accuracy to the Monte Carlo simulation results. A key advantage of this method is that it is far less computationally expensive than the conventional averaged Monte Carlo simulation.

To analyze the stability of the jump-diffusion model, methods based on the mean square stability are used in Topic-III. The jump-diffusion model is converted into a martingale to allow for the use of the Burkholder-Davis-Gundy (BDG) inequality. The method consists in computing the quadratic variation process and using the BDG inequality to derive bounds on the conditional moments of the system.

# ACKNOWLEDGMENTS

I would like to express my sincere gratitude and appreciation to my advisor, Dr. Jonathan Kimball, for providing me with the unique opportunity to work in a research area at the confluence of the stochastic theory and power systems. It has been quite a journey, and I thank Dr. Kimball for his patience, understanding and support throughout the course of this work.

I also thank my Ph.D. committee members, Dr. Mariesa Crow, Dr. Mehdi Ferdowsi, Dr. Pourya Shamsi, and Dr. Bruce McMillin, for their willingness to serve on my committee and review this dissertation.

A very special thanks to my family for their support and encouragement: my beloved wife, *Solange*, and our wonderful children, *Donny*, *Rosie* and *Joelle*. I could not accomplish this without you by my side. This dissertation is dedicated to you.

I am grateful to my parents: *Maman Isabelle* and *Papa Odon*, who early on instilled in me the passion for science and research.

Finally, I am thankful to the Boeing Company for funding my PhD program.

# TABLE OF CONTENTS

Page

PAPER

# LIST OF ILLUSTRATIONS

PAPER III

# LIST OF TABLES

# LIST OF SYMBOLS

| Symbol | Description |
|---|---|
| $(\Omega, \mathcal{A}, \mathbb{A}, \mathcal{P})$ | filtered probability space |
| $(\Omega, \mathcal{A}, \mathcal{P})$ | probability space |
| $A(t)$ | process of total variation |
| $A_i$ | state matrix associated with mode $i$ |
| $A_{sys}$ | system matrix |
| $B_i$ | input matrix associated with mode $i$ |
| $C = c_{ij}$ | covariance matrix of a stochastic process $X$ |
| $C_i$ | output matrix associated with mode $i$ |
| $D_i$ | feedthrough matrix associated with mode $i$ |
| $E(X)$ | expectation of a random variable $X$ |
| $E[X^p]$ | $p$th moment of a stochastic process $X$ |
| $G^{(m)}, H^{(m)}, G^{(m)}, J^{(m)}$ | matrices associated with the matrix representation of the evolution of the $m^{th}$ conditional moments |
| $I(N)$ | identity matrix of the $N$th order |
| $M(t)$ | martingale process |
| $M^{cont}(t)$ | continuous part of a martingale process |
| $M^{disc}(t)$ | discontinuous part of a martingale process |
| $N$ | number of stochastic modes |
| $N(t)$ | standard Poisson process |
| $N^{\ell}(t)$ | $\ell$th component of a multidimensional standard Poisson process |
| $N_u(N)$ | binomial coefficient |
| $P^*$ | reference active power |
| $P_k$ | $k^{th}$-inverter's active power |
| $Q^*$ | reference reactive power |

| | |
|---|---|
| $Q_i^+$ | set of outgoing transitions from mode $i$ |
| $Q_i^-$ | set of incoming transitions to mode $i$ |
| $Q_k$ | $k^{th}$-inverter's reactive power |
| $U(t)$ | input vector |
| $W(t)$ | standard Wiener process |
| $W_m, T_x, T_y$ | transformation matrices associated with the matrix representation |
| $X = \{X(t), 0 \leq t\}$ | one-dimensional stochastic process |
| $X_t^*$ | maximal process of a stochastic process $X$ |
| $Y(t) = \sum_{k=1}^{N(t)} \xi_k$ | compound Poisson process |
| $[X]_t = [X, X]_t$ | quadratic variation process of a stochastic process $X$ |
| $\Delta X(\tau_k)$ | jump size at time $\tau_k$ |
| $\Lambda$ | full transition rate matrix |
| $\Omega$ | sample space |
| $\beta$ | volatility constant |
| $\boldsymbol{X_i}$ | equilibrium operating point associated with mode $i$ |
| $\boldsymbol{X} = \{\boldsymbol{X}(t), 0 \leq t\}$ | multi-dimensional stochastic process |
| $\boldsymbol{y}$ | output vector |
| $\delta_k$ | $k^{th}$-inverter's phase angle |
| $\gamma_{d_k}$ | integral of error in filter inductor current, $d$-axis |
| $\gamma_{q_k}$ | integral of error in filter inductor current, $q$-axis |
| $\hat{N} = N_t - \lambda t$ | compensated Poisson process |
| $\hat{Y}(t)$ | compensated compound Poisson process |
| $\hat{\xi}$ | mean of all jumps |
| $\hat{f}(t, \boldsymbol{X}(t))$ | drift coefficient of an Itô formula of an SDE with jumps |
| $\hat{g}(t, \boldsymbol{X}(t))$ | diffusion coefficient of an Itô formula of an SDE with jumps |
| $\hat{h}(t, \boldsymbol{X}(t))$ | jump coefficient of an Itô formula of an SDE with jumps |

| | |
|---|---|
| $\lambda$ | intensity of a Poisson process |
| $\lambda_\ell$ | intensity of a Poisson process $N^\ell$ |
| $\lambda_{ij}$ | transition rate between modes $i$ and $j$ |
| $\mathbb{A}$ | filtration |
| $\mathcal{A}$ | collection of events, sigma-algebra, a family of subsets of $\Omega$ |
| $\mathcal{P}$ | probability measure |
| $\mu^p$ | $p$th moment of a stochastic process $X$ |
| $\mu_i^{(m)}$ | conditional moment of the $m^{th}$ order associated with mode $i$ |
| $\mu_{\boldsymbol{X}}$ | mean of $\boldsymbol{X}$ |
| $\omega_{PLL}$ | PLL's angular frequency |
| $\phi_{P_k}$ | $k^{th}$-inverter's integral of active power error |
| $\phi_{Q_k}$ | $k^{th}$-inverter's integral of reactive power error |
| $\phi_{pll_k}$ | $k^{th}$-inverter's integral $q$-axis voltage |
| $\psi = \psi(t, \boldsymbol{X}(t))$ | function of a stochastic process |
| $\psi(\hat{\xi})$ | mean jump size for the process function $\psi$ |
| $\sigma^2(X)$ | standard deviation of a stochastic process $X$ |
| $\tilde{x}_{sys}$ | state, system vector |
| $\xi_k$ | jump size of a compound Poisson process at time $\tau_k$ |
| $a_{pr}$ | elements of the state matrix $A_i$ |
| $e_p, e_r$ | unity vectors with a 1 at the $p^{th}$ ($r^{th}$) position and 0 elsewhere |
| $f(t, \boldsymbol{X}(t))$ | drift coefficient of an SDE with jumps |
| $g(t, \boldsymbol{X}(t))$ | diffusion coefficient of an SDE with jumps |
| $h(t, \boldsymbol{X}(t))$ | jump coefficient of an SDE with jumps |
| $i_{ld_k}$ | line $k$ current, $d$-axis |
| $i_{loadD_k}$ | bus $k$ load current, $d$-axis |
| $i_{loadQ_k}$ | bus $k$ load current, $q$-axis |
| $i_{lq_k}$ | line $k$ current, $q$-axis |

| | |
|---|---|
| $i_{od_k}$ | $k^{th}$-inverter's output current, $d$-axis |
| $i_{oq_k}$ | $k^{th}$-inverter's output current, $q$-axis |
| $m = (m_1, ..., m_N)$ | moment index vector |
| $n$ | dimension of the dynamic vector |
| $u_i$ | input vector associated with mode $i$ |
| $v_p^i$ | elements of the control vector augmented with an affine term |
| $v_{od_k}$ | $k^{th}$-inverter's output voltage, $d$-axis |
| $v_{oq_k}$ | $k^{th}$-inverter's output voltage, $q$-axis |
| $var(\boldsymbol{X})$ | variance of a multidimensional stochastic process $\boldsymbol{X}$ |
| $x_i$ | dynamic state associated with mode $i$ |

# 1. INTRODUCTION

## 1.1. MOTIVATION AND OUTCOME OF THE RESEARCH

The control of microgrids to ensure operational stability is of high interest for power engineers. Conventional techniques associated with the control of the main grid face challenges when applied to microgrids because of the randomness and sometimes the abruptness of the dynamics of microgrids. To develop an appropriate control scheme, a robust model of the microgrid is necessary, as well as stability criteria that apply to the stastistics of the system. Models based on Markov Jump Linear System (MJLS) combine a conventional dynamic representation of a microgrid with some random behavior that could include variations of the Wiener type and a Markovian random switching behavior. These models are derived in this dissertation and the resulting statistics are used to analyze the stochastic stability of the system.

The MJLS is a class of stochastic hybrid systems that consists of multiple linear modes representing the evolution of the states $\{\dot{x}_i = A_i x_i,\ i = 1, ..., N\}$, for which the modes $i$ are chosen stochastically following a continuous-time Markov chain (CTMC). For a microgrid, the system is considered to operate in some linear mode, with states experiencing linear variation of limited amplitudes around some equilibrium point. The switching mechanism corresponds, for instance, to random changes in the load or in power generation. In some cases and in the absence of adequate control, this non-linear and random behavior is susceptible to cause unit outages and transmission line faults. The model in Paper I borrows from the SHS's formulation and presents an MJLS with impulsive jumps in the dynamic states. Such model was used in [6] for a system subject to stochastic inputs, while the dynamic states were constrained to a linear behavior about a unique equilibrium point. In this study, the dynamics states evolve linearly around an equilibrium operating point but are also allowed to switch (or jump) between distinct operating points. When the

jump sizes are not bounded, the resulting impulses could be detrimental to the dynamics of the system. Paper II introduces a mean of constraining the jump size, based on the assumption that the system spends most of its time in a finite number of stochastic modes and barely in the transition between any two of them.

The modeling of the jump size is critical to accurately represent the transition behavior of a switching system.

## 1.2. ELEMENTS OF STOCHASTIC THEORY

The development of the microgrid stochastic models discussed in Papers I to III relies heavily on the terminology and concepts of the stochastic theory. These concepts may not be familiar to electrical and power system engineers. They are introduced here to provide a basic understanding of the conceptual framework used in Papers I to III. The definitions below are borrowed for the most part from [11, 28, 30, 29] and are presented here in a simplified way without all the complexity of the mathematical framework they were developed in.

**1.2.1. Probability Space.** All models developed in this study are based on the assumption that there exists an underlying probability space $(\Omega, \mathcal{A}, \mathcal{P})$ where: (i) $\Omega$ denotes the sample space, that is the set of all possible outcomes of a random experiment; (ii) $\mathcal{A}$ represents a collection of events (a family of subsets of $\Omega$), also called a sigma-algebra; and (iii) $\mathcal{P}$ is a function such that $\mathcal{P}(A)$ represents the probability that an event $A$ occurs, with $0 < \mathcal{P}(A) < 1$ and $\mathcal{P}(\Omega) = 1$. $\mathcal{P}$ is also called a probability measure.

**1.2.2. Stochastic Process.** A stochastic process with respect to a state space is a collection of random variables $X = \{X(t), 0 \leq t\}$ defined on the same probability space $(\Omega, \mathcal{A}, \mathcal{P})$. The state space is usually the set of real numbers $\mathbb{R}$. A trajectory, also called a sample path of the process $X(t)$ is the mapping $t \rightarrow X_t(\omega)$, for every fixed $\omega \in \Omega$. This thesis is interested in real-valued, multi-dimensional stochastic processes, $\boldsymbol{X}(t) \in \mathbb{R}^d$.

**1.2.3. Filtration.** A filtration on a probability space $(\Omega, \mathcal{A}, \mathcal{P})$, is an increasing family $\mathbb{A} = \{\mathcal{A}_t, 0 \leq t\}$ of sub-sigma-algebras of $\mathcal{A}$. The concept of sub-sigma-algebra means that for each $t$, $\mathcal{A}_t$ is a sigma-algebra included in $\mathcal{A}$ and if $s \leq t$, then $\mathcal{A}_s \subset \mathcal{A}_t$. A probability space endowed with a filtration $\mathbb{A}$ is termed a filtered probability space and is represented as $(\Omega, \mathcal{A}, \mathbb{A}, \mathcal{P})$.

**1.2.4. Moments of a Stochastic Process.** The expectation of a random variable $X$, denoted by $E(X)$, is defined as the integral of $X$ with respect to the probability measure $\mathcal{P}$

$$E(X) = \int_{\Omega} X d\mathcal{P} \tag{1.1}$$

where $\Omega$ is the sample space of the probability space $(\Omega, \mathcal{A}, \mathcal{P})$ the random variable $X$ is defined on.

The $p$th moment of a stochastic process $X(t)$ is defined by

$$\mu^p = E(X^p) \tag{1.2}$$

where $p \geq 1$. The process $X(t)$ is said to have a finite $p$th moment if $E(|X|^p) < \infty$. When $p = 1$, we obtain the mean or the expectation of $X$

$$\mu^{(1)}(t) = E(X_t) \tag{1.3}$$

and when $p = 2$, the $p$th moment corresponds to the moment of the second order

$$\mu^{(2)}(t) = E(X_t^2) \tag{1.4}$$

The variance of $X$ is calculated from the first and second moments as

$$var(X_t) = E\left[\left(X_t - \mu^{(1)}(t)\right)^2\right] \tag{1.5}$$

For a random vector process $\boldsymbol{X} = (X_1, ..., X_d)$ defined on a probability space $(\Omega, \mathcal{A}, \mathcal{P})$, the $p$th moment of $\boldsymbol{X}$ is defined as

$$\mu^{(p)}(t) = \mu^{(p_1, \cdots, p_d)}(t) = E\left[\prod_{i=1}^{d} X_i^{p_i}\right] \tag{1.6}$$

where $p_i \geq 0$ are integers such that $\sum_{i=1}^{d} p_i = p$. The mean or expectation of $\boldsymbol{X}$ is defined as the vector

$$E\left[\boldsymbol{X}\right] = \left(E[X_1] = \mu^{(1,0,...,0)}, ..., E[X_d] = \mu^{(0,...,0,1)}\right) \tag{1.7}$$

The covariance matrix of $\boldsymbol{X}$ is the $(d, d)$-matrix

$$C = c_{ij} = E\left[(X_i - E[X_i])(X_j - E[X_j])\right], \quad i, j = 1, ..., d \tag{1.8}$$

**1.2.5. Conditional Expectation.** The concept of conditional expectation is widely used in stochastic theory. Let $X$ be a stochastic process defined on a probability space $(\Omega, \mathcal{A}, \mathcal{P})$, and let $\mathcal{S}$ be a sub-sigma-algebra of $\mathcal{A}$. The *conditional expectation* of $X$ with respect to $\mathcal{S}$, denoted by $E(X|\mathcal{S})$ is defined as

$$\int_Q E(X|\mathcal{S})(\omega)dP(\omega) = \int_Q X(\omega)dP(\omega), \quad \forall Q \tag{1.9}$$

where $\omega \in \Omega$, and $\Omega$ is the sample space.

**1.2.6. Maximal Process.** For a stochastic process $X$, the corresponding maximal process is defined as

$$X_t^* = \sup_{s \leq t} |X_s| \tag{1.10}$$

The maximal process is an increasing process. It can be seen that if $s \leq t$ then $X_s^* \leq X_t^*$. Figure 1.1 shows a plot of a random process and its maximal process.

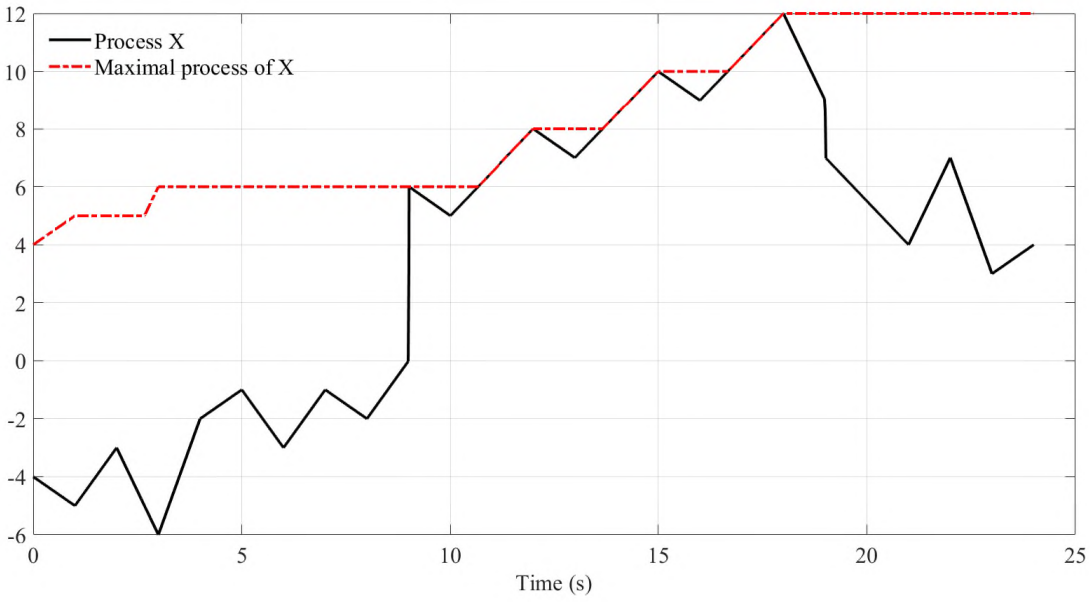


Figure 1.1. Process X and its maximal process

**1.2.7. Quadratic Variation Process.** The *quadratic variation process* of a stochastic process $X$, denoted by $[X, X]$ or $[X] = \{[X]_t, t \geq 0\}$, is an increasing process defined as

$$[X]_t \stackrel{\Delta}{=} \lim_{h \to 0} [X]_{h,t} \tag{1.11}$$

where $[X]_{h,t}$ is *the approximate quadratic variation* defined as the sums of squared increments of the process $X$

$$[X]_{h,t} = \sum_{k=1}^{\eta_t} (X_{t_k} - X_{t_{k-1}})^2 \tag{1.12}$$

In 1.12, $\eta_t$ is an integer such that

$$\eta_t = max\{k \in \mathcal{N} : t_k \leq t\} \tag{1.13}$$

and

$$\{t_k = kh : k \in \{0, 1, ...\}\} \tag{1.14}$$

represents an *equidistant time discretization.*

**1.2.8. Total Variation Process.** The *total variation process* of a stochastic process $X$, is the limit in probability as $h \longrightarrow 0$ defined as follows

$$\lim_{h \to 0} \sum_{k=1}^{\eta_t} |X_{t_k} - X_{t_{k-1}}| \tag{1.15}$$

A process is considered being of finite total variation if $\lim_{h \to 0} \sum_{k=1}^{\eta_t} |X_{t_k} - X_{t_{k-1}}| < \infty$.

Next, to illustrate the definitions above, examples of some of the most fundamental stochastic processes are presented and some of their properties described.

**1.2.9. Wiener Process.** The Wiener process is a continuous time stochastic process with stationary independent increments. The random increments of a Wiener process, $W_{t_k} - W_{t_{k-1}},\ k \in \{1, ..., n\}$ are independent for any sequence of times $t_0 < t_1 < ... < t_{n+1}, \forall n \in \mathcal{N}$. The stationary property implies that the increments $W_{t_k} - W_{t_{k-1}}$ have the same distribution as $W_h - W_0,\ \forall h > 0$ and $t \geq 0$. A formal definition for the Wiener Process from [28] is provided as follows: the Standard Wiener process $W = \{W_t,\ t \geq 0\}$ is defined as an $\mathcal{A}$-adapted process with Gaussian stationary independent increments and continuous

sample paths for which

$$W_0 = 0, \quad \mu(t) = E(W_t) = 0, \quad \sigma^2_{W_t}(t) = Var(W_t - W_s) = t - s, \quad \forall t \geq 0 \text{ and } s \in [0, t] \tag{1.16}$$

The Wiener process is very important in Stochastic theory. It is used to build more complex stochastic processes like martingales. It is used for instance to model noise in electronics or random variations (of limited magnitudes) in the dynamic states of a power system model.

The trajectories of 10 samples of a standard Wiener process are shown in Figure 1.2. To compute the mean and variance, 100 trajectories are used. According to 1.16, the standard Wiener process should have mean zero and variance $t - s$ and this is illustrated in Figure 1.2 . For a high number of trajectories (1000+), the variance is expected to be a straight line coinciding with the $x - axis$ as in the definition of a standard Wiener process.

The total variation and the quadratic variation processes are plotted in Figure 1.3 based on a Matlab code described in [29]. It can be seen that the Wiener process has an unbounded total variation and a bounded quadratic variation.

**1.2.10. Poisson Process.** The standard Poisson process is the most elementary and useful jump process. It is a counting process and has jumps of size +1 only. A formal definition from [28] is as follows: a Poisson process $N = \{N_t,\ t \geq 0\}$ with intensity $\lambda > 0$ is a piecewise constant process with stationary independent increments with initial value $N_0 = 0$ such that $N_t$ is Poisson distributed with intensity $\lambda$, that is, with probability

$$P(N_t - N_s = k) = \frac{e^{-\lambda(t-s)}(\lambda(t-s))^k}{k!} \tag{1.17}$$

for $k \in \{0, 1, ...\},\ t \geq 0\}$ and $s \in [0, t]$.

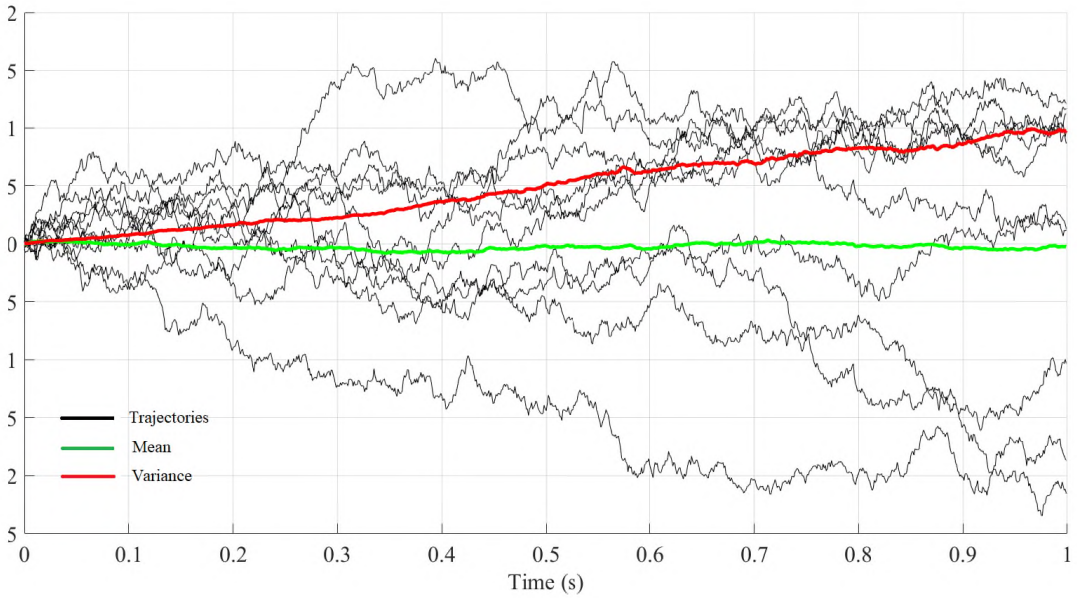


Figure 1.2. Sample trajectories of a Wiener process

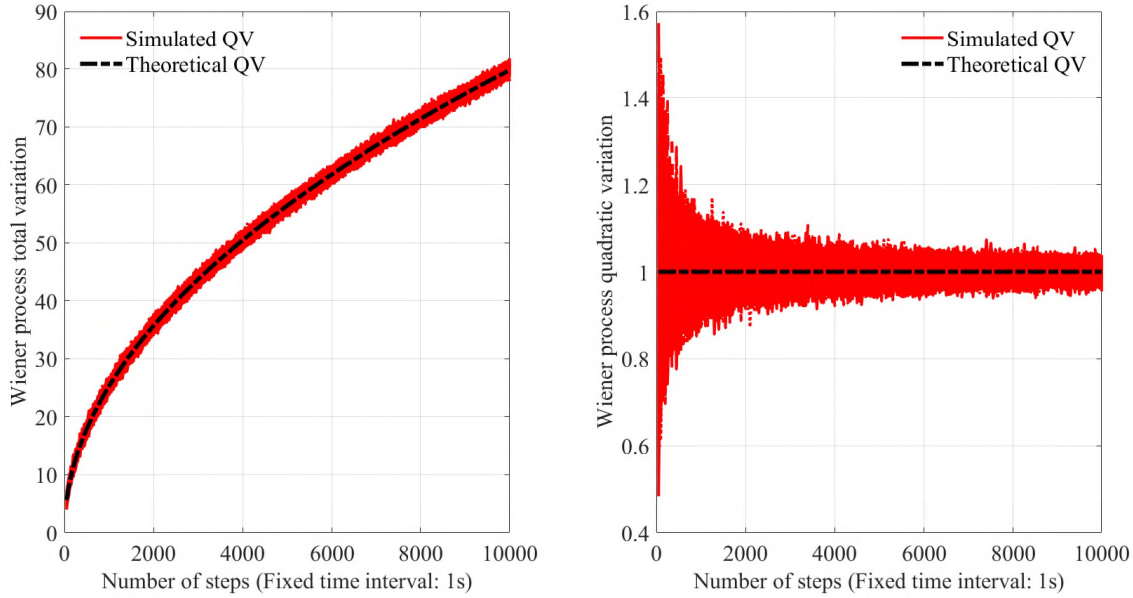


Figure 1.3. Wiener process total variation and quadratic variation processes

As a counting process, the number of events occurring up to a time instant $t$ is represented by

$$P(N_t = k) = \frac{e^{-\lambda t}(\lambda t)^k}{k!} \tag{1.18}$$

The mean of a standard Poisson process $N$ with intensity $\lambda$

$$\mu(t) = E(N_t) = \lambda t \tag{1.19}$$

and the variance

$$\sigma^2_{N_t}(t) = Var(N_t) = E\left[\left(N_t - \mu(t)\right)^2\right] = \lambda t \tag{1.20}$$

The process $\hat{N}_t = N_t - \lambda t$ is denoted as the compensated Poisson process and has a mean value of $E\left(\hat{N}_t\right) = 0$.

On the other hand, a compound Poisson process is also a counting process but with random jump sizes. It can be constructed as $Y = \{Y_t,\ t \geq 0\}$, with $Y_0 = 0$ and

$$Y_t = \sum_{k=1}^{N_t} \xi_k \tag{1.21}$$

where $N_t$ is a counting Poisson process with intensity $\lambda$, and $\xi_k$ represents the jump size at the jump time $\tau_k$. Figure 1.4 shows trajectories of a standard Poisson process and a compound Poisson process. According to the definition of the Poisson process, the number of jump events should be equal on average to the intensity, $\lambda$. It can also be seen that the jump size of the standard Poisson process equals 1 and that of the compound Poisson process is random.

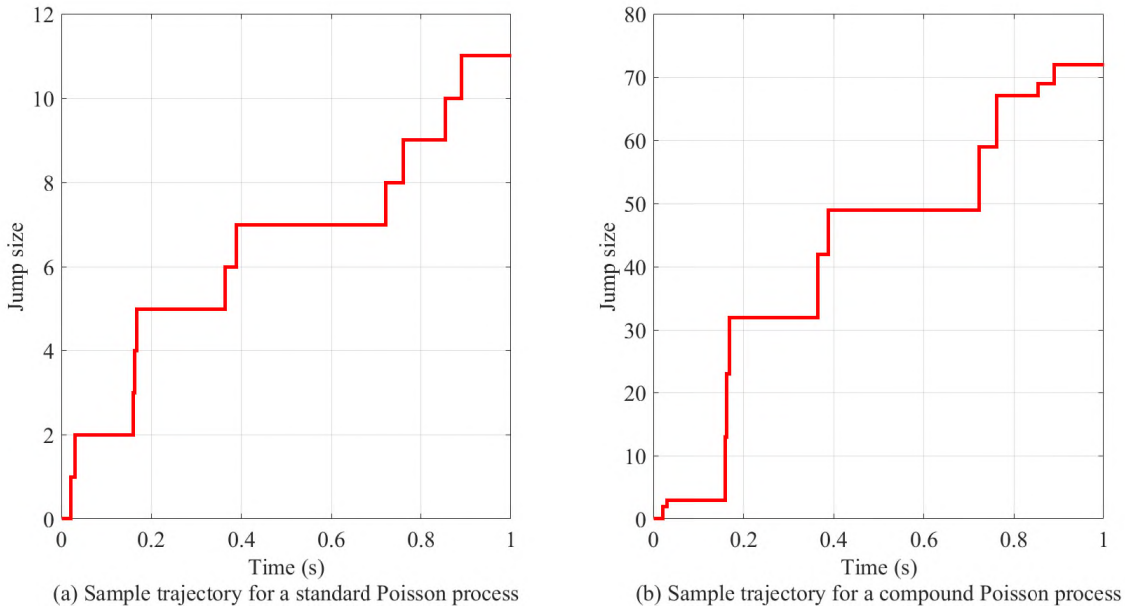


(a) Sample trajectory for a standard Poisson process

(b) Sample trajectory for a compound Poisson process

Figure 1.4. Sample trajectories of a Poisson and a compound Poisson processes

## 1.3. CONTRIBUTION TO DATE

This work uses techniques and concepts that apply to the stochastic theory and the financial modeling to develop stochastic models for a microgrid operating in grid-tied and standalone modes and analyzes the conditions of its stability.

Paper I develops a model for a microgrid in the SHS framework. The resulting ODEs representing the conditional moments are put into matrix form, and analytical solutions of the statistics of the system are computed. The paper also describes an algorithm based on the Gillespie method to accurately generate mode sequences for the underlying Markov Process of the switching process. To validate the model, comparison is made with the averaged Monte Carlo simulation. The Monte Carlo method turns out to be computationally, prohibitively expensive compared to the MJLS method. A limitation of the model is the impulses observed in the states during switching events that would make it difficult to control system dynamics. These impulses were observed during the Monte Carlo and are not present in the analytical solutions of the conditional moments.

In Paper II, the model in Paper I is improved with the addition of a Wiener process and an appropriate jump modeling to improve switching behavior. The procedure begins with a Stochastic differential equation with jumps where the jump term is represented by a compound Poisson process. Then, a method to derive a matrix representation of the systems of ODEs representing the evolution of the conditional moments is derived. The model yields improved system dynamics with higher convergence of the analytical solutions to the averaged Monte Carlo simulation . As in Paper I, the model is validated through the analysis of the modified IEEE 37-bus microgrid system.

Stability analysis is conducted in Paper III, using the statistics of the system derived in the jump-diffusion model of Paper II. The SDE with jumps is transformed into a compensated SDE to allow for the use of the martingale inequalities. The method allows for the computation of the quadratic variation process of the compensated Poisson stochastic integral. The mean-square stability criterion is applied to the quadratic variation process and bounds on the conditionals moments are derived using the Burkholder-Davis-Gundy inequality for martingales.

# PAPER

## I. MARKOV JUMP LINEAR SYSTEM ANALYSIS OF A MICROGRID OPERATING IN ISLANDED AND GRID-TIED MODES

Gilles Mpembele and Jonathan W. Kimball
Department of Electrical & Computer Engineering
Missouri University of Science and Technology
Rolla, Missouri 65409–0050
Email: gmhn7@umsystem.edu

## ABSTRACT

The analysis of power system dynamics is usually conducted using traditional models based on the standard nonlinear differential algebraic equations (DAEs). In general, solutions to these equations can be obtained using numerical methods such as the Monte Carlo simulations. The use of methods based on the Stochastic Hybrid System (SHS) framework for power systems subject to stochastic behavior is relatively new. These methods have been successfully applied to power systems subjected to stochastic inputs. This study discusses a class of SHSs referred to as Markov Jump Linear Systems (MJLSs), in which the entire dynamic system is jumping between distinct operating points, with different local small-signal dynamics. The numerical application is based on the analysis of the IEEE 37-bus power system switching between grid-tied and standalone operating modes. The Ordinary Differential Equations (ODEs) representing the evolution of the conditional moments are derived and a matrix representation of the system is developed. Results are compared to the averaged Monte Carlo simulation. The MJLS approach was found to have a key advantage of being far less computational expensive.

**Keywords:** Markov Jump Linear Systems, Monte Carlo simulations, Stochastic Hybrid Systems, Power System statistics.

## 1. INTRODUCTION

The objective of this paper is to analyze a microgrid using advanced techniques that apply to Markov Jump Linear Systems. The system under study is a modified IEEE 37-bus power system where seven inverters were added at selected buses [1] to represent Distributed Energy Resources (DERs). The application of stochastic methods to the analysis of microgrids has gained increased attention with a lot of research papers focused on the control and stability analysis of power systems subject to random disturbances [2, 3, 4]. However, previous works did not consider large signal disturbances such as those resulting from a microgrid switching between different operating equilibrium points.

In this paper, a microgrid is defined as a small-scale power grid that can operate independently or collaboratively with other small power grids [5]. This architecture based on the use of microgrids in a power system is also known as distributed, dispersed, decentralized, district or embedded power generation. Any small-scale and localized power system that includes localized generation resources and, but not always, storage capability, with well defined boundaries can be identified as a microgrid. In the case a microgrid is allowed to integrate with the main power grid, it is referred to as a grid-connected or hybrid microgrid. Typically, power production in microgrids is supported by generators or renewable energy systems such as wind and solar resources, and when integrated with the main grid they provide backup power or supplemental power during periods of heavy demand. This strategy provides redundancy for critical and essential services and makes the main grid more immune to temporary disasters [5].

In real-time operation, the control of distributed energy resources in a microgrid and the preservation of an adequate system inertia pose significant challenges to the stability of microgrids' operation. This is particularly true in the absence of a stiff grid, when a

microgrid is operating in standalone or islanded mode. Because of the combination of factors such as low microgrid inertia, limited power storage capability and tight coupling among various elements in the system, fluctuations in the output power of distributed energy resources or changes in local load may lead to power quality or frequency/voltage stability concerns [6]. For example, if an important load is switched on and off, frequency and voltage may change dramatically, and could even result in a collapse of the entire system. Additionally, with an increasing penetration of microgrids, the main power grid could face a similar challenge when subject to active/reactive power injections resulting from a random coupling and decoupling of multiple DERs [2].

To characterize the randomness in system operation as described above, methods based on Stochastic Hybrid Systems were proposed [2, 7, 8]. These methods combine the conventional power system dynamic model and a stochastic representation. In this study, focus is on one particular class of SHSs referred to as Markov Jump Linear Systems. An MJLS is composed of two coupled sub-systems [9].

The first sub-system is based on a linearized power system dynamic model. Each mode of the stochastic model is mapped to a linear system with continuous state variables. These linear systems correspond to continuous-time small-signal models of the microgrid linearized around well defined operating points.

The second sub-system is a continuous-time Markov process, which has a defined number of discrete states, $N$, also described as stochastic modes of the Markov process. These discrete states correspond to the steady-state operating points of the microgrid. Hence, the system is described as "jumping" between different modes $(i, j)$ at a transition rate $\lambda_{ij}$.

The two coupled models are represented in Figure 1.

The general SHS model framework for a power system is discussed in [2], where a power system is subject to stochastic power injections resulting from the coupling and decoupling of microgrids. The power system is operating around an identified stable

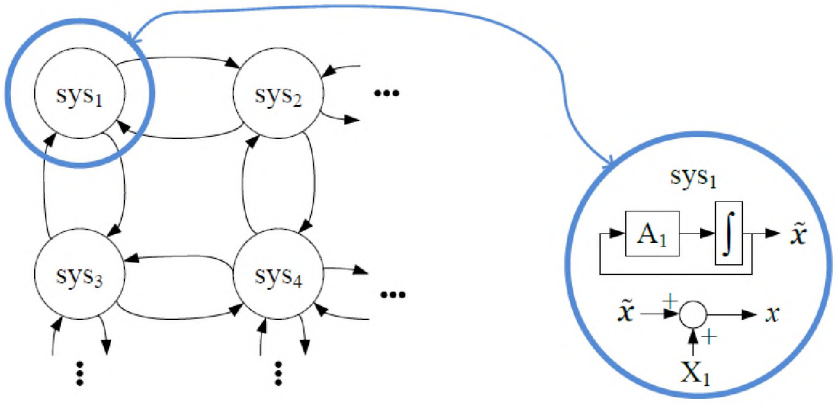


Figure 1. Markov Jump Linear System architecture, where each node on the left maps to a linear system as on the right.

operating point, only the control variables are randomly switching between a finite set of discrete values. The method results in a set of ODEs that describe the evolution of the conditional moments of the power system. The integration of these ODEs yield the statistics of the dynamic and algebraic states. This method is also used in [7] to predict the influence of random load behavior on the dynamics of dc microgrids and distribution systems.

Following a method described in [2], a set of ODEs representing the evolution of the conditional moments is derived to represent the dynamics of a *microgrid system oscillating between distinct operating equilibrium points*, with different local small-signal dynamics.

For the system under study, the IEEE 37-bus microgrid, the analysis begins with a description of the power system dynamics by standard nonlinear differential algebraic equations. Based on the derivation in [1, 10], a total of 225 dynamic states and a collection of non-linear equations are identified to represent the microgrid dynamics. These non-linear equations are then linearized around equilibrium points, and the result is a $225^{th}$ order state space representation. The system is considered switching between three equilibrium points (one grid-tied mode and two standalone modes). Therefore, there are three state space representations of the $225^{th}$ order corresponding to each operating mode. However, the linearized system is a two-time scale system that combines fast and slow dynamic states.

By applying the singular perturbation method [1, 11], slow states can be separated from the fast states. The procedure results in a system order reduction to 56 dynamic states. The stochastic modelling consists in characterising the random switching of the system from one operating mode to another. This switching behavior is appropriately represented as a Continuous Time Markov Chain [2, 8, 9]. In practice, this corresponds to including a *jump term* in the state equations to represent jump events at Poisson distributed jump times [8]. To solve this combined system (linear dynamics and jumps), there are two possible methods: the numerical integration of the system of ODEs representing the dynamics of the conditional moments, or the averaged solution of repeated Monte Carlo simulations. The solutions obtained using either method represent the conditional moments of the stochastic system. This study *computes these moments* using the two methods mentioned above and demonstrates that the MJLS results converge to the averaged Monte Carlo simulations. The steps discussed above are represented in Figure 2.

This paper is structured as follows. Section 2 describes the system under study: the modified IEEE 37-bus power system. In Section 3, the power system model is cast as an MJLS and, using the equations developed in [2, 12], a matrix representation of the system is derived for the computation of the conditional moments. In Section 4, the solutions to the ODEs of the system dynamics are computed and discussed using the two methods described above (MJLS and averaged Monte Carlo simulations). Conclusion and avenues for future work are summarized in Section 5. In the appendix, the transition rate matrix of the stochastic process, the state vectors for the three stochastic modes of the MJLS, as well as the matrix representation of the dynamics of the second moments are presented.

## 2. SYSTEM UNDER CONSIDERATION

The method developed in this study is applied to the IEEE 37-bus power system. The standard IEEE 37-bus system was modified with the addition of seven inverters at selected nodes to represent inverter-based DERs. The one-line diagram is represented in

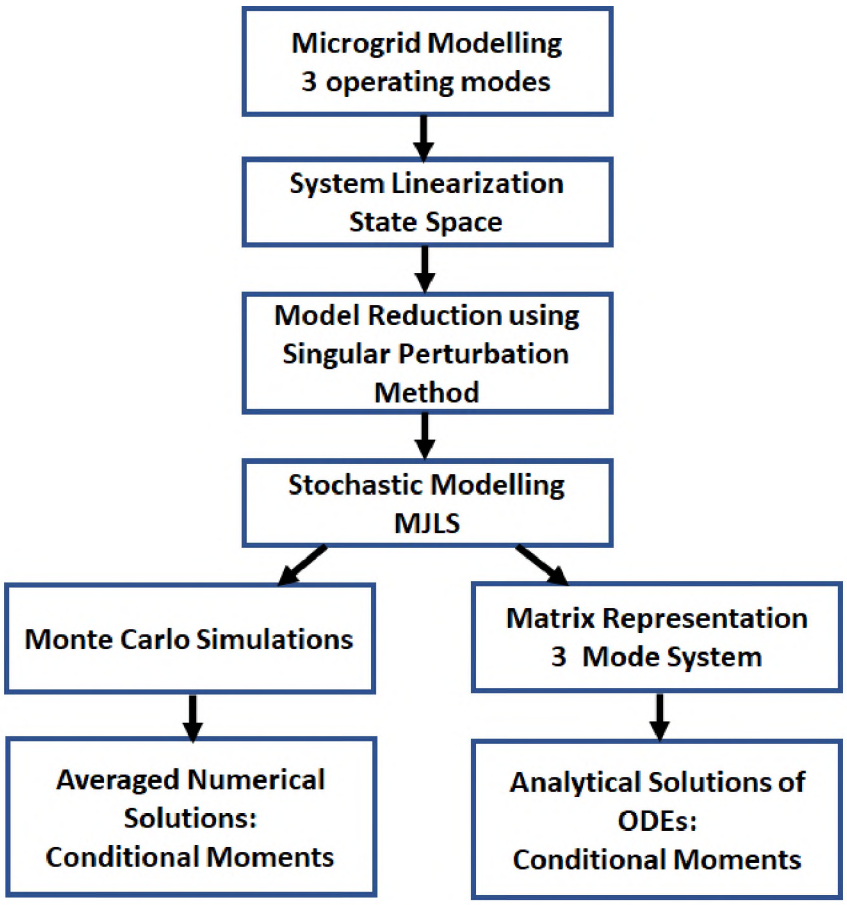


Figure 2. Analysis steps of a microgrid using MJLS and Monte Carlo simulations

Figure 3, where the larger dots at designated bus locations represent the inverters. Static loads are spot loads at various nodes and represent consumers of constant power ($PQ$), constant current or constant impedance. Details of the modified system including the load and line parameters are given in [1, 11].

For the purpose of this study, the system is considered switching between the grid-tied and two distinct islanded operating modes. The connection to the main power grid is made at the point of common coupling (PCC). In the grid-tied mode, all the bus voltages and the system frequency are maintained by the stiff main grid. However, in the islanded mode, voltage and frequency are controlled by the DERs using the droop control strategy [13]. The numerical application considers one grid-tied operating mode, and two distinct

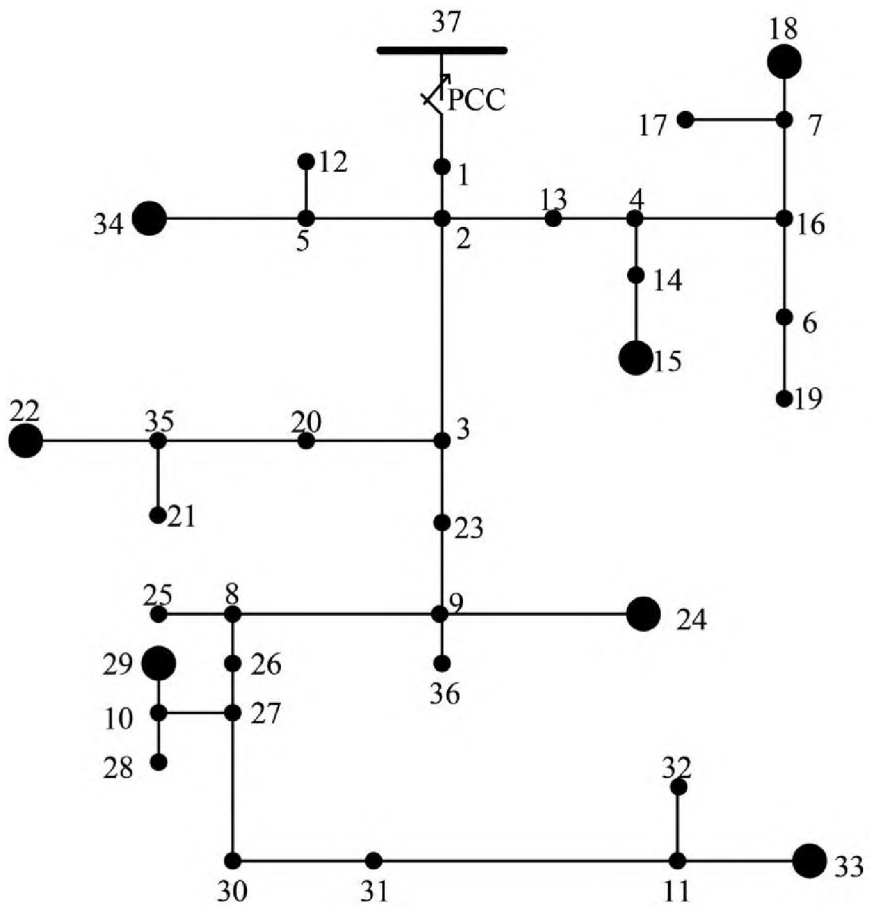


Figure 3. One-line diagram of the IEEE-37 node distribution test feeder. Large circles represent inverters.

islanded (standalone) operating modes. The two standalone operating modes correspond to *two distinct equilibrium points* characterized by *two distinct sets of bus loads and inverter settings*. A sample of numerical values for the dynamic states of the IEEE 37-bus microgrid operating in grid-tied and standalone modes are presented in Table 1. The definition of all parameters can be found in [1, 10, 11].

The small-signal model of the overall system was developed in [1, 11] using the *dq* reference frame and resulted in a $225^{th}$ order system. The derivation of the linearized dynamic model is also presented in details in the same papers. Each inverter system contains 15 states. Load and line models contain two states: the load currents *(d, q)* and the line

Table 1. Sample Dynamic States Equilibrium Points

| **States** | **Grid-tied** | **Standalone 1** | **Standalone 2** |
|---|---|---|---|
| $P_4(W)$ | 5000 | 8444 | 11600 |
| $Q_4(Var)$ | 1000 | 5239 | 7201 |
| $V_{22_D}(Volts)$ | -9.954 | -42.64 | -47.29 |
| $V_{22_Q}(Volts)$ | 298.6 | 291.1 | 282.7 |
| $\delta_4(rad)$ | 0.07868 | -0.01768 | -0.03615 |
| $I_{22-35_D}(A)$ | -0.307 | -7.869 | -11.03 |
| $I_{22-35_Q}(A)$ | -8.816 | -17.17 | -24.90 |
| $Iload_{22_D}(A)$ | 1.261 | 0.9777 | 0.894 |
| $Iload_{22_Q}(A)$ | 2.26 | 2.37 | 2.344 |

currents *(d, q)*. These dynamic states are presented below for the grid-tied operating mode

$$x_{inv} = [\delta \quad P \quad Q \quad \varphi_P \quad \varphi_Q \quad \gamma_d \quad \gamma_q \quad i_{ld} \quad i_{lq} \quad i_{od} \quad i_{oq} \quad v_{od} \quad v_{oq} \quad \varphi_{PLL} \quad v_{od,f}]^T \tag{1}$$

$$x_{load} = [i_{load_d} \quad i_{load_q}]^T \tag{2}$$

$$x_{line} = [i_{line_d} \quad i_{line_q}]^T \tag{3}$$

For the islanded system [10, 11], the inverter states $\varphi_P$ and $\varphi_Q$ in the voltage controller of the grid-tied system are replaced with $\phi_d$ and $\phi_q$ in the power controller, respectively. It can be shown that in the two cases (grid-tied and islanded), the system matrices are compatible and therefore a transition islanded mode to grid-tied mode (and vice versa) can be envisaged. In the standalone mode, $\phi_d$ represents the integral of the error

between the angular frequency $\omega_{PLL}$ generated by the PLL and the reference frequency $\omega^*$. Similarly, $\phi_q$ is equivalent to the integral of the error between the reference voltage and the measured $q$-axis voltage $v_{oq}$. In the grid-tied mode, $\phi_P$ is the integral of the error between the reference active power $P^*$ and the measured active power $P$, in the power controller, and $\phi_Q$ is the integral of the error between the reference reactive power $Q^*$ and the measured reactive power $Q$.

Another difference between the two operating modes is in the inputs to the system. In the grid-tied mode, the inputs are the active and reactive power references $(P^*, Q^*)$. However, in the islanded mode, the inverters are droop controlled and the inputs can be defined as the bus voltages. As explained in [11], to accurately predict the effects of load perturbations when bus voltages are used as inputs, a method based on a virtual resistor is used. The virtual resistor with high resistance is connected at the inverter bus and has a negligible effect on the system dynamics. With this method, the terms related to the bus voltages are included in the system matrix.

An analysis of the dynamic model reveals the existence of a two-time-scale behavior [14], which requires small time steps for the fast dynamics and a long simulation time for the slow dynamics. Using the singular perturbation method [1, 11], fast transients can be eliminated and, as a result, the system order is reduced. In the case of the modified IEEE 37-bus microgrid, the system order is reduced from 225 to 56 dynamic states [1, 11].

Following the procedure described above: non-linear model identification, linearization around steady-state operating points, system order reduction, and with help of the Matlab symbolic toolbox, the small-signal mathematical model of the grid-tied system is

$$\begin{aligned} \dot{\tilde{x}}_{sys} &= A\tilde{x}_{sys} + B\tilde{u} \\ \tilde{y} &= C\tilde{x}_{sys} + D\tilde{u} \end{aligned} \tag{4}$$

where the control vector $\tilde{u} = [P^* \quad Q^*]^T$. In the case of the islanded operating modes, the small-signal dynamic model is

$$\begin{aligned} \dot{\tilde{x}}_{sys} &= A_p \tilde{x}_{sys}; \quad p = 1, 2 \\ \tilde{y} &= C\tilde{x}_{sys} \end{aligned} \tag{5}$$

where, as indicated above and in [10, 11], the input vector of bus voltages has been expressed in terms of the dynamic states.

## 3. IEEE 37-BUS POWER SYSTEM AS AN MJLS

In this section, the IEEE-37 bus power system is framed as an MJLS. The system is switching between three operating modes in a random manner. The conjoint modeling of the linear dynamic system and the stochastic system was developed in [2, 7, 8, 15]. The resulting system of ODEs that represent the evolution of the conditional moments were derived in [2]. The ODE for the $m^{th}$ order conditional moment with respect to the stochastic mode $i$ is represented as

$$\begin{aligned} \dot{\mu}_i^{(m)}(t) = \sum_{p=1}^{n} m_p \left( \sum_{r=1}^{n} a_{pr}^i \mu_i^{\left(m-e_p+e_r\right)}(t) + \mu_i^{\left(m-e_p\right)}(t)\, v_p^i \right) \\ + \sum_{j \in Q_i^-} \lambda_{ji}(t)\, \mu_j^{(m)}(t) - \sum_{k \in Q_i^+} \lambda_{ik}(t)\, \mu_i^{(m)}(t), \forall i \in Q \end{aligned} \tag{6}$$

where $\dot{\mu}_i^{(m)}$ denotes the time derivative of the conditional moment of the $m^{th}$ order associated with mode $i$, $m_p$ is the $p^{th}$ element of the moment index vector $m = (m_1, ..., m_N)$, $a_{pr}^i$ are elements of the state matrix $A_i$, $v_p^i$ represents the elements of the control vector augmented with an affine term, $\lambda_{ji}$ is the transition rate from $j$ to $i$, $Q_i^-$ is the set of incoming transitions, and $Q_i^+$ is the set of outgoing transitions, $e_p$, $e_r$ are unity vectors with a 1 at the $p^{th}$ ($r^{th}$, respectively) position and 0 elsewhere. The solutions to the MJLS model can be computed

using two approaches. The first method is a discrete time approximation using the averaged Monte Carlo simulation, and the second method is based on a matrix representation of equation (6). The two approaches are explained below.

### 3.1. AVERAGED MONTE CARLO SIMULATION

The method consists in solving the dynamic equations in (4) or (5) numerically along the paths resulting from the CTMC. Therefore, the procedure begins with generating the CTMC integration paths based on a given transition rate matrix. The procedure to generate these integration paths is summarized in Algorithm 1, where $\mathbf{j} = max(j)$ and the operation $mode = k + 1$ is defined such as $1 + 1 = 2$, $2 + 1 = 3$, and $3 + 1 = 1$, for $k = 1, 2, 3$, respectively. The method described in Algorithm 1 is an adaptation of the Gillepsie's Stochastic Simulation Algorithm (SSA) [16].

**Algorithm 1:** CTMC modes sequence generation

**Require:** $T_s$, $T_{final}$, $\Lambda$
**Initialize:** $t = 0$, $mode = initial\_mode$, $lam = tr(\Lambda)$
**while** $t <= T_{final}$ **do**
  $r_1 = rand(1)$
  $tsw = -ln(r_1)/\Lambda(mode, mode)$
  $r_2 = rand(1)$
  **if** $mode = k$ **then**
    **if** $\big(\sum_{i=1}^{k-1}\sum_{\substack{j=1\\ j\neq i}}^{N}\lambda_{ij}\big)/lam < r_2$ *and* $r_2 \leq \big(\sum_{i=1}^{k}\sum_{\substack{j=1\\ j\neq i}}^{N}\lambda_{ij} - \lambda_{k\mathbf{j}}\big)/lam$ **then**
      $mode = k + 1$; continue;
    **end**
    **if** $\big(\sum_{i=1}^{k}\sum_{\substack{j=1\\ j\neq i}}^{N}\lambda_{ij} - \lambda_{k\mathbf{j}}\big)/lam < r_2$ *and* $r_2 \leq \big(\sum_{i=1}^{k}\sum_{\substack{j=1\\ j\neq i}}^{N}\lambda_{ij}\big)/lam$ **then**
      $mode = k + 2$; continue;
    **end**
  **end**
**end**

The next step is to solve the dynamic states using the Euler method along each path generated by Algorithm 1. This procedure is repeated during successive runs, the number of which will determine the accuracy of the final result. The final solutions for the dynamic and algebraic states are calculated by averaging the results from all runs. This yields the statistics of the system: zeroth, first and second moments, which are usually sufficient to characterize a distribution. The procedure for the repetitive MC simulations is described in Algorithm 2 where $X_i$ represents the state vector at equilibrium for mode $i = 1, 2, 3$.

**Algorithm 2:** Repetitive Monte Carlo simulations

**Require:** $T_s$, $T_{final}$, $Mode\ sequence\ from\ Algorithm\ 1$
**Initialize:** $max\_iter$, $X_{init}$, $x_{iter} = 0$
**for** $iter = 1 : max\_iter$ **do**
  **for** $k = 1 : length(t)$ **do**
    $x(1) = X_{init}$
    **if** $modes(k) = i$ **then**
      $x(k+1) = x(k) + Ts * A_i * (x(k) - X_i) + Ts * B_i * u_i$
    **end**
  **end**
  $x_{iter} = x_{iter} + x$
**end**
$x_{iter} = x_{iter}/max\_iter$

## 3.2. MATRIX REPRESENTATION OF THE MJLS

For small systems, with a very small number of dynamic states (for instance the SMIB system described in [2]), an analytical solution of the equation above is pretty straightforward. However, for larger systems with a higher number of dynamic states, an analytical solution becomes quickly very complex. It was discussed in [17, 18] that, for a larger system, the solutions are more conveniently computed when equation (6) is put in matrix form. This matrix representation is derived below, following the methods discussed in [18, 7]. Fortunately, the system of ODEs (6) representing the evolution of the conditional moments are finite-dimensional. Each term on the left hand side of (6) depends only on

moments of equal order or lower on the right hand side. Therefore, moment-closure methods are not necessary. It can be seen from (6), that $\dot{\mu}_i^{(m)}(t)$ depends only on $\mu_i^{(m-e_p+e_r)}(t)$, $\mu_i^{(m-e_p)}(t)$, $\mu_i^{(m)}(t)$, and $\mu_j^{(m)}(t)$. It turns out the operation $m - e_p + e_r$ results in only two possible outcomes $m$ and $m-1$, associated respectively with $\mu_i^{(m)}(t)$ and $\mu_i^{(m-1)}(t)$. On the other hand, the moments $\mu_i^{(m)}(t)$ and $\mu_j^{(m)}(t)$, associated with modes $i$ and $j$ are of the same dimension $m$. Regrouping all terms associated with moments of the same order [7], the system of ODEs represented in (6) can now be expressed as follows

$$\dot{\mu}^{(m)}(t) = G^{(m)}\mu^{(m)}(t) + H^{(m)}\mu^{(m-1)}(t) \tag{7}$$

This expression is equivalent to (6) and matrices $G^{(m)}$ and $H^{(m)}$ can be derived using the method detailed in [7]. They are essentially block diagonal combinations of sub-matrices related to each mode of the stochastic system. The general structure of $G^{(m)}$ and $H^{(m)}$ are provided in (8) and (9). $G^{(m)}$ is a sum of two terms. The first term is a block diagonal matrix which elements $G_i^{(m)}$ $(i = 1...N)$ include the state matrices corresponding to the modes of the stochastic model. The second term contains elements of the transition rate matrix.

$$G^{(m)} = \begin{bmatrix} G_1^{(m)} & 0 & \cdots & 0 \\ 0 & G_2^{(m)} & \cdots & 0 \\ \vdots & \vdots & \ddots & \vdots \\ 0 & 0 & \cdots & G_N^{(m)} \end{bmatrix} + \left(\Lambda^T \otimes I\left(N^m\right)\right) \tag{8}$$

In (8), $I(N^m)$ is the $N^m$-dimensional identity matrix and $\Lambda^T$ is the transpose of the full transition matrix, which includes the self-transition elements $\lambda_{ii}$.

$H^{(m)}$ is also a block-diagonal matrix which elements correspond to the input term of equation (4) augmented with an affine term: $Bu^i + C = v^i$.

$$H^{(m)} = \begin{bmatrix} H_1^{(m)} & 0 & \cdots & 0 \\ 0 & H_2^{(m)} & \cdots & 0 \\ \vdots & \vdots & \ddots & \vdots \\ 0 & 0 & \cdots & H_N^{(m)} \end{bmatrix} \tag{9}$$

The method to derive these matrices is described in length in [7, 18] and succinctly presented here for the lower order moments: zeroth, first and second.

The $0^{th}$ order moments are the occupational probabilities of the stochastic model, i.e., they represent the probability for the system to be in a particular mode $i$. To obtain the $0^{th}$ order moments, we replace $m = 0$ in equations (6) and (7). It follows

$$G^{(0)} = \Lambda^T \tag{10}$$

$$H^{(0)} = 0 \tag{11}$$

It is worth noting that $\mu^{(0-1)}$ is not permitted as it would result in a negative order moment.

The first order moments are the statistical means of the system. It can be shown that

$$G_i^{(1)} = A_i \tag{12}$$

$$H_i^{(1)} = v^i \tag{13}$$

The second order moments are the uncentered second moments of the system.

$G^2$ and $H^2$ elements result from the Kronecker product of $I(N)$ and $A_i$ (respectively, $v^i$), subsequently multiplied by $W_m$, which is a transformation matrix that describes the structure and ordering of the second moment [7]

$$G_i^{(2)} = W_m(I(N) \otimes A_i) \tag{14}$$

$$H_i^{(2)} = W_m(I(N) \otimes v^i) \tag{15}$$

The next step in the calculation of the second moment is to eliminate the redundant second order moments. The procedure results in the reduction of the order and size of $G^{(2)}$ and $H^{(2)}$. After the redundant second order moments are eliminated, the equations (8) and (9) can now be rewritten as follows:

$$\hat{G}^{(m)} = \begin{bmatrix} \hat{G}_1^{(m)} & 0 & . & . & 0 \\ 0 & \hat{G}_2^{(m)} & . & . & 0 \\ . & . & . & . & . \\ . & . & . & . & . \\ 0 & 0 & . & . & \hat{G}_N^{(m)} \end{bmatrix} + \left(\Lambda^T \otimes I\left(N_u(N)\right)\right) \tag{16}$$

$$\hat{H}^{(m)} = \begin{bmatrix} \hat{H}_1^{(m)} & 0 & . & . & 0 \\ 0 & \hat{H}_2^{(m)} & . & . & 0 \\ . & . & . & . & . \\ . & . & . & . & . \\ 0 & 0 & . & . & \hat{H}_N^{(m)} \end{bmatrix} \tag{17}$$

$$\hat{G}_i^{(2)} = W_m(I(N_u) \otimes A^i) \tag{18}$$

$$\hat{H}_i^{(2)} = W_m(I(N_u) \otimes v^i) \tag{19}$$

In (16), $N_u(N)$ is the binomial coefficient,

$$N_u(N) = \begin{pmatrix} N+1 \\ 2 \end{pmatrix} = \frac{N(N+1)}{2} \tag{20}$$

Finally, the expressions for the low order moments are summarized as follows:

$$\begin{aligned} \dot{\mu}^{(0)}(t) &= G^{(0)}\mu^{(0)}(t) \\ \dot{\mu}^{(1)}(t) &= G^{(1)}\mu^{(1)}(t) + H^{(1)}\mu^{(0)}(t) \\ \dot{\mu}^{(2)}(t) &= \hat{G}^{(2)}\mu^{(2)}(t) + \hat{H}^{(2)}\mu^{(1)}(t) \end{aligned} \tag{21}$$

Distributions are usually described with means and variances. For a stochastic variable, $X$, the variance is derived from the uncentered second moment as follows

$$\sigma^2_{[X]} = \mu^{(2)} - (\mu^{(1)})^2 \tag{22}$$

Next, the derivation of the low order moments ($0^{th}$, $1^{st}$, and $2^{nd}$) is illustrated with a simple example.

*Example:* The solutions for the case of a 2-state, 2-mode system were discussed in [2]. The matrix representation for this small system is shown here.

For the $0^{th}$ order moment (occupational probabilities), the matrix representation of the ODE (6) is

$$\begin{bmatrix} \dot{\mu}_1^{(0)} \\ \dot{\mu}_2^{(0)} \end{bmatrix} = \begin{bmatrix} -\lambda_{12} & \lambda_{12} \\ \lambda_{21} & -\lambda_{21} \end{bmatrix}^T \begin{bmatrix} \mu_1^{(0)} \\ \mu_2^{(0)} \end{bmatrix} \tag{23}$$

The computation of equation (23) requires the knowledge of an initial condition. Let us assume that the system is in mode 2 at time $t = 0$, therefore the initial condition is $[0 \quad 1]^T$. The solution to (23) yields a $2 \times 1$ vector

$$\mu^{(0)} = e^{\Lambda' t} \, [0 \quad 1]^T \tag{24}$$

The evolution of the $1^{st}$ order moments is represented in the matrix equation (25)

$$\begin{bmatrix} \dot{\mu}_1^{(1,0)} \\ \dot{\mu}_1^{(0,1)} \\ \dot{\mu}_2^{(1,0)} \\ \dot{\mu}_2^{(0,1)} \end{bmatrix} = \left( \begin{bmatrix} a1_{11} & a1_{12} & 0 & 0 \\ a1_{21} & a1_{22} & 0 & 0 \\ 0 & 0 & a2_{11} & a2_{12} \\ 0 & 0 & a2_{21} & a2_{22} \end{bmatrix} + \begin{bmatrix} -\lambda_{11} & 0 & \lambda_{21} & 0 \\ 0 & -\lambda_{11} & 0 & \lambda_{21} \\ \lambda_{12} & 0 & -\lambda_{22} & 0 \\ 0 & \lambda_{12} & 0 & -\lambda_{22} \end{bmatrix} \right) \begin{bmatrix} \mu_1^{(1,0)} \\ \mu_1^{(0,1)} \\ \mu_2^{(1,0)} \\ \mu_2^{(0,1)} \end{bmatrix} + \begin{bmatrix} c1_1 & 0 \\ c1_2 & 0 \\ 0 & c2_1 \\ 0 & c2_2 \end{bmatrix} \begin{bmatrix} \mu_1^{(0,0)} \\ \mu_2^{(0,0)} \end{bmatrix} \tag{25}$$

The first order moment is a $n \times 1$ vector that represents the statistic means of the dynamic states, and is computed as

$$\mu^{(1)} = \begin{bmatrix} \mu_1^{(1,0)} + \mu_2^{(1,0)} \\ \mu_1^{(0,1)} + \mu_2^{(0,1)} \end{bmatrix} \tag{26}$$

The matrix equation of the $2^{nd}$ order moments (uncentered second moments) is too large to be include here, and instead is given as (1) in the appendix. The second order moment is an $n(n+1)/2 \times 1$ vector whose elements are the uncentered second moments of the dynamic states, and is computed as

$$\mu^{(2)} = \begin{bmatrix} \mu_1^{(2,0)} + \mu_2^{(2,0)} \\ \mu_1^{(0,2)} + \mu_2^{(0,2)} \\ \mu_1^{(1,1)} + \mu_2^{(1,1)} \end{bmatrix} \tag{27}$$

The computation of the ODEs (25) and (1) requires the knowledge of the transition matrix, which contains the transition rates between different stochastic modes. These rates are either calculated or evaluated based on empirical observations of the system. In this study, the transition rates are considered given. For a 3-mode system, the incoming and outgoing transition rates are represented by a $3 \times 3$ matrix

$$\Lambda_{trans} = \begin{bmatrix} 0 & \lambda_{12} & \lambda_{13} \\ \lambda_{21} & 0 & \lambda_{23} \\ \lambda_{31} & \lambda_{32} & 0 \end{bmatrix} \tag{28}$$

Notice that the diagonal elements are equal to zero. To obtain the full transition matrix, the self-transition elements $\lambda_{ii}$ are added in such a way that the sum of row elements is equal to zero. This matrix $\Lambda$ should not be confused with the Transition Probability Matrix (TPM) in a discrete-time Markov process where the sum of row elements is equal to 1. The full transition matrix is

$$\Lambda = \begin{bmatrix} -(\lambda_{12}+\lambda_{13}) & \lambda_{12} & \lambda_{13} \\ \lambda_{21} & -(\lambda_{21}+\lambda_{23}) & \lambda_{23} \\ \lambda_{31} & \lambda_{32} & -(\lambda_{31}+\lambda_{32}) \end{bmatrix} \tag{29}$$

## 4. RESULTS AND DISCUSSION

This section examines the results of both the MJLS analysis and the Monte Carlo simulations. The system of ODEs representing the evolution of the system statistics are solved in the time domain. The solutions represent the conditional moments of the dynamic and algebraic states. These results are compared to those obtained by averaging the solutions of 20,000 Monte Carlo simulations.

The numerical values of the state vectors corresponding to the three modes of the stochastic model are presented in the appendix section. The transition rates matrix is also provided in the appendix. Its values are representative of a slow switching system, with the states spending most of the time at the equilibrium operating points of the different stochastic modes and barely any time in-between.

Figures 4, 5, 6, 7, and 8 represent the averaged results of 20,000 Monte Carlo simulations and the solutions to the ODEs representing the evolution of the conditional moments. The averaged Monte Carlo solutions (red) are superimposed to the MJLS results (black) for comparison purposes.

Figure 4 shows the results for the zeroth moments (occupational probabilities). The averaged Monte Carlo simulations converge with great accuracy to the solutions of the MJLS (24).

The solutions for the first moments of the dynamic and algebraic states are represented in Figures (5) and (6). The Monte Carlo results converge pretty well to the MJLS solutions. However, small spikes are noticeable, which will be greatly exacerbated in the second moments plots, as it can be seen in Figures (7) and (8). This phenomena is due to

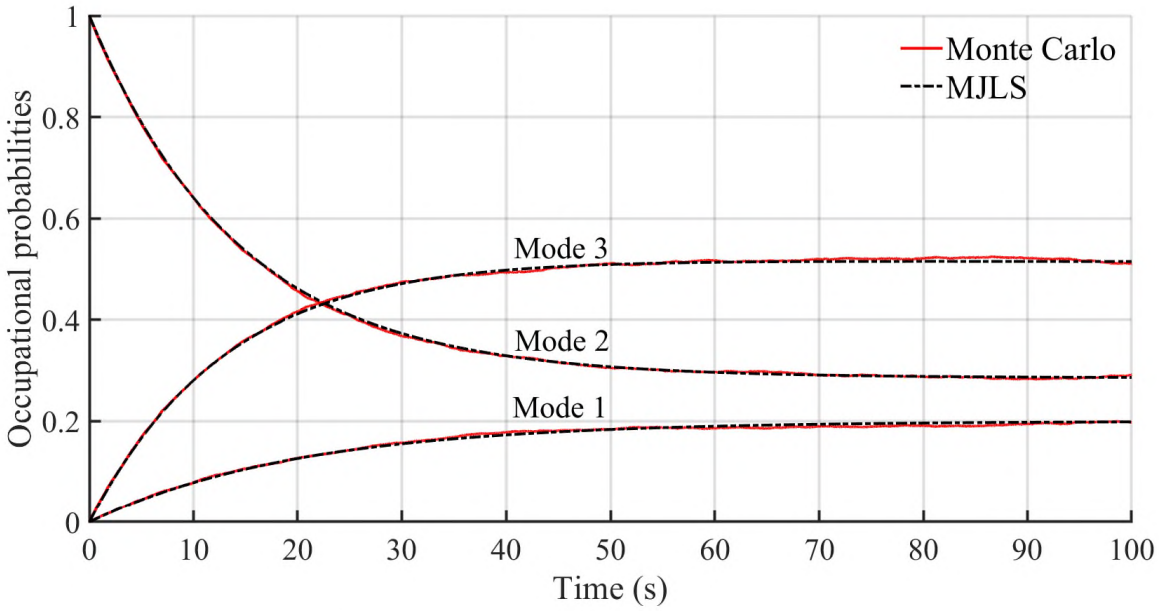


Figure 4. Zeroth moments: occupational probabilities

the way stochastic jumps are characterized in the model (6). In the Monte Carlo simulation, this translates to unbounded transient overshoots during switching between two stochastic modes. The jump term in the model represented by (6) needs to be refined to accurately represent transient events when the power system switches from one equilibrium point to another one.

## 5. CONCLUSION AND FUTURE WORK

A method based on the MJLS was applied to a microgrid operating in grid-tied and standalone operating modes. The microgrid is represented by the modified IEEE-37 bus power system, that includes seven inverters at selected bus locations. The ODEs representing the time evolution of the conditional moments were solved to derive the statistics of the system (zeroth, first and second moments). These solutions were compared to the results of the averaged Monte Carlo simulations. The objective was to demonstrate that the model developed in previous works [2, 7] also applies to a switching system and that the results

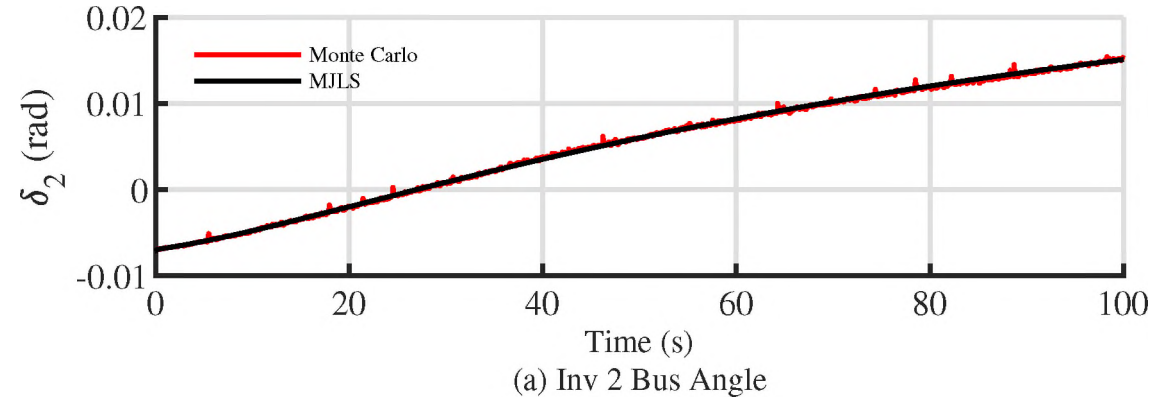


(a) Inv 2 Bus Angle

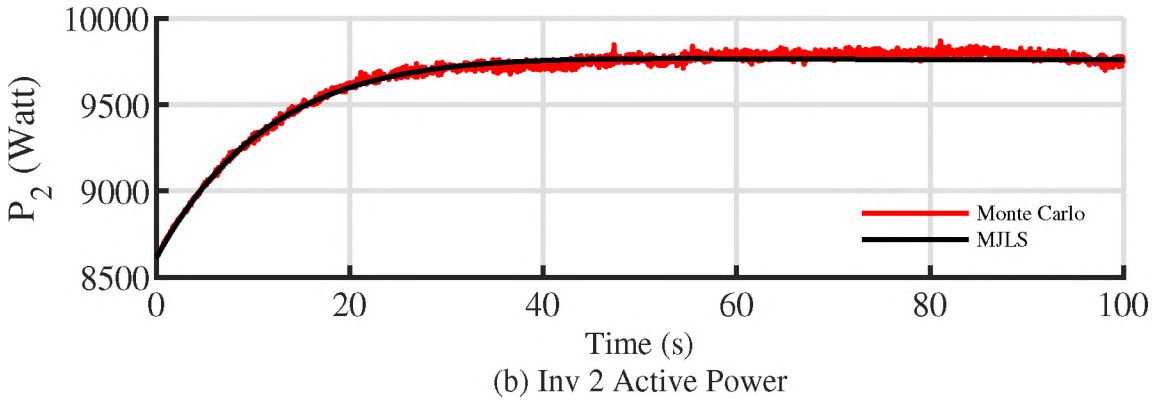


(b) Inv 2 Active Power

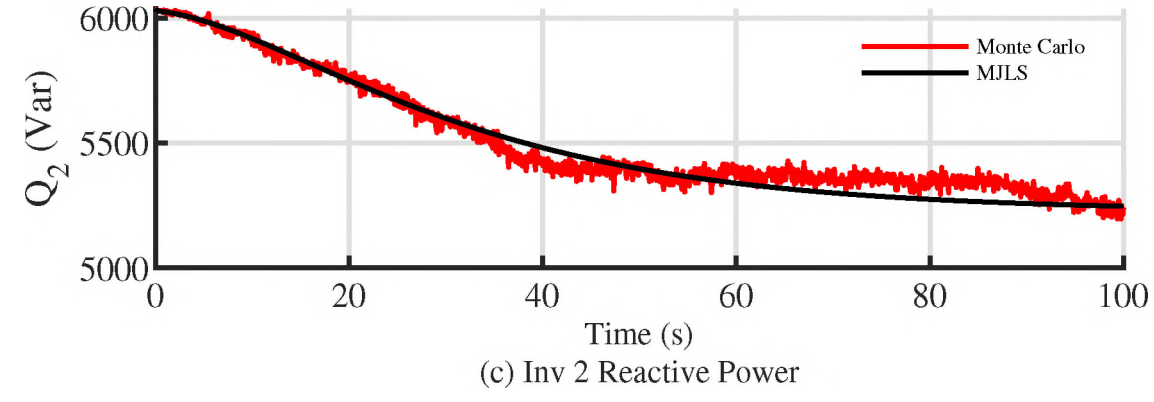


(c) Inv 2 Reactive Power

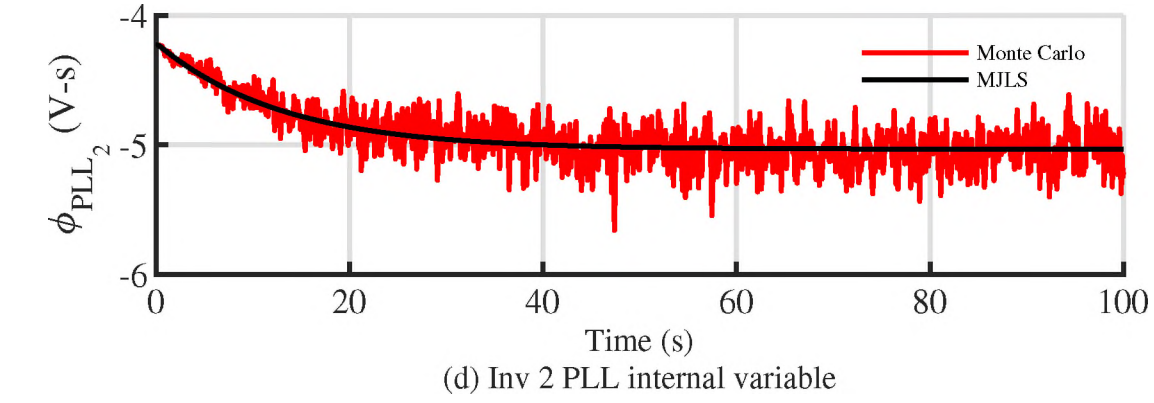


(d) Inv 2 PLL internal variable

Figure 5. A sample of first moments of the dynamic states

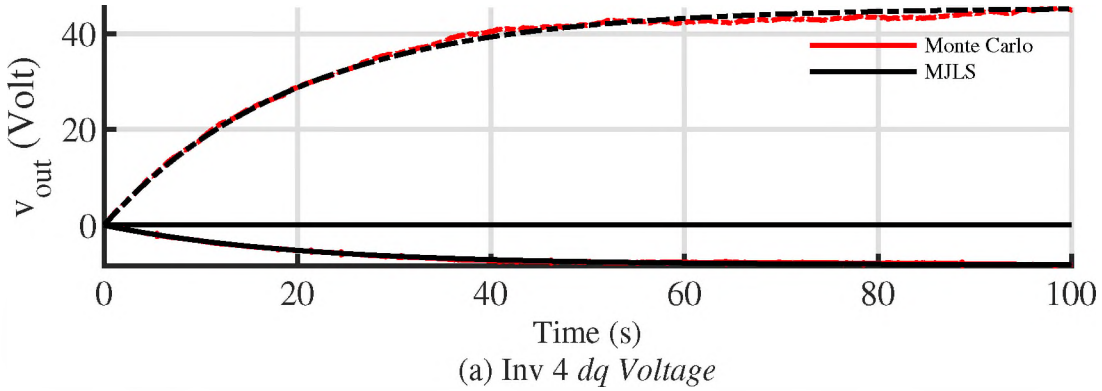


(a) Inv 4 *dq Voltage*

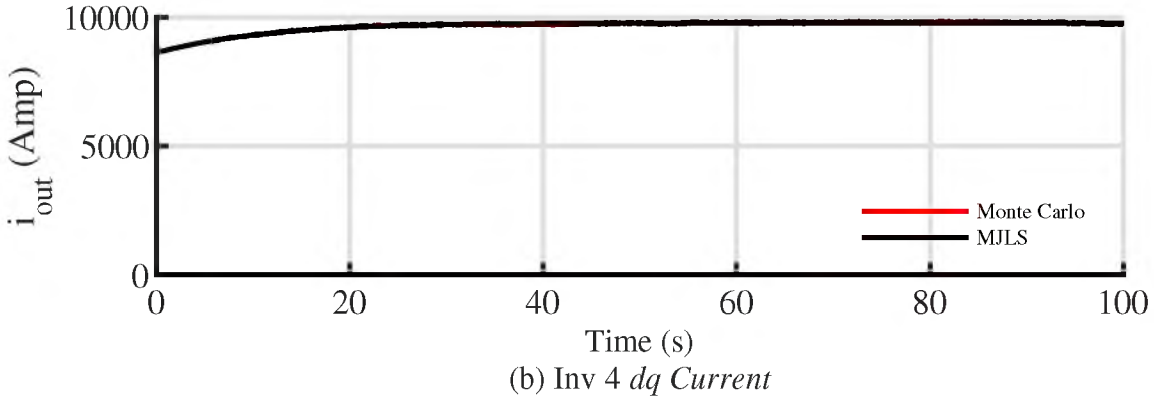


(b) Inv 4 *dq Current*

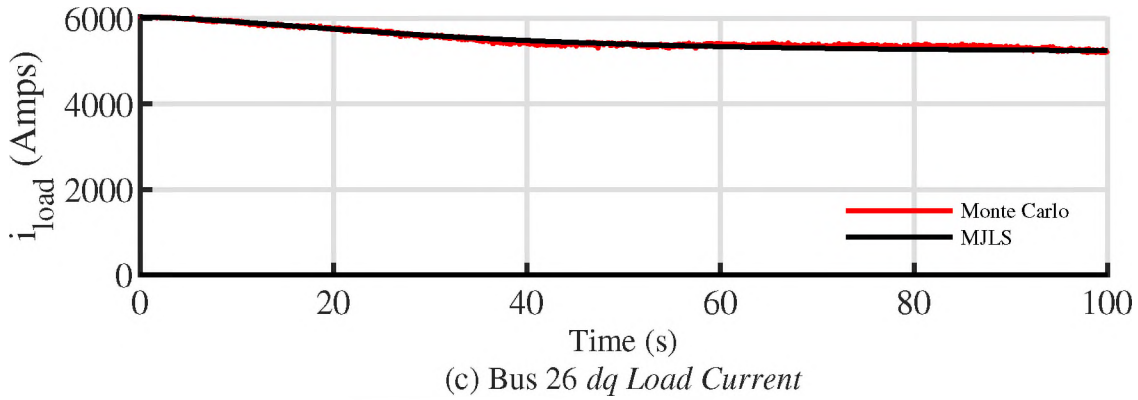


(c) Bus 26 *dq Load Current*

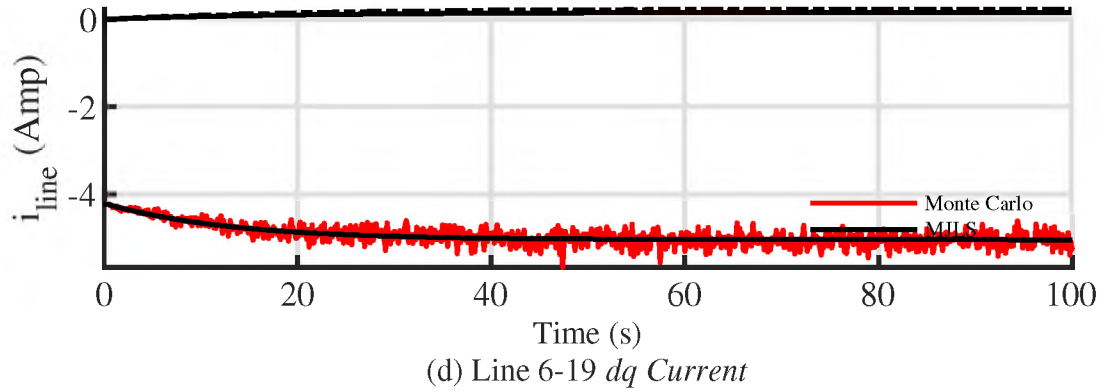


(d) Line 6-19 *dq Current*

Figure 6. A sample of first moments of the algebraic states

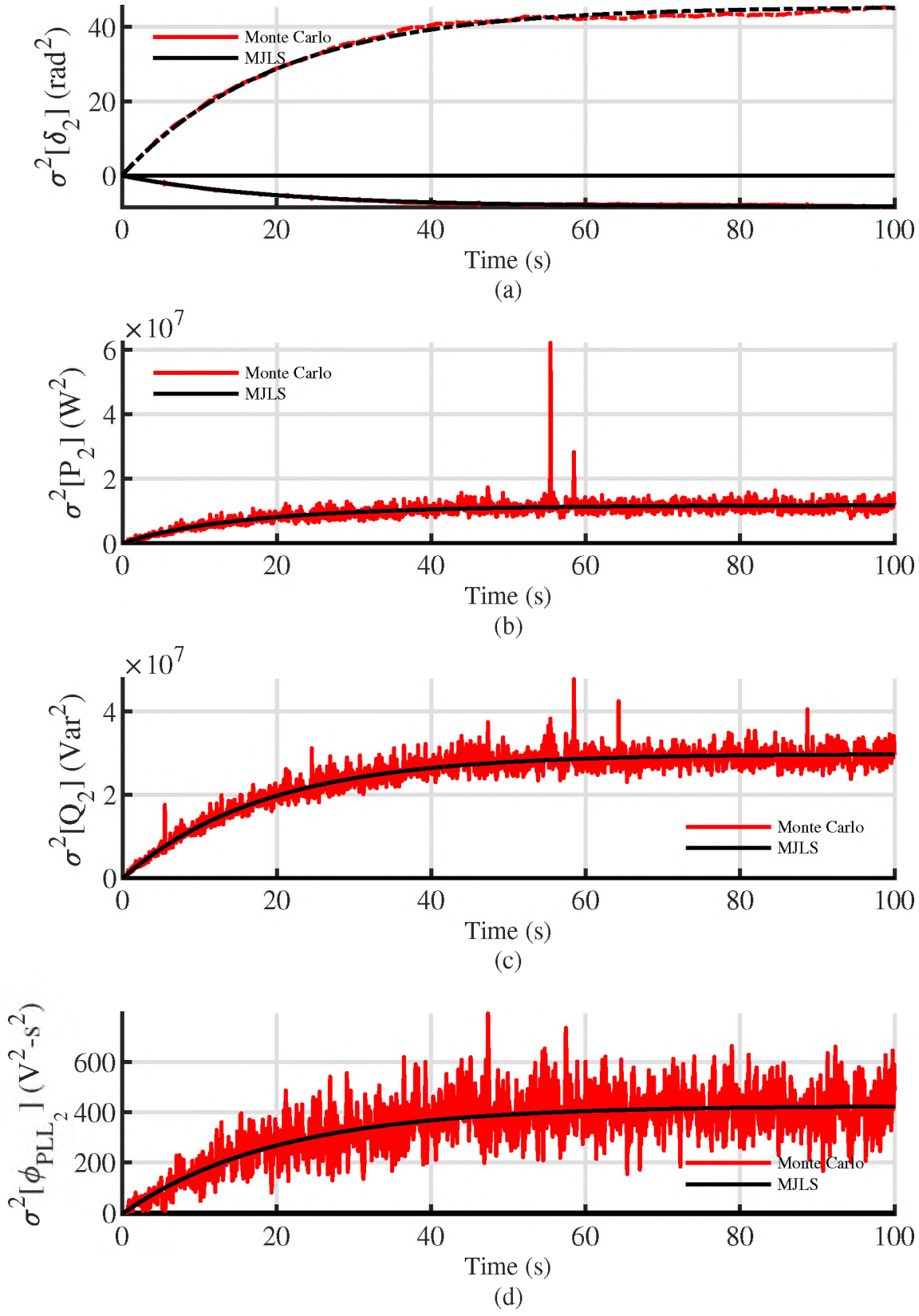


Figure 7. A sample of second moments of the dynamic states

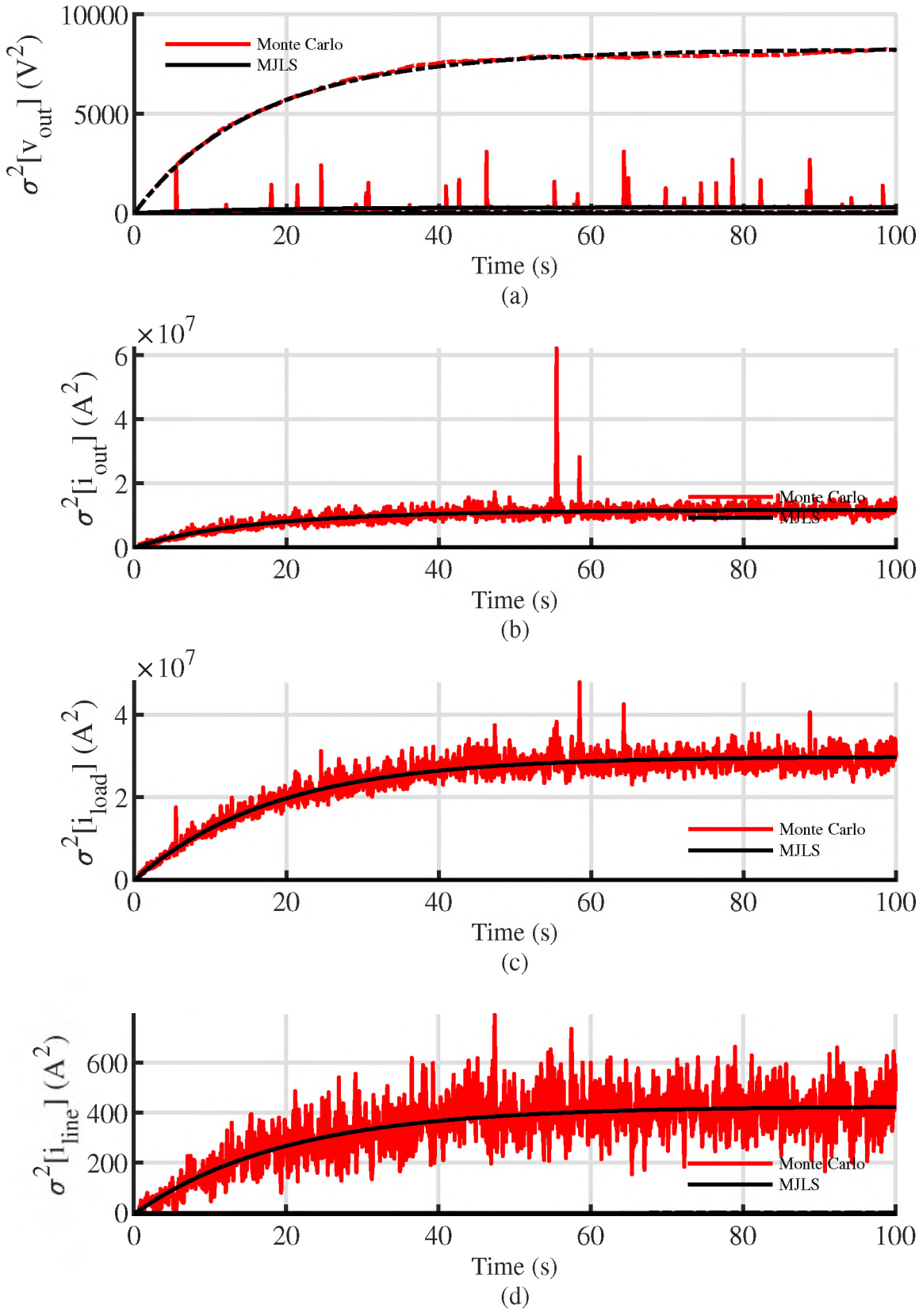


Figure 8. A sample of second moments of the algebraic states

remain valid for a larger system (56 dynamic states). It was observed that the averaged Monte Carlo simulations of the lower order conditional moments converge pretty well to the solutions of the MJLS. Avenues for future works include improving the model to better characterize the jumps between distinct operating modes and by doing so, eliminate the spikes that occur during the Monte Carlo simulation. Another study will focus on the stability of the system when subject to stochastic switching between distinct operating equilibrium points.

# APPENDIX A.

# SECOND ORDER MOMENT ODEs

The ODEs representing the evolution of the second order moments for a 2-state, 2-mode system are represented below

$$\begin{bmatrix} \dot{\mu}_1^{(2,0)} \\ \dot{\mu}_1^{(0,2)} \\ \dot{\mu}_1^{(1,1)} \\ \dot{\mu}_2^{(2,0)} \\ \dot{\mu}_2^{(0,2)} \\ \dot{\mu}_2^{(1,1)} \end{bmatrix} = \left( \begin{bmatrix} 2a1_{11} & 0 & 2a1_{12} & 0 & 0 & 0 \\ 0 & 2a1_{22} & 2a1_{21} & 0 & 0 & 0 \\ a1_{21} & a1_{12} & a1_{11}+a1_{22} & 0 & 0 & 0 \\ 0 & 0 & 0 & 2a2_{11} & 0 & 2a2_{12} \\ 0 & 0 & 0 & 0 & 2a2_{22} & 2a2_{21} \\ 0 & 0 & 0 & a2_{21} & a2_{12} & a2_{11}+a2_{22} \end{bmatrix} + \begin{bmatrix} -\lambda_{11} & 0 & 0 & \lambda_{21} & 0 & 0 \\ 0 & -\lambda_{11} & 0 & 0 & \lambda_{21} & 0 \\ 0 & 0 & -\lambda_{11} & 0 & 0 & \lambda_{21} \\ \lambda_{12} & 0 & 0 & -\lambda_{22} & 0 & 0 \\ 0 & \lambda_{12} & 0 & 0 & -\lambda_{22} & 0 \\ 0 & 0 & \lambda_{12} & 0 & 0 & -\lambda_{22} \end{bmatrix} \right) \begin{bmatrix} \mu_1^{(2,0)} \\ \mu_1^{(0,2)} \\ \mu_1^{(1,1)} \\ \mu_2^{(2,0)} \\ \mu_2^{(0,2)} \\ \mu_2^{(1,1)} \end{bmatrix} + \begin{bmatrix} 2c1_1 & 0 & 0 & 0 \\ 0 & 2c1_2 & 0 & 0 \\ c1_2 & c1_1 & 0 & 0 \\ 0 & 0 & 2c2_1 & 0 \\ 0 & 0 & 0 & 2c2_2 \\ 0 & 0 & c2_2 & c2_1 \end{bmatrix} \begin{bmatrix} \mu_1^{(1,0)} \\ \mu_1^{(0,1)} \\ \mu_2^{(1,0)} \\ \mu_2^{(0,1)} \end{bmatrix} \tag{1}$$

# APPENDIX B.

# NUMERICAL VALUES FOR THE SYSTEM UNDER STUDY

The transition rates matrix for the stochastic model is represented below

$$\lambda = \begin{bmatrix} -0.04 & 0.02 & 0.02 \\ 0.01 & -0.05 & 0.04 \\ 0.01 & 0.02 & -0.03 \end{bmatrix} \tag{1}$$

The state vectors for the three modes of the stochastic system are as follows

$$\begin{aligned} X1sp = [&0.054593; 0.1535; 101.2; -28.411; -0.28274; \\ &3.3159; -1381.6; -9531.5; 0.067361; 0.083983; 102.41; \\ &-12.402; -0.29516; 3.2348; 505.86; -4888.9; 0.076545; \\ &0.026086; 105.42; 0.84976; -0.30503; 3.1674; 2595.3; \\ &-1038.8; 0.066538; 0.046265; 106.07; -4.1122; -0.3021; \\ &3.1459; 2070.1; -2448; 0.066959; 0.021063; 108.54; \\ &1.623; -0.30833; 3.0967; 3222.5; -756.5; 0.061937; \\ &0.061937; 0.0026639; 110.71; 5.0832; -0.31835; 3.0575; \\ &4159.9; 396.33; 0.062938; -0.0050023; 112.82; 7.4309; \\ &-0.31733; 3.0143; 4658.6; 974.77]^T \end{aligned} \tag{2}$$

$$X2sp = [0; -4.2281; 0.57922; 0.73305; -0.297; 3.0808; 8634.6; 7499.7; -0.0071639; -4.2289; 0.44488; 0.72922; -0.31123; 3.0955; 8621.1; 6041.3; -0.01641; -4.23; 0.30195; 0.72508; -0.32647; 3.1115; 8589.9; 4482.5; -0.017274; -4.2299; 0.38662; 0.72879; -0.31791; 3.1031; 8595.1; 5418.7; -0.025885; -4.2305; 0.307; 0.72557; -0.32627; 3.1114; 8585; 4542.7; -0.046846; -4.2326; 0.10269; 0.72126; -0.34661; 3.1387; 8454.6; 2234.6; -0.035132; -4.2311; 0.26683; 0.72391; -0.33086; 3.1156; 8581.8; 4110.7]^T \quad (3)$$

$$X3sp = [0; -5.8204; 0.95561; 1.0018; -0.25278; 3.0486; 11932; 11591; -0.017088; -5.8224; 0.6683; 0.99312; -0.28371; 3.0821; 11866; 8532.7; -0.037865; -5.8248; 0.37074; 0.98493; -0.31642; 3.1183; 11782; 5318.1; -0.035314; -5.8242; 0.56114; 0.99138; -0.296; 3.0962; 11820; 7392.1; -0.048431; -5.8251; 0.46465; 0.98727; -0.30661; 3.1066; 11812; 6349.4; -0.085731; -5.829; 0.11172; 0.97846; -0.34325; 3.1546; 11597; 2402.5; -0.073223; -5.8269; 0.28715; 0.98276; -0.32642; 3.129; 11747; 4415.6]^T \quad (4)$$

## REFERENCES


[1] L. Luo and S. V. Dhople, "Spatiotemporal model reduction of inverter-based islanded microgrids," *IEEE Transactions on Energy Conversion*, vol. 29, no. 4, pp. 823–832, 2014.

[2] S. V. Dhople, Y. C. Chen, L. DeVille, and A. D. Dominguez-Garcia, "Analysis of power system dynamics subject to stochastic power injections," *IEEE Transactions on Circuits and Systems I: Regular Papers*, vol. 60, no. 12, pp. 3341–3353, 2013.

[3] S. Dhople, L. DeVille, and A. Dominguez-Garcia, "A stochastic hybrid systems framework for analysis of markov reward models," *Reliability Engineering & System Safety*, vol. 123, pp. 158–170, 2014.

[4] Y. Xu, F. Wen, H. Zhao, M. Chen, Z. Yang, and H. Shang, "Stochastic small signal stability of a power system with uncertainties," *Energies*, vol. 11, no. 11, p. 2980, 2018.

[5] A. Hirsch, Y. Parag, and J. Guerrero, "Microgrids: A review of technologies, key drivers, and outstanding issues," *Renewable & sustainable energy reviews*, vol. 90, pp. 402–411, 2018.

[6] T. C. Green and M. Prodanović, "Control of inverter-based micro-grids," *Electric Power Systems Research*, vol. 77, no. 9, pp. 1204–1213, 2007.

[7] J. A. Mueller and J. W. Kimball, "Modeling and analysis of dc microgrids as stochastic hybrid systems," *IEEE Transactions on Power Electronics*, pp. 1–1, 2021.

[8] J. Hespanha, "Modelling and analysis of stochastic hybrid systems," *IEE Proceedings - Control Theory and Applications*, vol. 153, no. 5, pp. 520–535, 2006.

[9] O. L. V. Costa, M. G. Todorov, M. D. Fragoso, and S. O. service), *Continuous-Time Markov Jump Linear Systems*. Berlin, Heidelberg: Springer Berlin Heidelberg, 2013.

[10] M. Rasheduzzaman, J. A. Mueller, and J. W. Kimball, "An accurate small-signal model of inverter- dominated islanded microgrids using *dq* reference frame," *IEEE Journal of Emerging and Selected Topics in Power Electronics*, vol. 2, no. 4, pp. 1070–1080, 2014.

[11] M. Rasheduzzaman, J. Mueller, and J. W. Kimball, "Reduced-order small-signal model of microgrid systems," *IEEE Transactions on Sustainable Energy*, vol. 6, no. 4, pp. 1292–1305, 2015.

[12] P. Hespanha, "Modeling and analysis of networked control systems using stochastic hybrid systems," *Annual Reviews in Control*, vol. 38, no. 2, pp. 155–170, 2014.

[13] V. Mariani, F. Vasca, J. C. Vasquez, and J. M. Guerrero, "Model order reductions for stability analysis of islanded microgrids with droop control," *IEEE Transactions on Industrial Electronics*, vol. 62, no. 7, pp. 4344–4354, 2015.

[14] A. Teel, L. Moreau, and D. Nesic, "A unified framework for input-to-state stability in systems with two time scales," *IEEE Transactions on Automatic Control*, vol. 48, no. 9, pp. 1526–1544, 2003.

[15] J. P. Hespanha, "A model for stochastic hybrid systems with application to communication networks," *Nonlinear Analysis: Theory, Methods & Applications*, vol. 62, no. 8, pp. 1353–1383, 2005.

[16] D. T. Gillespie, "Exact stochastic simulation of coupled chemical reactions," *The Journal of Physical Chemistry*, vol. 81, pp. 2340–2361, 1977.

[17] G. Mpembele and J. Kimball, "Analysis of a standalone microgrid stability using generic markov jump linear systems," in *2017 IEEE Power and Energy Conference at Illinois (PECI)*, Feb 2017, pp. 1–8.

[18] G. Mpembele and J. W. Kimball, "A matrix representation of a markov jump linear system applied to a standalone microgrid," in *2018 9th IEEE International Symposium on Power Electronics for Distributed Generation Systems (PEDG)*, June 2018, pp. 1–8.

# II. JUMP-DIFFUSION MODELING OF A MARKOV JUMP LINEAR SYSTEM WITH APPLICATIONS IN MICROGRIDS

Gilles Mpembele and Jonathan W. Kimball
Department of Electrical & Computer Engineering
Missouri University of Science and Technology
Rolla, Missouri 65409–0050
Email: gmhn7@umsystem.edu

## ABSTRACT

This paper proposes a jump-diffusion model for the analysis of a microgrid operating in grid-tied and standalone modes. The model framework combines a linearized power system dynamic model with a continuous-time Markov chain (CTMC). The power system has a stochastic input modeled with a one-dimensional Wiener process and multiplicative diffusion coefficient. The CTMC gives rise to a compound Poisson process that represents jumps between different operating modes. Starting from the resulting stochastic differential equation (SDE), the proposed approach uses Itô calculus and Dynkin's formula to derive a system of ordinary differential equations (ODEs) that describe the evolution of the moments of the system. The approach is validated with the IEEE 37-bus system modified to form a microgrid. The results match a Monte Carlo simulation but with far lower computational complexity. In addition, the ODEs are amenable to further analysis, such as stability analysis and determination of operational bounds.

**Keywords:** Jump-Diffusion, Markov Jump Linear Systems (MJLSs), Monte Carlo simulations, Power System statistics, Stochastic Differential Equation (SDE), Stochastic Hybrid Systems (SHSs).

# 1. INTRODUCTION

The stochastic jump-diffusion model is well suited to dynamic systems subject to random disturbances of a limited amplitude, as well as to random and abrupt perturbations of a relatively higher magnitude [1]. Disturbances of limited (small) amplitude correspond to the diffusion component of the model and are described using the Wiener process. Higher (large) magnitude disturbances apply to the jump component of the model and are represented by the Poisson process [1, 2, 3]. The objective of this study is to develop such jump-diffusion model for a microgrid that oscillates between standalone (islanded) and grid-tied operating modes. Preceding works focused on deterministic systems controlled by stochastic inputs of the jump type [4, 5] and, in other cases, on stochastic systems subject to switching behaviors of a pure-jump type [6, 7]. This work extends previous models: 1) the *entire system* is considered switching between distinct stochastic modes, 2) this switching behavior involves *all dynamic and algebraic states*, and not just the system inputs as in [4, 5], 3) the modeling of the stochastic process includes a *Wiener process* as well *Poisson jump processes* in the derivation of the ordinary differential equations that govern the evolution of the system statistics.

The jump-diffusion model finds many applications in finance to describe the dynamics of market variables such as stock pricing, asset and commodity prices, credit ratings, exchange rates, etc [1]. The mathematical framework for stochastic models was first developed for the finance industry, and to this day, most publications remain in this area. The theory has also been successfully applied to biology and chemistry [3], and more generally to any areas that involves random quantities.

The application of stochastic models to the analysis of the dynamics of power systems is relatively new [4, 8]. This representation is particularly relevant for a class of stochastic processes called Stochastic Hybrid Systems (SHSs). In this framework, the linearized power system dynamic model is combined with discrete transitions of the system variables triggered by stochastic events [9, 10, 11, 4, 5, 7]. The linearized model is represented by a

system of differential algebraic equations (DAEs) that includes the evolution of the dynamic states, and of the output variables expressed as a linear combination of the dynamic states and the control variables [4, 7, 5]. In a particular class of SHSs called Markov Jump Linear Systems (MJLSs), the stochastic discrete transitions of the system are explicitly modeled as continuous time Markov chains. The jump-diffusion model developed in this study is based on the Markovian property of the jumps, appropriately supplied by a Poisson process, while the diffusion component is supplied by a Wiener process.

For a microgrid, a jump in a dynamic state is defined as a variation of significant magnitude that cannot be represented by a linear drift or a noise perturbation. For instance, when an abrupt change occurs in the loading condition or in the characteristics of distributed power sources, and because of the finite and limited inertia of the system, the bus voltages and the system frequency can experience drastic variations that, in the absence of adequate control, could result in instabilities and even in the collapse of the entire system [12, 7]. In the context of this paper, discrete jumps result in the switching of the microgrid between one grid-tied operating mode and two distinct standalone (islanded) operating modes. The difference between the two standalone modes results from a difference in load conditions and corresponds to two distinct sets of dynamic states and output variables [7, 13].

Figure 1 shows bus voltages and load currents at an arbitrary bus (labeled 26) of the IEEE 37-bus microgrid. In Figure 2, inverter 2's active and reactive powers are represented. These plots were obtained from a Simulink®/PLECS® simulation of the IEEE 37-bus microgrid and from results from an experimental testbed [14]. A one-line diagram of the IEEE 37-bus power system is presented in the appendix.

The derivation of a small-signal model of an inverter-based microgrid system was carried out in [14]. For the IEEE 37-bus microgrid, the resulting state space model is of the $225^{th}$ order and represent a two-time scale system where states with slow dynamics are mixed with those with fast dynamics [15, 7]. A reduction method based on the singular perturbation technique was presented in [16, 15, 17]. In the case of the $225^{th}$ order

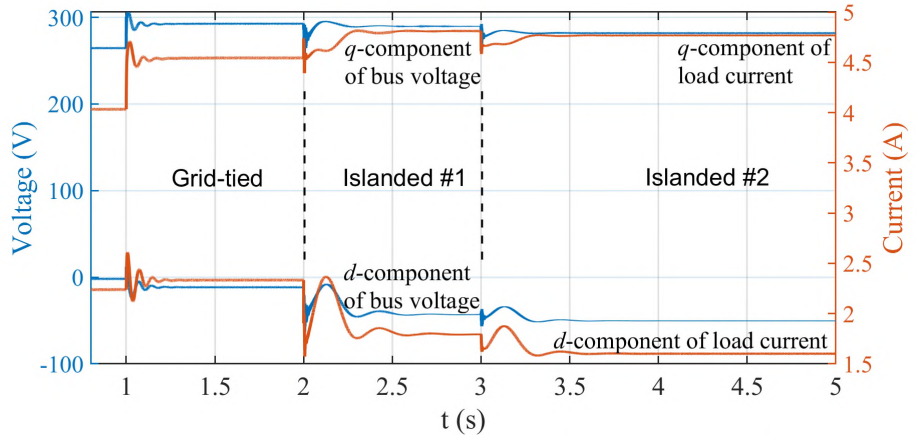


Figure 1. Voltage and Load current at bus 26

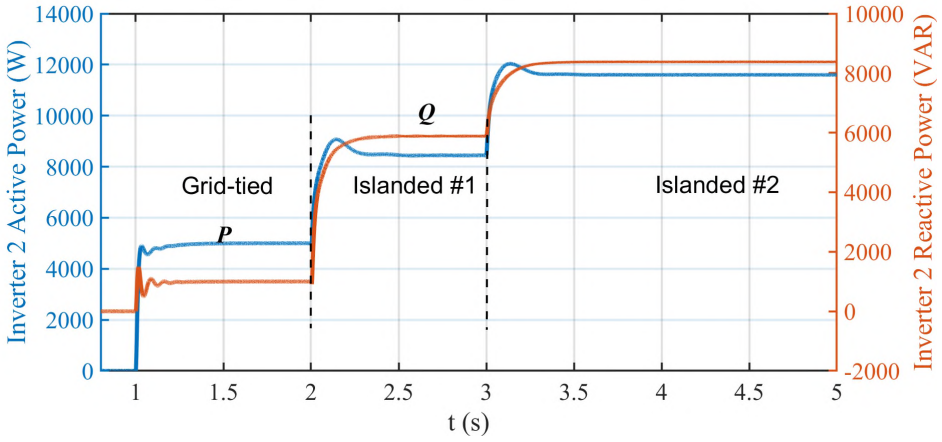


Figure 2. Inverter 2 Active Power and Reactive Power

system (IEEE 37-bus system), the technique allowed to reduce the system to the $56^{th}$ order by eliminating the fast states. Accuracy of this method was evaluated in [15], where the system's dynamic response was evaluated in grid-tied and islanded modes, as well as during transitions between the two modes. Results obtained using the reduced model were found to match experimental results from a hardware testbed [15].

A SHS model for a power system was developed in [4] to represent the dynamic behavior of a system subject to stochastic inputs. The resulting ODEs representing the evolution of the conditional moments were derived using stochastic inputs and did not include random variations of the Wiener type. This model was used in [7] for a system

switching between different equilibrium points. It was shown in [5, 18, 7] that a matrix representation of the system can be used along with analytical tools to compute the system statistics. In this study, the model is adapted for a slow-switching system, and includes a Wiener process component. The derivation of the model is carried out directly from the jump-diffusion stochastic differential equation (SDE), rather than from the SHS framework as in [4, 6, 7].

This paper is organized as follows. In section 2, the development of a jump-diffusion model of a power system is presented. In section 3, the Dynkin's formula is applied to the Itô formula of the Stochastic Differential Equation to derive the ODEs that represent the evolution of the system statistics. In section 4, a numerical application of the jump-diffusion model to the IEEE-37 bus microgrid system is discussed. A conclusion and avenues for future work are presented in Section 5.

## 2. JUMP-DIFFUSION MODEL OF A POWER SYSTEM

Let $X = \{X(t),\ t \geq 0\}$ be a one-dimensional continuous stochastic process. In the most general sense, a jump-diffusion process can be represented by a stochastic differential equation with jumps

$$\begin{aligned} dX(t) = f\big(t, X(t)\big)dt + g\big(t, X(t)\big)dW(t) \\ + h\big(t, X(t-)\big)dN(t) \end{aligned} \tag{1}$$

for $t \geq 0$ with initial value $X(0) = X_0$. Here, $W = \{W(t),\ t \geq 0\}$ represents a standard Wiener process and $N = \{N(t),\ t \geq 0\}$ a Poisson process with intensity $\lambda$. The processes $f$, $g$, and $h$ are called respectively drift, diffusion, and jump coefficient functions. These coefficient functions could be deterministic, time dependent and non linear, in general. In accordance with power system models, this study considers deterministic, state dependent and linear coefficient functions. Furthermore, the existence and uniqueness of the solution

to the SDE (1) are guaranteed only if the drift, diffusion and jump coefficient functions satisfy the Lipschitz conditions, as well as the linear growth conditions, the definition of which can be found in [1, 19, 20].

When given in the differential form, the SDE (1) is considered an informal or short hand notation for its integral form. The integral form yields the solution to (1) and is called an Itô process with jumps or a jump-diffusion process

$$\begin{aligned} X(t) =& X_0 + \int_0^t f(s, X(s))ds + \int_0^t g(s, X(s))dW(s) \\ &+ \sum_{k=1}^{N(t)} h\big(\tau_k, X(\tau_k-)\big) \end{aligned} \tag{2}$$

The first integral is an ordinary Riemann integral. The second integral is an Itô integral with respect to the Wiener process $W(t)$. The third term represents a compound Poisson process where, as noted above, $\{N(t),\ t > 0\}$ is a Poisson process with intensity $\lambda$.

In a Poisson process, jumps occur at discrete times $\tau_k \in \{\tau_1, \tau_2, ..., \tau_{N(t)}\}$ where $\tau_{N(t)} \leq t$. These jump times are exponentially distributed with parameter[1] $\lambda > 0$ and density $\lambda e^{\lambda\tau_i}$. The probability for a Poisson process $N(t)$ to be equal to $k$ (in other words, the probability to obtain $k$ jumps between time 0 and time $t$) is given by

$$P(N(t) = k) = \frac{(\lambda t)^k}{k!} e^{-\lambda t} \tag{3}$$

It results from (3) that for a Poisson process $N(t)$ with intensity $\lambda$ and for $t \geq 0$, the mean [1]

$$\mu(t) = E\big[N(t)\big] = \lambda t \tag{4}$$

and the variance [1]

$$Var(N(t)) = E\Big[\big(N(t) - \mu(t)\big)^2\Big] = \lambda t \tag{5}$$

[1]Also called jump intensity, transition intensity, or transition rate.

In (2), $\{h(\tau_k, X_{\tau_k-}),\ k > 0\}$ is a family of independent and identically distributed (i.i.d) random variables (independent of $N$) called jump sizes.

The notation $X_{\tau_k}-$ corresponds to the almost sure left-hand limit of $X(t)$ at time $\tau_k$, and if a jump occurred at time $\tau_k$, the jump size is defined as

$$\Delta X(\tau_k) = X(\tau_k) - X(\tau_k-) \tag{6}$$

The generalization of (1) and (2) to a multidimensional system is straightforward. The evolution of the stochastic vector $\boldsymbol{X} = \{\boldsymbol{X}(t) \in \mathbb{R}^n,\ t \geq 0\}$, is described by an $n$-dimensional SDE with jumps [1]

$$\begin{aligned} d\boldsymbol{X}(t) = f(t, \boldsymbol{X}(t))dt + g(t, \boldsymbol{X}(t))d\boldsymbol{W}(t) \\ + \sum_{\ell=1}^{d} h^{\ell}(t, \boldsymbol{X}(t-))dN^{\ell}(t) \end{aligned} \tag{7}$$

for $t \in [0, T]$, with initial value $\boldsymbol{X_0} \in \mathbb{R}^n$, an $q$-dimensional Wiener process $\boldsymbol{W} = \{\boldsymbol{W}(t) = W^1(t), ..., W^q(t)\}$, $t \in [0, T]$ and $d$ independent compound Poisson processes, $N^{\ell}$, with parameters $\lambda_{\ell}$, $\ell = 1, ..., d$, and jump sizes $h^{\ell}(t, \boldsymbol{X}(t-))$.

The integral form is derived from (7) as

$$\begin{aligned} \boldsymbol{X}(t) = \boldsymbol{X_0} + \int_0^t f(s, \boldsymbol{X}(s))ds + \int_0^t g(s, \boldsymbol{X}(s))d\boldsymbol{W}(s) \\ + \sum_{\ell=1}^{d} \sum_{k=1}^{N^{\ell}(t)} h^{\ell}\left(\tau_k, \boldsymbol{X}(\tau_k-)\right) \end{aligned} \tag{8}$$

To develop a jump-diffusion model for a microgrid system, the conventional dynamic model needs to be cast into the stochastic differential equation with jumps defined by (7). The deterministic dynamic model is represented by the differential algebraic equation (DAE) [5, 4]

$$\begin{aligned} \dot{x} &= f(x, y, u) \\ 0 &= g(x, y, u) \end{aligned} \tag{9}$$

where $x(t) \in \mathbb{R}^n$ is referred to as the dynamic states; $y(t) \in \mathbb{R}^v$ denotes the algebraic states or outputs of the system; and $u(t) \in \mathbb{R}^w$ represents the inputs of the system.

The linearization of (9) around a given stable equilibrium point results in a linear affine model [5, 4]

$$\begin{aligned} \dot{x} &= Ax + Bu + C \\ y &= Dx + Eu + F \end{aligned} \tag{10}$$

Following [7, 14, 15], the equilibrium points correspond to the steady-state operating points of a microgrid operating in grid-tied mode ($\boldsymbol{X}_1$) or in two distinct standalone modes ($\boldsymbol{X}_2, \boldsymbol{X}_3$). The difference between the two standalone modes is based on different load conditions on the system. The affine term, $C$, is defined in such a way that small variations are modelled around the equilibrium points $X_1, X_2, X_3$

$$C = -A_i X_i, \quad i = 1, 2, 3 \tag{11}$$

In the output equation, $F$ is set to zero: the outputs depend on the dynamic states and input vector.

The first step in developing a stochastic model for a power system is to convert the deterministic variables in equation (10) into stochastic variables

$$\begin{aligned} d\boldsymbol{X}(t) &= (A(t)\boldsymbol{X}(t) + B(t)\boldsymbol{U}(t) + C(t))\, dt \\ \boldsymbol{Y}(t) &= D(t)\boldsymbol{X}(t) + E(t)\boldsymbol{U}(t) \end{aligned} \tag{12}$$

To establish a correspondence between (7) and (12), the state equation of the dynamic model is cast as the drift term of the SDE with jumps, i.e.,

$$f(\boldsymbol{X}(t),t) = A(t)\boldsymbol{X}(t) + B(t)\boldsymbol{U}(t) + C(t) \tag{13}$$

The diffusion term is modeled as a multiplicative diffusion component, with a noise generated ripple proportional to the dynamic state. The diffusion coefficient is adequately chosen to limit the ripple to about 10% of the steady-state value of the dynamic state,

$$g(\boldsymbol{X}(t),t) = \beta\boldsymbol{X}(t) \tag{14}$$

where $\beta = 0.1$.

For the jump term of a slow switching system, the states spend most of the time at the stable operating points of the different modes and barely any time in-between. The system jumps from one operating mode to another with $t_{jump} \rightarrow 0$, and the jump size

$$h\big(t, \boldsymbol{X}(t-)\big) = \boldsymbol{X}(t) - \boldsymbol{X}(t-) \tag{15}$$

where $\boldsymbol{X}(t)$ is set to the steady-state operating point corresponding to the destination mode (*i.e. mode the system has jumped to*), and $\boldsymbol{X}(t-)$ is the value of the dynamic state just prior to the jump event

With all the terms of the SDE (7) defined, the jump-diffusion model of a power system based on the deterministic model (10) can now be represented by the SDE with jumps

$$\begin{aligned} d\boldsymbol{X}(t) = &\big[A_i(t)\big(\boldsymbol{X}(t) - \boldsymbol{X}_i(t)\big) + B_iU_i(t)\big]dt + \beta\boldsymbol{X}(t)dW(t) \\ &+ \sum_{\ell=1}^{d} \big(\boldsymbol{X}(\tau_k) - \boldsymbol{X}(\tau_k-)\big)dN^{\ell}(t) \end{aligned} \tag{16}$$

where $W(t)$ is a one-dimensional Wiener process[2] and $N^{\ell}$, $\ell = 1, ..., d$, represents the $\ell^{th}$ Poisson process with intensity $\lambda_{\ell}$, and $i \in \{1, 2, 3\}$ represents the system operating mode.

[2]A one-dimensional Wiener process is used here to simplify the equations, without loss of generality.

# 3. DERIVATION OF THE CONDITIONAL MOMENTS

The procedure to derive the conditional moments include the following steps:

- Derivation of the Itô formula for the SDE with jumps
- Application of the Dynkin's formula to the Itô formula
- Derivation of the conditional moments dynamics
- Derivation of a matrix representation

## 3.1. ITÔ FORMULA FOR THE SDE WITH JUMPS

The aim of this sub-section is to derive the expression of the stochastic differential equation for a process that is function of the solution of equation (7). In a more formal way, the problem can be stated as follows:

Given a stochastic differential equation with jumps of the type (7), and a process $\psi(t)$ which is a function of $\boldsymbol{X}(t)$

$$\psi = \psi(t, \boldsymbol{X}(t)) \tag{17}$$

where the function $\psi(t, \boldsymbol{X}(t))$ is continuously differentiable in $t$ and twice continuously differentiable in $\boldsymbol{X}$, determine the stochastic differential equation for the process $\psi(t)$

$$\begin{aligned} d\psi(t, \boldsymbol{X}(t)) = \tilde{f}(t, \boldsymbol{X}(t))dt + \tilde{g}(t, \boldsymbol{X}(t))d\boldsymbol{W}(t) \\ + \tilde{h}(t, \boldsymbol{X}(t-))d\boldsymbol{N}(t) \end{aligned} \tag{18}$$

Equation (18) is called the Itô formula (or Itô rule) and the definitions of the coefficient functions $\tilde{f}$, $\tilde{g}$, $\tilde{h}$ are based on the rules of the stochastic calculus. The Itô formula is the equivalent to the chain rule in classical calculus and it can be interpreted as a stochastic generalization of the fundamental theorem of calculus. It is used to quantify the changes in $\psi(t, \boldsymbol{X}(t))$ that are caused by changes in $\boldsymbol{X}(t)$.

To derive the Itô formula, equation (18) is first considered without the jump term. The process begins with a one-dimensional stochastic variable $X(t)$, which will be generalised afterwards to the multi-dimensional case. The Taylor expansion of $\psi\big(t, X(t)\big)$ is as follows

$$\begin{aligned} d\psi\big(t, X(t)\big) &= \psi\big(t + dt, X(t) + dX(t)\big) - \psi\big(t, X(t)\big) \\ &= \frac{\partial \psi\big(t, X(t)\big)}{\partial t} dt + \frac{1}{2} \frac{\partial^2 \psi\big(t, X(t)\big)}{\partial t^2} dt^2 \\ &+ \frac{\partial \psi\big(t, X(t)\big)}{\partial x} dX + \frac{1}{2} \frac{\partial^2 \psi\big(t, X(t)\big)}{\partial x^2} dX^2 \\ &+ h.o.t. \end{aligned} \tag{19}$$

Inserting the expression of the one-dimensional $dX(t)$ (equation (1) without the jump term) yields

$$\begin{aligned} d\psi(t, X(t)) &= \frac{\partial \psi\big(t, X(t)\big)}{\partial t} dt + \frac{1}{2} \frac{\partial^2 \psi\big(t, X(t)\big)}{\partial t^2} dt^2 \\ &+ \frac{\partial \psi\big(t, X(t)\big)}{\partial x} \Big( f(t, X(t)) dt + g(t, X(t)) dW(t) \Big) \\ &+ \frac{1}{2} \frac{\partial^2 \psi\big(t, X(t)\big)}{\partial x^2} \Big( f(t, X(t)) dt + g(t, X(t)) dW(t) \Big)^2 \\ &+ h.o.t. \end{aligned} \tag{20}$$

After neglecting higher order terms and with the help of stochastic calculus rules ($dW^2(t) = dt$, $dt^2 = 0$, $dtdW = 0$), it results the Itô formula for an SDE (one-dimensional), without the jump term

$$\begin{aligned} d\psi(t, X(t)) &= \left( \frac{\partial \psi\big(t, X(t)\big)}{\partial t} + \frac{\partial \psi\big(t, X(t)\big)}{\partial x} f\big(t, X(t)\big) \right. \\ &\left. + \frac{1}{2} \frac{\partial^2 \psi\big(t, X(t)\big)}{\partial x^2} g^2(t, X(t)) \right) dt \\ &+ \frac{\partial \psi\big(t, X(t)\big)}{\partial x} g\big(t, X(t)\big) dW(t) \end{aligned} \tag{21}$$

The addition of the jump term results in

$$d\psi(t,X(t)) = \left(\frac{\partial\psi\left(t,X(t)\right)}{\partial t} + \frac{\partial\psi\left(t,X(t)\right)}{\partial x} f\left(t,X(t)\right) + \frac{1}{2}\frac{\partial^2\psi\left(t,X(t)\right)}{\partial x^2} g^2(t,X(t))\right)dt + \frac{\partial\psi\left(t,X(t)\right)}{\partial x} g\left(t,X(t)\right)dW(t) + \sum_{\ell=1}^{d}\left(\psi\left(t,X(t)\right) - \psi\left(t-,X(t-)\right)\right)dN^{\ell}(t) \tag{22}$$

The generalization of (22) to the multidimensional case yields

$$d\psi(t,\boldsymbol{X}(t)) = \left(\frac{\partial\psi\left(t,\boldsymbol{X}(t)\right)}{\partial t} + \sum_{i=1}^{n}\frac{\partial\psi\left(t,\boldsymbol{X}(t)\right)}{\partial x^i} f^i\left(t,\boldsymbol{X}(t)\right) + \frac{1}{2}\sum_{i,j=1}^{n}\frac{\partial^2\psi\left(t,\boldsymbol{X}(t)\right)}{\partial x^i x^j}\left[g(t,\boldsymbol{X}(t))g^T(t,\boldsymbol{X}(t))\right]^{i,j}\right)dt + \sum_{i=1}^{n}\frac{\partial\psi\left(t,\boldsymbol{X}(t)\right)}{\partial x^i} g^i\left(t,\boldsymbol{X}(t)\right)dW(t) + \sum_{\ell=1}^{d}\left(\psi\left(t,\boldsymbol{X}(t)\right) - \psi\left(t-,\boldsymbol{X}(t-)\right)\right)dN^{\ell}(t) \tag{23}$$

where $\boldsymbol{X}(t)$ is a $n$-dimensional continuous stochastic vector process

$$\boldsymbol{X}(t) = \{X_1(t), X_2(t), ..., X_n(t),\ t \geq 0\} \tag{24}$$

and $f$ and $g$ are $n$-dimensional drift and diffusion coefficient functions, respectively

$$f(t,\boldsymbol{X}(t)) = \{f^1(t,\boldsymbol{X}(t)), ..., f^n(t,\boldsymbol{X}(t)),\ t \geq 0\} \tag{25}$$

$$g(t,\boldsymbol{X}(t)) = \{g^1(t,\boldsymbol{X}(t)), ..., g^n(t,\boldsymbol{X}(t)),\ t \geq 0\} \tag{26}$$

.

As mentioned above, $W(t)$ is a one-dimensional Wiener process, and $N^{\ell}(t)$ is the $\ell^{th}$ component of a $d$-dimensional Poisson process, with $\ell = 1, ..., d$.

Equations (18) and (23) are equivalent. As a result, the coefficient functions of equation (18) are defined as follows

$$\tilde{f}(t, X(t)) = \frac{\partial \psi(t, \boldsymbol{X}(t))}{\partial t} + \sum_{i=1}^{n} \frac{\partial \psi(t, \boldsymbol{X}(t))}{\partial x^i} f^i(t, \boldsymbol{X}(t)) + \frac{1}{2} \sum_{i,j=1}^{n} \frac{\partial^2 \psi(t, \boldsymbol{X}(t))}{\partial x^i x^j} \left[ g(t, \boldsymbol{X}(t)) g^T(t, \boldsymbol{X}(t)) \right]^{i,j} \tag{27}$$

$$\tilde{g}(t, X(t)) = \sum_{i=1}^{n} \frac{\partial \psi(t, \boldsymbol{X}(t))}{\partial x^i} g^i(t, \boldsymbol{X}(t)) \tag{28}$$

$$\tilde{h}(t, X(t)) = \psi(t, \boldsymbol{X}(t)) - \psi(t-, \boldsymbol{X}(t-)) \tag{29}$$

## 3.2. APPLICATION OF DYNKIN'S FORMULA

In stochastic analysis, Dynkin's formula is a theorem that relates the expectation of a function of a jump-diffusion process and a functional of the backward jump-diffusion operator [3]. For a jump-diffusion SDE of the type (7), the Dynkin's formula consists in taking the expectation of (23)

$$\begin{aligned} d\boldsymbol{E}[\psi(t, \boldsymbol{X}(t))] = \\ \boldsymbol{E}\left[ \frac{\partial \psi(t, \boldsymbol{X}(t))}{\partial t} + \sum_{i=1}^{n} \frac{\partial \psi(t, \boldsymbol{X}(t))}{\partial x^i} f^i(t, \boldsymbol{X}(t)) \right. \\ \left. + \frac{1}{2} \sum_{i,j=1}^{n} \frac{\partial^2 \psi(t, \boldsymbol{X}(t))}{\partial x^i x^j} \left[ g(t, \boldsymbol{X}(t)) g^T(t, \boldsymbol{X}(t)) \right]^{i,j} \right] dt \\ + \sum_{\ell=1}^{d} \boldsymbol{E}\left[ \psi(t, \boldsymbol{X}(t)) - \psi(t-, \boldsymbol{X}(t-)) \right] \lambda_{\ell} dt \end{aligned} \tag{30}$$

Notice the term with $dW(t)$ has disappeared from (30). In fact, the expected value of the Wiener process $\boldsymbol{E}[dW(t)] = 0$. In addition, the differential term $dN^{\ell}(t)$ has been replaced by its expected value $\lambda_{\ell} dt$ where $\lambda_{\ell}$ represents the parameter of a Poisson process $N^{\ell}(t)$.

## 3.3. DERIVATION OF THE CONDITIONAL MOMENTS DYNAMICS

The Dynkin's formula, combined with the law of total expectation allows for a derivation of the ODEs that describe the evolution of the conditional moments.

The law of total expectation can simply be defined as follows: given a set of stochastic events $\mathcal{A}_i,\ i = 1, ...N$, the expectation of a random variable $X$ equals the sum of the expectations of $X$ given $\mathcal{A}_i$

$$\boldsymbol{E}(X) = \sum_{i=1}^{N} \boldsymbol{E}(X|\mathcal{A}_i) Pr(\mathcal{A}_i) \tag{31}$$

where $Pr(\mathcal{A}_i)$ denotes the probability of event $\mathcal{A}_i$.

The conditional moment of a process function $\psi(t)$ given a stochastic event $\mathcal{A}_i$ is expressed as

$$\mu_i(t) = \boldsymbol{E}[\psi(t, X(t))|\mathcal{A}_i] Pr(\mathcal{A}_i) \tag{32}$$

It follows from (31) that the total expectation of $\psi(t, X(t))$ equals the sum of all conditional moments given the events $\mathcal{A}_i$

$$\mu(t) = \boldsymbol{E}[\psi(t, X(t))] = \sum_{i=1}^{N} \mu_i(t) \tag{33}$$

and the evolution of a conditional moment:

$$\dot{\mu}_i(t) = \frac{d}{dt} \boldsymbol{E}[\psi(t, X(t))|\mathcal{A}_i] Pr(\mathcal{A}_i) \tag{34}$$

The right hand side of equation (34) represents the Dynkin's formula (30), expressed here with respect to a stochastic mode $i$, where $i = 1, ..., N$

$$\begin{aligned}\dot{\mu}_i(t) = \\ \boldsymbol{E}\Bigg[\frac{\partial\psi\big(t, \boldsymbol{X}(t)\big)}{\partial t} + \sum_{i=1}^{n}\frac{\partial\psi\big(t, \boldsymbol{X}(t)\big)}{\partial x^i}f^i\big(t, \boldsymbol{X}(t)\big) \\ + \frac{1}{2}\sum_{i,j=1}^{n}\frac{\partial^2\psi\big(t, \boldsymbol{X}(t)\big)}{\partial x^i x^j}\big[g(t, \boldsymbol{X}(t))g^T(t, \boldsymbol{X}(t))\big]^{i,j}\Bigg] \\ + \sum_{\ell=1}^{d}\boldsymbol{E}\Big[\psi\big(t, \boldsymbol{X}(t)\big) - \psi\big(t-, \boldsymbol{X}(t-)\big)\Big]\lambda_\ell \end{aligned} \tag{35}$$

For a power system jump-diffusion model (16), jump sizes correspond to jumps in dynamic and algebraic states when the system switches between one equilibrium point to another one. They can subsequently be represented as follows

$$\psi(t, X(t)) - \psi(t-, X(t-)) = \psi_j(t, X(t)) - \psi_i(t, X(t)) \tag{36}$$

where "$i$" represents the origin mode and "$j$" the destination mode. Therefore, these poissonian jumps between different modes of the stochastic system can be characterised by a set of jump parameters (or transition rates) $\lambda_{ij}$, $i, j = 1, ..., N$. The full transition rate matrix for a stochastic system with $N$ stochastic modes is defined as

$$\Lambda = \{\lambda_{ij},\ i, j = 1, ..., N\} \tag{37}$$

where, in accordance with the Markov chain theory, the self-transitions[3]

$$\lambda_{ii} = -\sum_{\substack{j=1 \\ j\neq i}}^{N}\lambda_{ij},\ \forall i = 1, ..., N \tag{38}$$

[3]To not confuse with diagonal elements of a transition probability matrix of a Markov chain, $\lambda_{ii} = \sum_{\substack{j=1 \\ j\neq i}}^{N}\lambda_{ij}$

The jump term in (35) can now be written as

$$\sum_{i,j=1}^{N} \boldsymbol{E}\Big[\psi_j\big(t,\boldsymbol{X}(t)\big) - \psi_i\big(t,\boldsymbol{X}(t)\big)\Big]\lambda_{ij} =$$
$$\sum_{\substack{j=1\\ j\neq i}}^{N} \boldsymbol{E}\Big[\psi_j\big(t,\boldsymbol{X}(t)\big)\Big]\lambda_{ij} - \boldsymbol{E}\Big[\psi_i\big(t,\boldsymbol{X}(t)\big)\Big]\lambda_{ii} \tag{39}$$

The function process $\psi_i(t,\boldsymbol{X}(t))$ of a stochastic variable $\boldsymbol{X}(t)$ has not been defined yet. It can be expressed in many different ways. For instance, for $\psi_i(t,\boldsymbol{X}(t)) = \big(\boldsymbol{X}(t)\big)_i^0$, equation (35) corresponds to the $0^{th}$ order moment dynamics and will be denoted by $\dot{\mu}_i^{(0)}(t)$. For $\psi_i(t,\boldsymbol{X}(t)) = \big(\boldsymbol{X}(t)\big)_i^1$, equation (35) represents the evolution of the conditional moment of the first order (mean) and will be denoted by $\dot{\mu}_i^{(1)}(t)$, and for $\psi_i(t,X(t)) = \big(\boldsymbol{X}(t)\big)_i^2$, equation (35) represents the evolution of the conditional moment of the second order (also called uncentered second moment) and will be denoted by $\dot{\mu}_i^{(2)}(t)$.

In general, conditional moments of order $m$ will be denoted by $\mu_i^{(m)}$ and for an n-dimensional vector $\boldsymbol{X}(t)$, $m = (m_1, m_2, ..., m_n)$, and

$$\mu_i^{(m)}(t) = \mu_i^{(m_1,m_2,...,m_n)}(t) \tag{40}$$

It results, for the $0^{th}$ order moment

$$\mu_i^{(0)}(t) = \mu_i^{(0,...,0)}(t)$$
$$= E\left[X_1^0 X_2^0 ... X_n^0\right] \tag{41}$$

For the $k^{th}$ element of $\boldsymbol{X}(t)$, $X_k$, the first moment is defined as

$$\mu_i^{(1)}(t) = \mu_i^{(0,..,1,...0)}(t)$$
$$= E\left[X_1^0 ... X_k^1 ... X_n^0\right] \tag{42}$$

The uncentered second moment can be defined with respect to one element ($k^{th}$) of $\boldsymbol{X}(t)$ or two elements, ($k^{th}$) and ($\ell^{th}$)

$$\begin{aligned}\mu_i^{(2)}(t) &= \mu_i^{(0,..,2,...,0)}(t) \\ &= E\left[X_1^0 ... X_k^2 ... X_n^0\right]\end{aligned} \tag{43}$$

$$\begin{aligned}\mu_i^{(2)}(t) &= \mu_i^{(0,..,1,...,1,...,0)}(t) \\ &= E\left[X_1^0 ... X_k^1 ... X_l^1 ... X_n^0\right]\end{aligned} \tag{44}$$

It follows from (41), (42), (43), (44) and from the jump-diffusion model of a power system in (16)

$$\begin{aligned}&\dot{\mu}_i^{(m)}(t) = \\ &\boldsymbol{E}\left[\sum_{r=1}^{n} \frac{\partial \psi_i^{(m)}(t, \boldsymbol{X(t)})}{\partial x^r} \cdot \left(A_i(t)\boldsymbol{X}(t) + B_i(t)\boldsymbol{U_i}(t) + C_i(t)\right)\right] \\ &+ \frac{1}{2}\beta^2 \boldsymbol{E}\left[\sum_{r,s=1}^{n} \frac{\partial^2 \psi_i^{(m)}(t, \boldsymbol{X(t)})}{\partial x^r x^s} \boldsymbol{X}^2(t)\right] \\ &+ \sum_{\substack{j=1 \\ j\neq i}}^{N} \boldsymbol{E}\left[\psi_j\left(t, \boldsymbol{X}(t)\right)\right]\lambda_{ij} - \boldsymbol{E}\left[\psi_i\left(t, \boldsymbol{X}(t)\right)\right]\lambda_{ii}\end{aligned} \tag{45}$$

A more detailed derivation of the conditional moments of a stochastic hybrid system is described in [4]. However, the resulting model in [4] is different from the one developed in this paper, for the reason that the power system in [4] is subjected to stochastic inputs whereas in this study, the entire system is switching stochastically between distinct equilibrium points.

In (45), $\psi_j(t, \boldsymbol{X}(t)$ is set to the equilibrium operating point of the destination mode (slow switching system) after a jump event has occurred. In addition, the second term of the right hand side of (45) is equal to zero for $m < 2$.

The resulting system of ODEs that describes the evolution of the conditional moment of the jump-diffusion model of a power system is

$$\dot{\mu}_i^{(m)}(t) = \sum_{p=1}^{n} m_p \left( \sum_{r=1}^{n} a_{pr}^i \mu_i^{m-e_p+e_r}(t) + \mu_i^{m-e_p}(t) v_p^i \right)$$
$$+ \frac{1}{2}\beta^2 \sum_{p=1}^{n} \left( m_p(m_p - 1) + \sum_{\substack{r=1 \\ r \neq p}}^{n} m_p m_r \right) \mu_i^{(m)}(t) + \sum_{\substack{j=1 \\ j \neq i}}^{N} \lambda_{ij} \boldsymbol{X}_i^{(m)} \mu_j^{(0)}(t) - \lambda_{ii} \mu_i^{(m)}(t) \qquad (46)$$

$\forall i = 1, ..., N$, where $v_p^i$ represents the $p^{th}$ element of the vector $B_i U_i + C_i$ and $e_p, e_r$ are two unit vectors with a 1 at the $p^{th}$, $r^{th}$ entry, respectively.

## 3.4. MATRIX REPRESENTATION

The derivation of the matrix representation of equation (46) follows the procedure described in [5, 7, 18]. However, the resulting matrices for the power system jump-diffusion model presented here are different from the matrices developed in [5, 7, 18], excepted for the $0^{th}$ order as indicated below:

1) The $0^{th}$ moments represent the occupational probabilities, which are the probabilities for the system to be in a particular operating mode. The matrix representation of the ODEs (46) is described in equation (47). This corresponds to the expression that was obtained in [5, 7, 18]

$$\dot{\mu}^{(0)} = \Lambda^T \mu^{(0)} \qquad (47)$$

where $\Lambda^T$ is the transpose of the full transition rate matrix (37). Equation (47) corresponds to the well-known Chapman-Kolmogorov equation.

2) The $1^{st}$ conditional moments are the statistical means of the stochastic distribution. The general form of the $1^{st}$ moment ODEs derived in [5, 7] was as follows

$$\dot{\mu}^{(1)} = G^{(1)} \mu^{(1)}(t) + H^{(1)} \mu^{(0)}(t) \qquad (48)$$

where the evolution of the first moments is function of the moments of the $1^{st}$ and $0^{th}$ orders. Using Matlab notation, the coefficient functions $G^{(1)}$ and $H^{(1)}$ in [5, 7] were defined as

$$G^1 = blkdiag(A_1, ..., A_N) + (\Lambda^T \otimes I(N)) \tag{49}$$

$$H^1 = blkdiag(-A_1X_1, ..., -A_NX_N) \tag{50}$$

Because of the way the jump term is defined in the jump-diffusion model developed here, the matrices $G^{(1)}$ and $H^{(1)}$ are modified as follows

$$G^1 = blkdiag(A_1, ..., A_N) + diag(\Lambda^T \otimes I(N)) \tag{51}$$

$$H^1 = blkdiag(-A_1\boldsymbol{X}_1, ..., -A_N\boldsymbol{X}_N) + [\boldsymbol{X}1; \boldsymbol{X}2; \boldsymbol{X}3] \circ \left(\Lambda^T_{trans} \otimes \mathbb{1}_{n\times 1}\right) \tag{52}$$

where $\circ$ represents the Hadamard product (element-wise multiplication, Matlab '.*'), $\Lambda_{trans} = \Lambda - diag(\Lambda)$, and $\mathbb{1}_{n\times 1}$ is an $n \times 1$ matrix of all ones (Matlab $ones(n, 1)$).

3) The $2^{nd}$ conditional moments represent the uncentered second moments. From [5, 7]

$$\dot{\mu}^{(2)} = G^{(2)}\mu^{(2)}(t) + H^{(2)}\mu^{(1)}(t) \tag{53}$$

where the evolution of the second moment is function of the moments of the $2^{nd}$ and $1^{st}$ orders. The structure of the coefficient functions $G^{(2)}$ and $H^{(2)}$ is pretty complex and was described in length in [5]. However, for the jump-diffusion model, because of the way the jump term is defined and of the inclusion of the Wiener term, the equation of the ODEs representing the evolution of the second moment is as follows

$$\dot{\mu}^{(2)} = G^{(2)}\mu^{(2)}(t) + H^{(2)}\mu^{(1)}(t) + J^{(2)}\mu^{(0)}(t) \tag{54}$$

Matrix $G^{(2)}$ contains the contributions from the state matrices $A_i$, $i = 1, 2, 3$, from the diagonal elements of the transition rate matrix ($\lambda_{ii}$, self-transitions), and from the square of the Wiener coefficient $\frac{1}{2}\beta^2$. Each block entry of $G^{(2)}$ is defined as

$$G_i^{(2)} = (T_x + T_y)\,(I(n) \otimes A_i)\,T_x' + diag\left(\Lambda' \otimes I(n + n_z)\right) + \beta^2\, I\left(n(n+1)/2\right) \tag{55}$$

where $n_z$ is the binomial coefficient of $n$ and 2, $T_x, T_y$ (and $T_z$ below) are reordering matrices. These matrices are not unique, they ensure the elements of $G^{(2)}$ are ordered in a desired fashion.

Matrix $H^{(2)}$ is constructed with the affine term in the drift component of the SDE (16), $-A_i \boldsymbol{X}_i + B_i \boldsymbol{U}_i$, $i = 1, 2, 3$. Each bloc entry is

$$H_i^{(2)} = (T_x + T_y)\left(I(n) \otimes (-A_i X_i + B_i U_i)\right) \tag{56}$$

Matrix $J^{(2)}$ is a Kronecker product of the transition rates (non-diagonal elements of $\Lambda$) with the steady-state vectors. The block elements of $J^{(2)}$ are of the form

$$J_{ij}^{(2)} = \frac{\lambda_{ij}}{2}\, T_z\,(Xj \otimes Xj) \tag{57}$$

where $i, j = 1, 2, 3$ and $i \neq j$.

## 4. NUMERICAL APPLICATION

In this section, a numerical application of the jump-diffusion model to the IEEE 37-bus microgrid is presented and discussed. The ODEs representing the conditional moments are solved using the matrix representation of the jump-diffusion model. Computation of the conditional moments is limited to the lower order moments (zeroth, first and second orders). These lower order moments correspond respectively to the occupational probabilities, the statistic means and the uncentered second moments (from which the variances are derived

according to equation (5)), and are in general sufficient to characterise a probability density function of a distribution. Conceivably, moments of higher order can be calculated, but the analytical expression of the system of ODEs becomes too complex and the solutions too computational expensive, they are not addressed in this paper.

The jump-diffusion results are superimposed to the averaged results of 20,000 Monte Carlo simulations of the DAE model of the IEEE 37-bus microgrid, augmented with a multiplicative diffusion term and subject to random switching between three distinct equilibrium points. The occupational probabilities (zeroth moments) are simulated using the Gillespie algorithm ([21, 7]). The mode sequences generated by each run of the Gillespie algorithm are used as integration paths to compute the first and second order moments during each run. To obtain a good accuracy for the first and second order moments, a large number of Monte-Carlo runs is necessary (in excess of 100,000 for the IEEE 37-bus microgrid). The results presented in this study were limited to 20,000 runs and the computer execution time was 55 hr 20 min 23 s, on a PC with a 3.2 GHz Intel® Core™ i7-800 CPU processor with 32GB memory in the MATLAB's environment. The computer execution time increases significantly as the number of runs is increased. In this regard, the jump-diffusion method developed here is vastly superior to the averaged Monte Carlo method. The execution time to compute the zeroth, first and second order conditional moments was 2 hr 18 min 54 s, a reduction of 95.8% relative to the Monte Carlo approach.

## 4.1. ZEROTH MOMENT RESULTS

For the zeroth moments, the jump-diffusion model corresponds to the Chapman-Kolmogorov equations, the differential expression of which is provided in (3). The exact solution of these equations is easy to obtain in the jump-diffusion model. On the other hand, the Monte Carlo simulation requires a large number of iterations for greater accuracy. The solutions for the zeroth order moments are identical to those obtained in [7], they are represented here again, in Figure 3, for completeness.

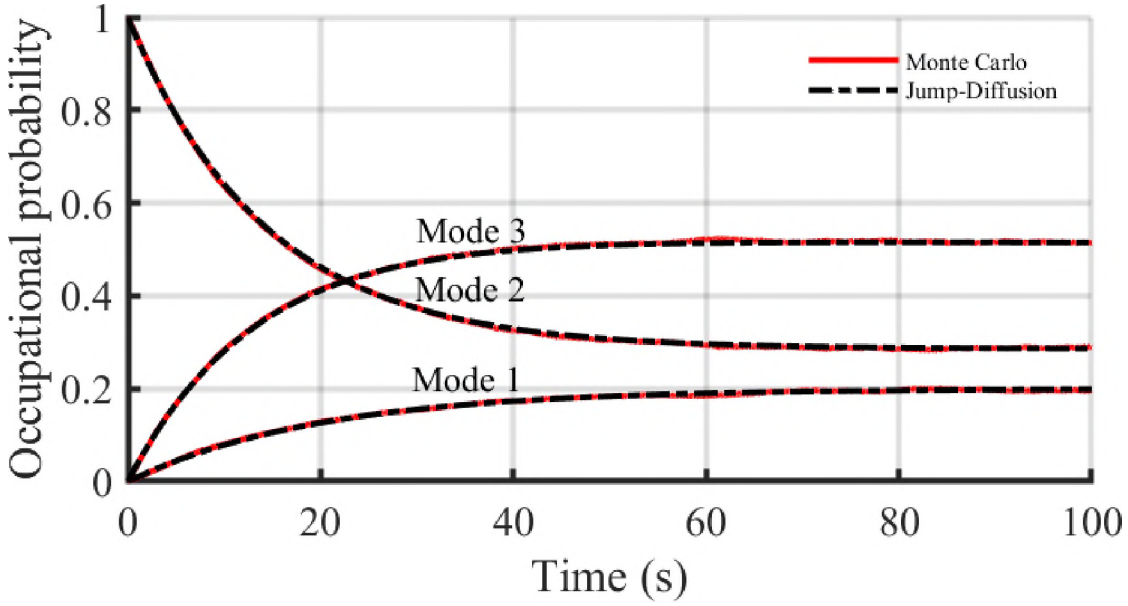


Figure 3. Zeroth Moments of the stochastic system (occupational probabilities)

## 4.2. FIRST MOMENT RESULTS

The solutions for the first moments are obtained by solving the system of ODEs represented by the matrix equation (48), where the moment order $m = 1$. In (48), matrix $G^{(1)}$ is $168 \times 168$ and matrix $H^{(1)}$ is $168 \times 3$. To obtain the means for the 56 dynamic states, the solutions corresponding to the three stochastic modes and embedded in the column vector $\mu^{(1)}$ are summed up, in accordance with the law of total expectation

$$\mu_{[56\times1]} = [I(56) \quad I(56) \quad I(56)]\mu^{(1)} \tag{58}$$

The first moments represented in Figure (4) correspond to the dynamic states associated with Inverter 2 of the modified IEEE 37-bus power system [22, 18, 14, 15]. The plots in red represent the averaged Monte Carlo simulations. They closely match the jump-diffusion plots in dashed-black. The error observed in Figure 4 *(b)* and *(h)* can be considerably reduced by increasing the number of Monte Carlo runs, but at the expense of the execution

time. In Figure (5), results for the algebraic states (or outputs) are represented, as linear algebraic combinations of the moments of the dynamic states. A comparison between the results from the Jump-Diffusion model developed in this paper and from the Markov Jump Linear System model in [7] is represented in Figure 8 and 9. It can be seen, from Figure 8 *(a)* that the steady-state is reached more quickly for the Jump-diffusion model, whereas the MJLS result reaches steady-state at about 200s (not shown on the plot). On the other hand, the spikes observed in the Monte Carlo simulation of the MJLS model [7] have disappeared from the Jump-Diffusion's Monte Carlo results (Figure 9), and this is indicative of a better modeling of the jumps.

### 4.3. SECOND MOMENT RESULTS

To obtain the solutions for the uncentered second moments, the moment order is set as $m = 2$ in matrix ODEs (54). It results from (54), $G^{(2)}$ is $4788 \times 4788$, $H^{(2)}$ is $4788 \times 168$, and $J^{(2)}$ is a $4788 \times 3$. Following the argument developed for the first order moments, the uncentered second moments for the dynamic states is a $1596 \times 1$, and the second moments for the algebraic states is a $1540 \times 1$ vector. The results are shown in Figure (6) for the dynamic states (inverter 2), and in Figure (7) for the algebraic states (inverter 2 outputs, bus and load currents). An examination of Figure (6) and Figure (7) indicates the averaged Monte Carlo simulation results converge to the jump-diffusion results. The comments related to the comparison between the first moments obtained from the Jump-Diffusion model and form the MJLS model from [7] are also valid for the second moments and the variances, Figure (8) and Figure (9).

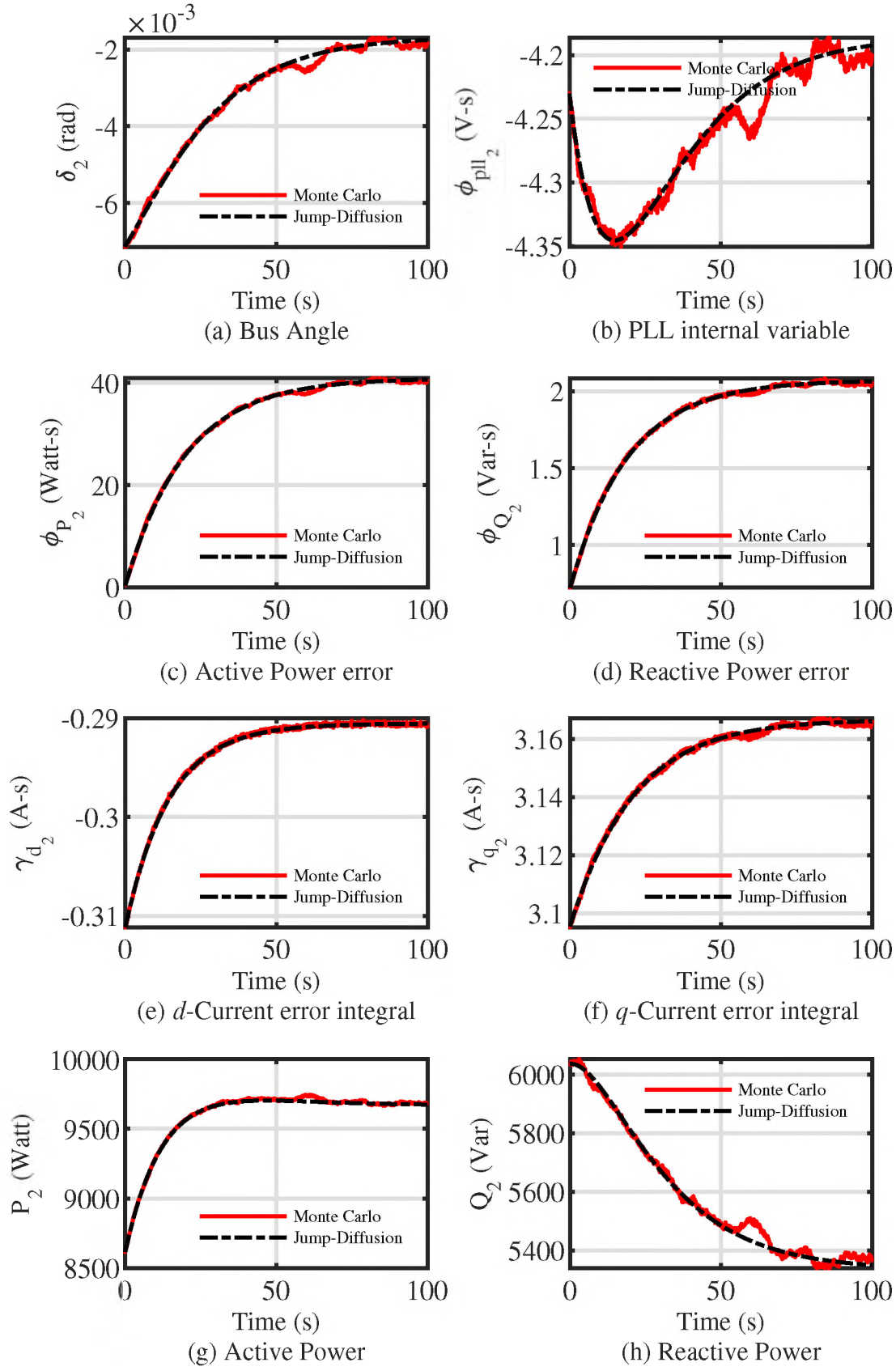


Figure 4. First Moments of the dynamic states

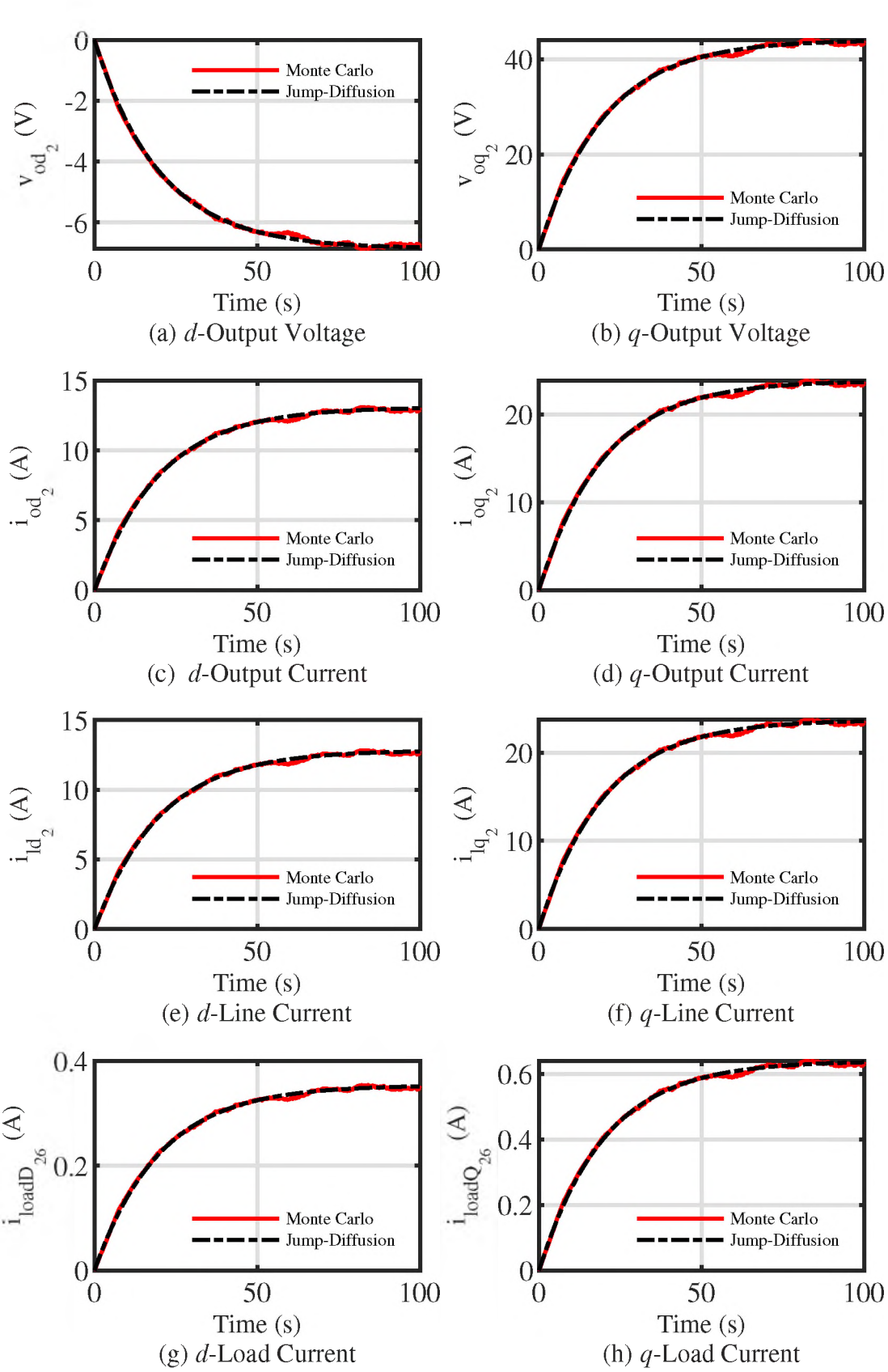


Figure 5. First Moments of the algebraic states

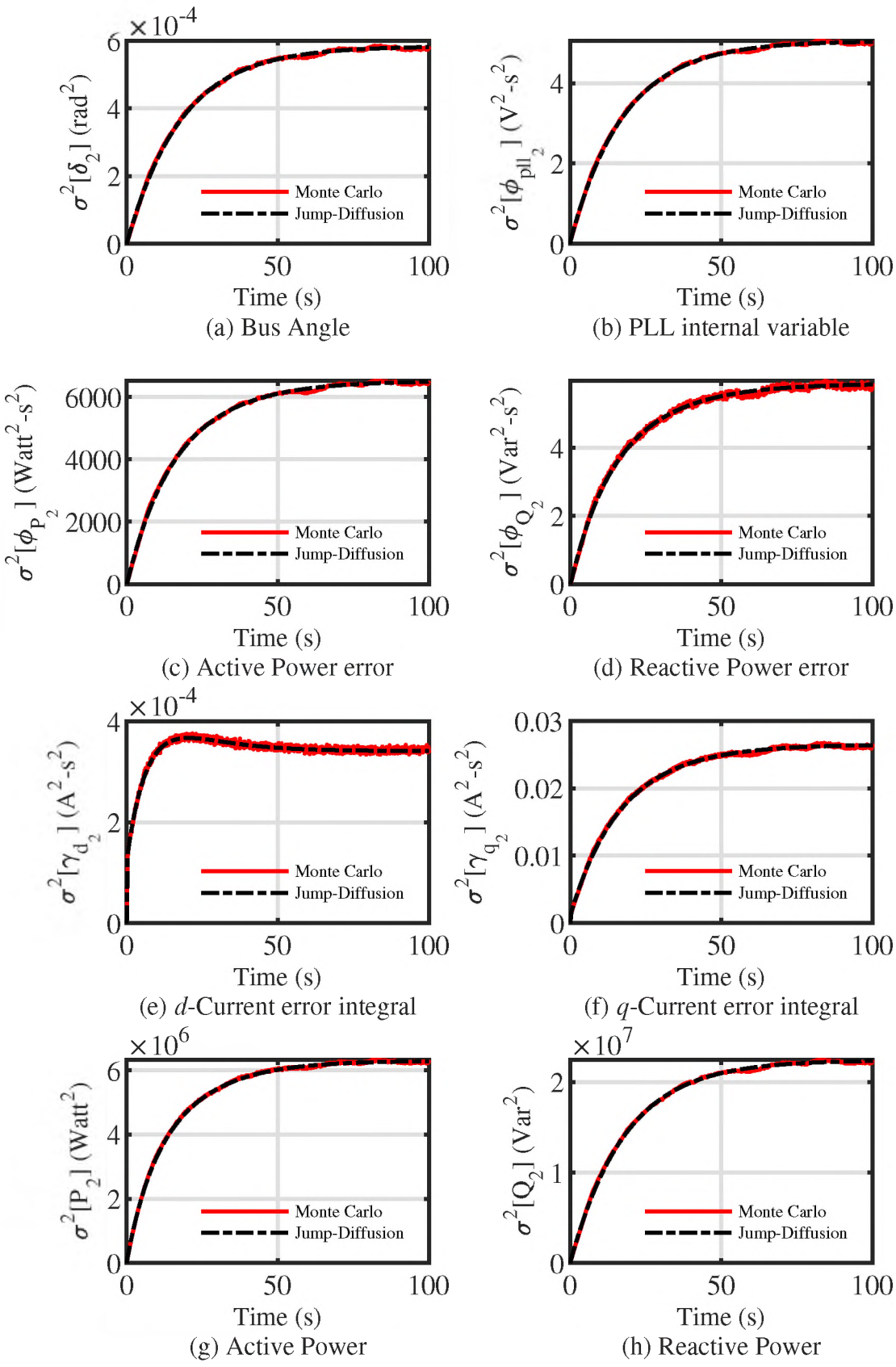


Figure 6. Second Moments of the dynamic states

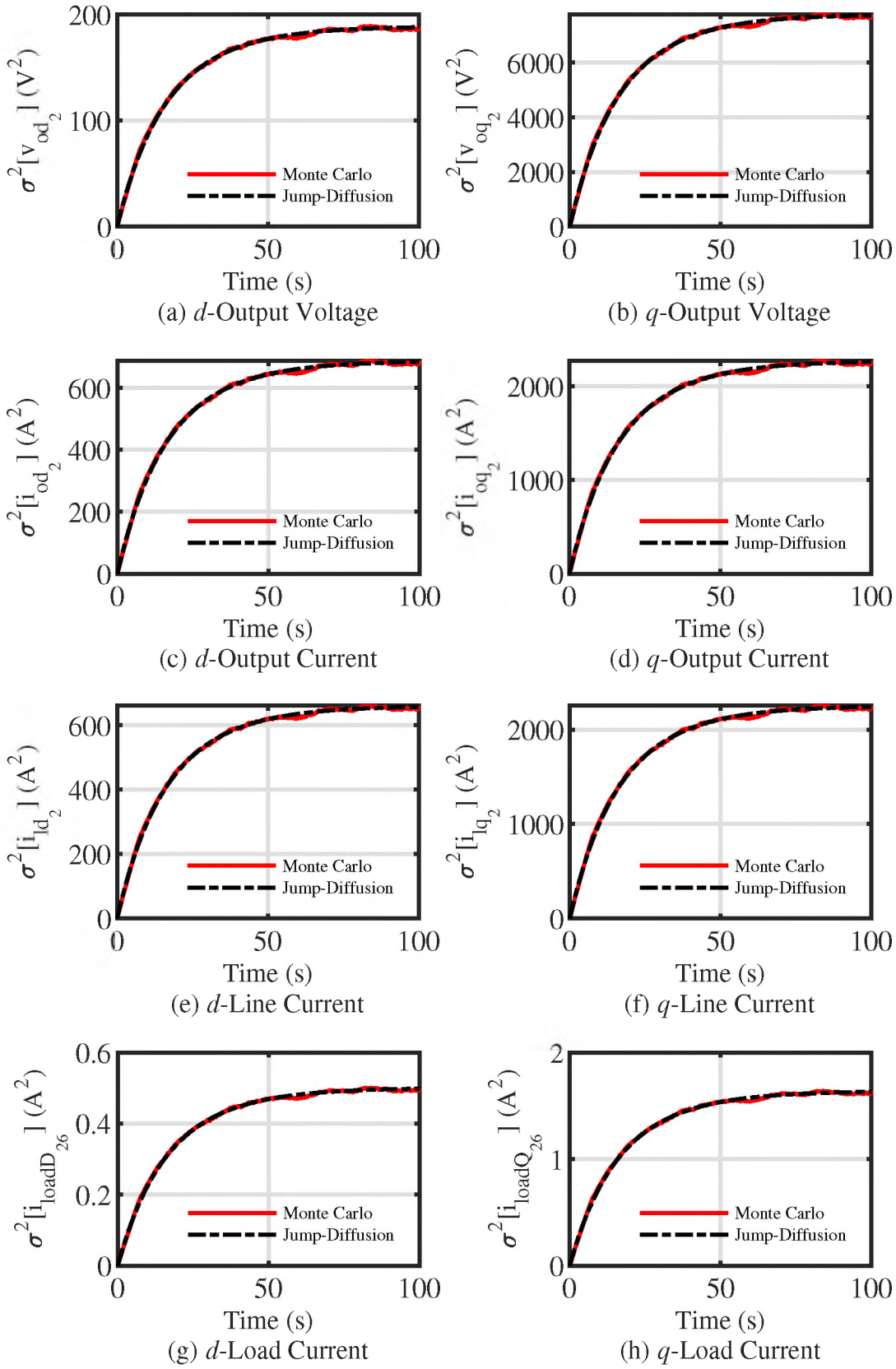


Figure 7. Second Moments of the algebraic states

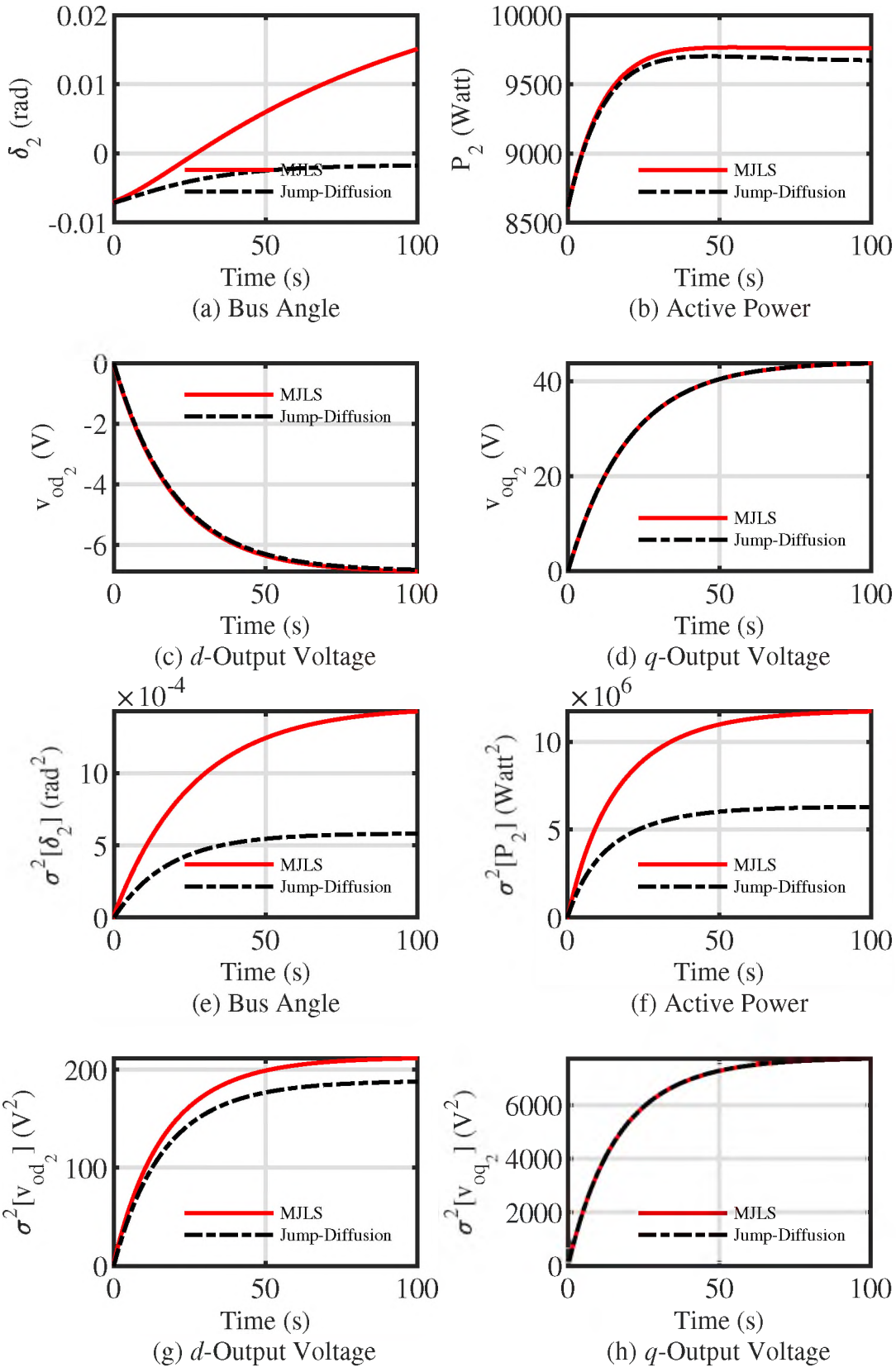


Figure 8. Comparison between stochastic modeling results from [7] (referred to as "MJLS") and from this study (referred to as "Jump-Diffusion")

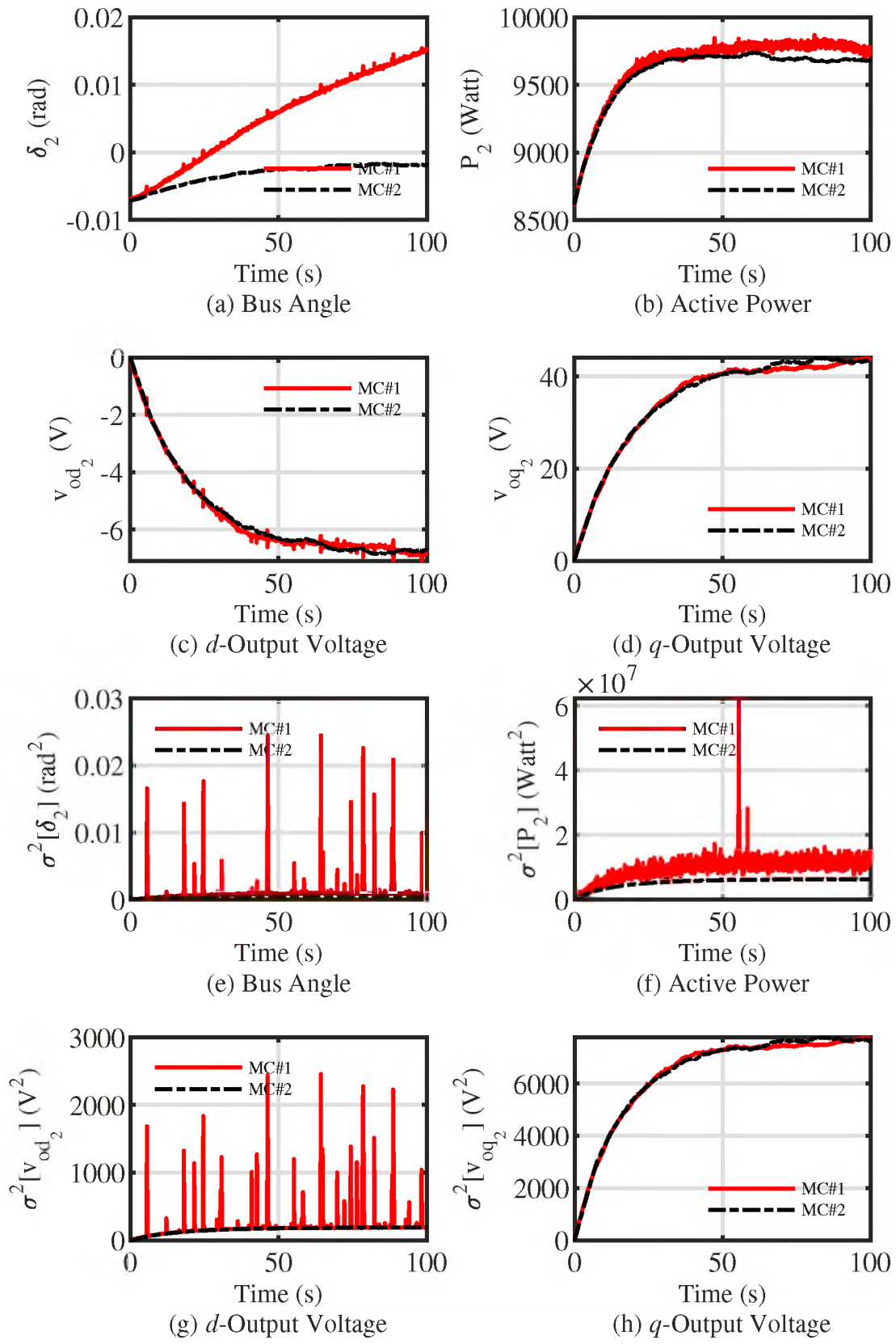


Figure 9. Comparison between Monte Carlo results from [7] (referred to as "MC#1") and from this study (referred to as "MC#2")

# 5. CONCLUSION AND FUTURE WORK

This study presented a jump-diffusion model to analyze the dynamics of a microgrid operating in grid-tied and standalone modes. For a system subject to stochastic behavior affecting dynamic and algebraic states, a statistical approach based on the computation of the conditional moments is suitable for the analysis of the system dynamics. The SDE representing the system included the Wiener process as well as Poisson processes to represent the stochastic jumps between different operating modes of the power system. The solution of the jump-diffusion SDE led to a system of ODEs that represent the evolution of the conditional moments of the system. A matrix representation of the system of ODEs, and the numerical solutions were shown to converge to the results of the averaged Monte Carlo simulation. Future work will include using the Jump-Diffusion model developed in this study to analyse the stability of a microgrid system subjected to random and abrupt transitions between different operating modes.

# APPENDIX A.

# IEEE 37-BUS MICROGRID DYNAMIC STATES

The dynamic and algebraic states of the IEEE 37-bus microgrid represented in figures 4, 5, 6, 7 above are defined in Table A1.

Table A1. Power System Dynamic and Algebraic States

| Variable | Definition |
|---|---|
| $\delta_2$ | Inverter 2 phase angle |
| $\phi_{pll_2}$ | Integral of Inverter 2 $q$-axis voltage |
| $\phi_{P_2}$ | Integral of Inverter 2 Active Power error |
| $\phi_{Q_2}$ | Integral of Inverter 2 Reactive Power error |
| $\gamma_{d_2}$ | Integral of error in filter inductor current, $d$-axis |
| $\gamma_{q_2}$ | Integral of error in filter inductor current, $q$-axis |
| $P_2$ | Inverter 2 Active Power |
| $Q_2$ | Inverter 2 Reactive Power |
| $v_{od_2}$ | Inverter 2 output voltage, $d$-axis |
| $v_{oq_2}$ | Inverter 2 output voltage, $q$-axis |
| $i_{od_2}$ | Inverter 2 output current, $d$-axis |
| $i_{oq_2}$ | Inverter 2 output current, $q$-axis |
| $i_{ld_{619}}$ | Line 619 current, $d$-axis |
| $i_{lq_{619}}$ | Line 619 current, $q$-axis |
| $i_{loadD_{26}}$ | Bus 26 load current, $d$-axis |
| $i_{loadQ_{26}}$ | Bus 26 load current, $q$-axis |

# APPENDIX B.

# THE IEEE 37-BUS MICROGRID

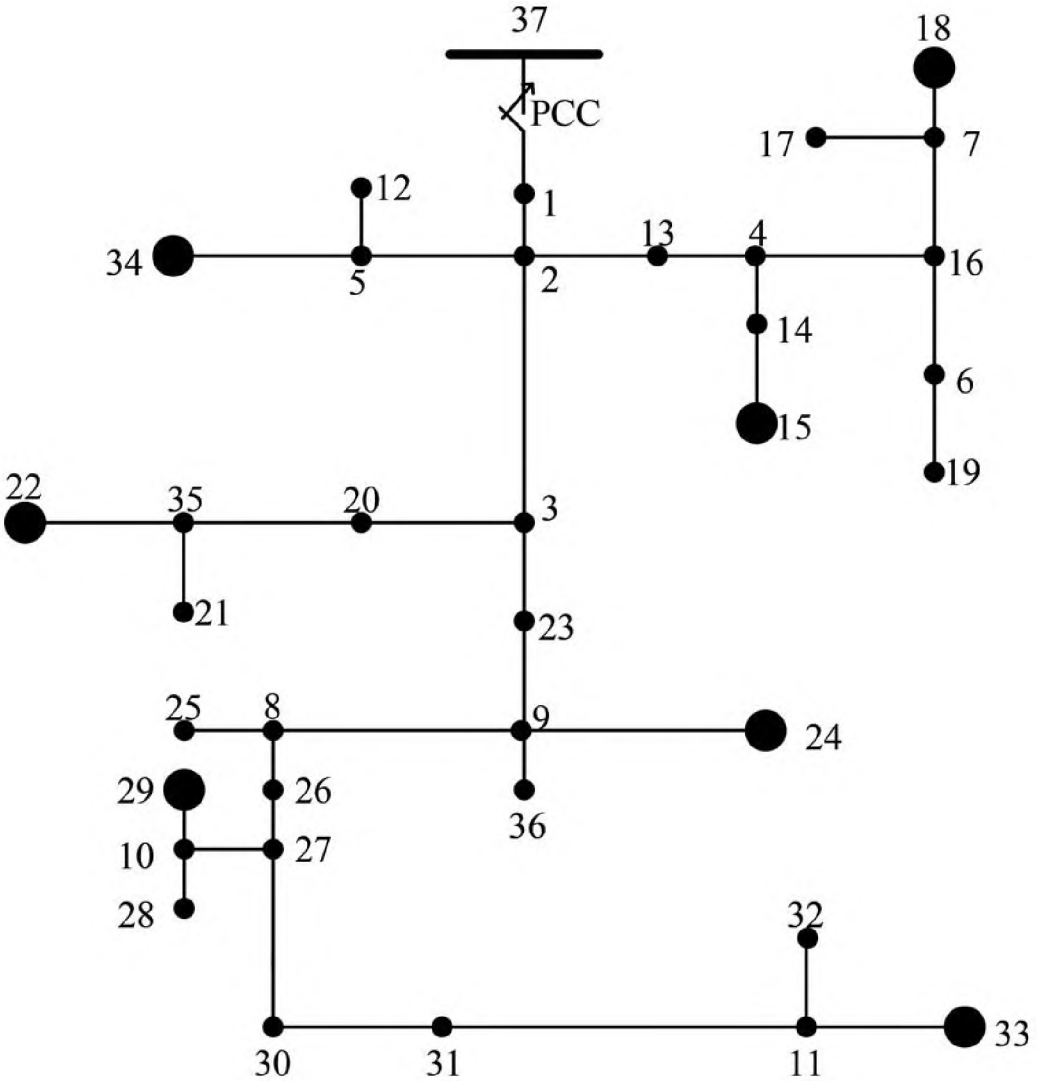


Figure B.1. A one-line diagram of the modified IEEE-37 microgrid. Larger circles indicate locations of inverters.

# REFERENCES


[1] E. Platen and N. Bruti-Liberati, *Numerical solution of stochastic differential equations with jumps in finance*, ser. Stochastic modelling and applied probability. Springer-Verlag, 2010, vol. 64.

[2] A. Seierstad, *Stochastic control in discrete and continuous time*. Springer, 2009.

[3] F. B. Hanson, *Applied Stochastic Processes and Control for Jump-Diffusions: Modeling, Analysis and Computation*, ser. Advances in Design and Control. Society for Industrial and Applied Mathematics, 2007.

[4] S. V. Dhople, Y. C. Chen, L. DeVille, and A. D. Dominguez-Garcia, "Analysis of power system dynamics subject to stochastic power injections," *IEEE Transactions on Circuits and Systems I: Regular Papers*, vol. 60, no. 12, pp. 3341–3353, 2013.

[5] J. A. Mueller and J. W. Kimball, "Modeling and analysis of dc microgrids as stochastic hybrid systems," *IEEE Transactions on Power Electronics*, pp. 1–1, 2021.

[6] S. Dhople, L. DeVille, and A. Dominguez-Garcia, "A stochastic hybrid systems framework for analysis of markov reward models," *Reliability Engineering & System Safety*, vol. 123, pp. 158–170, 2014.

[7] G. Mpembele and J. Kimball, "Markov jump linear system analysis of a microgrid operating in islanded and grid tied modes," *TechRxiv*, 2020.

[8] Y. Xu, F. Wen, H. Zhao, M. Chen, Z. Yang, and H. Shang, "Stochastic small signal stability of a power system with uncertainties," *Energies*, vol. 11, no. 11, p. 2980, 2018.

[9] J. Hespanha, "Modelling and analysis of stochastic hybrid systems," *IEE Proceedings - Control Theory and Applications*, vol. 153, no. 5, pp. 520–535, 2006.

[10] P. Hespanha, "Modeling and analysis of networked control systems using stochastic hybrid systems," *Annual Reviews in Control*, vol. 38, no. 2, pp. 155–170, 2014.

[11] J. P. Hespanha, "A model for stochastic hybrid systems with application to communication networks," *Nonlinear Analysis: Theory, Methods & Applications*, vol. 62, no. 8, pp. 1353–1383, 2005.

[12] J. A. Mueller, M. Rasheduzzaman, and J. W. Kimball, "A model modification process for grid-connected inverters used in islanded microgrids," *IEEE Transactions on Energy Conversion*, vol. 31, no. 1, pp. 240–250, 2016.

[13] T. C. Green and M. Prodanović, "Control of inverter-based micro-grids," *Electric Power Systems Research*, vol. 77, no. 9, pp. 1204–1213, 2007.

[14] M. Rasheduzzaman, J. A. Mueller, and J. W. Kimball, "An accurate small-signal model of inverter- dominated islanded microgrids using *dq* reference frame," *IEEE Journal of Emerging and Selected Topics in Power Electronics*, vol. 2, no. 4, pp. 1070–1080, 2014.

[15] M. Rasheduzzaman, J. Mueller, and J. W. Kimball, "Reduced-order small-signal model of microgrid systems," *IEEE Transactions on Sustainable Energy*, vol. 6, no. 4, pp. 1292–1305, 2015.

[16] L. Luo and S. V. Dhople, "Spatiotemporal model reduction of inverter-based islanded microgrids," *IEEE Transactions on Energy Conversion*, vol. 29, no. 4, pp. 823–832, 2014.

[17] V. Mariani, F. Vasca, J. C. Vasquez, and J. M. Guerrero, "Model order reductions for stability analysis of islanded microgrids with droop control," *IEEE Transactions on Industrial Electronics*, vol. 62, no. 7, pp. 4344–4354, 2015.

[18] G. Mpembele and J. W. Kimball, "A matrix representation of a markov jump linear system applied to a standalone microgrid," in *2018 9th IEEE International Symposium on Power Electronics for Distributed Generation Systems (PEDG)*, June 2018, pp. 1–8.

[19] N. Ikeda and S. Watanabe, *Stochastic differential equations and diffusion processes*. North-Holland, 2011.

[20] P. E. Protter, *Stochastic Integration and Differential Equations*. Springer-Verlag, 2013.

[21] D. T. Gillespie, "Exact stochastic simulation of coupled chemical reactions," *The Journal of Physical Chemistry*, vol. 81, pp. 2340–2361, 1977.

[22] G. Mpembele and J. Kimball, "Analysis of a standalone microgrid stability using generic markov jump linear systems," in *2017 IEEE Power and Energy Conference at Illinois (PECI)*, Feb 2017, pp. 1–8.

# III. MEAN SQUARE STABILITY OF A MICROGRID'S JUMP DIFFUSION MODEL

Gilles Mpembele and Jonathan W. Kimball
Department of Electrical & Computer Engineering
Missouri University of Science and Technology
Rolla, Missouri 65409–0050
Email: gmhn7@umsystem.edu

## ABSTRACT

This paper discusses the stability of a Jump-Diffusion model of a microgrid operating in grid-tied and standalone modes. The system is modeled as a Markov Jump Linear System represented by a Jump-Diffusion Stochastic Differential Equation (SDE). The multi-dimensional compound Poisson process in the jump term was modified to include a compensator to allow for the application of the Burkholder-Davis-Gundy (BDG) inequality for martingales. The analysis proceeds with the derivation of bounds on the conditional moments of the compensated Jump-Diffusion model and the mean-square stability criterion is used to characterize the asymptotic stability of the system. An illustration of the method is described for the IEEE 37-bus microgrid system.

**Keywords:** Jump-Diffusion, Markov Jump Linear Systems (MJLSs), Mean-square stability, Monte Carlo simulations, Power System statistics, Stochastic Differential Equation (SDE), Stochastic Hybrid Systems (SHSs).

## 1. INTRODUCTION

One of the most difficult challenges facing microgrids is implementing a control system in the face of uncertainty and randomness in their operating conditions. For a microgrid operating in grid-tied mode, the control of the frequency and bus voltages

can rely on the mains power system's ability to set these parameters for the entire grid. However, in standalone mode, the microgrid is more susceptible to variations in loads and local sources and if not adequately controlled it could experience operating instabilities. To develop an efficient and resilient control strategy, accurate models for the microgrid's operation are needed, not only during standalone operation but during switching between different operating equilibrium points.

The Jump-diffusion process [1] provides an excellent mathematical framework to analyze the dynamics of a microgrid operating between different equilibrium points. The system can equivalently be represented in the Stochastic Hybrid System (SHS) framework, and particularly, as a Markov Jump Linear System, with potentially impulsive jumps in the dynamic and algebraic states. The SHS formulation was used to derive a model for a power system with stochastic inputs in [2, 3], and an MJLS model of a system with random switching between multiple equilibrium points was discussed in [4]. In [1], a Jump-diffusion model for a microgrid was developed, where a multi-dimensional compound Poisson process is used to represent the random and abrupt jumps between different operating modes.

The modeling process in both cases is theoretically founded and empirically validated. The resulting Ordinary Differential Equations (ODEs) provide an accurate statistical representation of the evolution of the dynamic and algebraic states. They also provide a basis for the analysis of the stochastic stability of the system. The stability analysis of SHSs encompasses a wide range of methods and stability criteria. There are methods that focus on the stability of the numerical methods used to solve the SDEs. Other methods establish criteria on the parameters of the stochastic model such as the dwell time (defined as the amount of time that passes between two consecutive switching instants). There are also methods that evaluate the bounds on the conditional moments of the stochastic system using appropriate inequalities.

Various types of SHSs are surveyed in [5]. These methods are essentially based on global stability. The global asymptotic stability method, for instance, includes Lyapunov stability, Lagrange stability, and global attractivity. The Lyapunov stability method is used in [6, 7] where the Lyapunov function is equated to the Itô formula for a stochastic differential equation with jumps. The stability analysis is performed through the evaluation of bounds on the expected value of the extended generator. The method is applied to the trivial solution of the SHS, based on the fact that the origin is an equilibrium state for the asymptotic stability.

In [8, 9], the objective is to assess the transient stability of a power system subject to uncertainties such as load levels and system faults. For that purpose, the deterministic DAEs of the power system are converted into SDEs with the addition of stochastic components. The solutions to the SDEs are computed using numerical integration methods such as the Euler method and the Milstein method. Although not explicitly stated in these papers, the stability of the discrete-time approximation methods is evaluated using the asymptotically p-stable criterion [10]. The study demonstrates convergence of the numerical methods to the exact solution, hence the stability of the method as applied to the system under study.

The analysis in [11, 12] uses essentially the Lyapunov functions method to derive the minimum dwell time that guarantees system stability when subjected to stochastic switching. In [13], the exponential stability method is discussed with respect to the dwell times. The analysis shows that the expected value of the euclidean norm of the dynamic states is exponentially bounded.

The almost sure exponential stability method is used in [14], for a Markov Jump Linear System subject to deterministic switching dynamics. The conditions of stability are established under either hard or average constraints on the dwell times between switching instants. The method consists in determining the minimum dwell time that guarantees the stability of the system.

In [15], the stability of a power system is analyzed from an MJLS perspective, where every transition may be impulsive and the exponentially distributed dwell times may be arbitrarily small. The representation of the microgrid in the MJLS framework allows for a derivation of bounds on the expected values of the dynamic states based on a combination of the Markov process parameters (transition rates), the dynamics of each linear system, and the magnitude of the impulses. The study makes the assumption that each mode of the MJLS is stable, and the impulsive transitions between stochastic modes of the power system are also bounded. The bounds on the expected values of the dynamic states, defined in terms of the transition matrices and the impulses are in general very conservative and could be arbitrarily large.

In [16], moment bounds for the solutions to the stochastic differential equation with jumps are derived using the martingale framework and the Burkholder-Davis-Gundy (BDG) inequality. The method results in the $p$-moment stability equivalent to the one described in [6, 7]. The paper includes cases where $p \in [1, 2]$ and a generalization to $p > 2$.

The BDG inequality method is used in this paper to derive bounds on the conditional moments of the Jump-Diffusion model for a microgrid developed in [1]. The BDG inequality is applied to the solutions of the SDE with jump representing the dynamics of the system. It will be shown that these solutions can be described as semimartingales and hence they satisfy the applicability condition of the BDG inequality.

The paper is subdivided as follows:

In Section 2, a compensated Jump-Diffusion model is presented based on a method described in [10], and a matrix representation of the conditional moments is derived. In Section 3, standard inequalities [10] related to martingales as well as the BDG inequality [16, 17] are presented. In Section 4, a stability method based on the mean-square stability criterion and the application of the BDG inequality to the compensated Poisson stochastic

integral process is described. Section 5 discusses the application of the stability criterion to a modified IEEE 37-bus microgrid system. Section 6 concludes this study and avenues for future work are presented.

## 2. COMPENSATED JUMP-DIFFUSION MODEL OF A MICROGRID

A Jump-Diffusion model based on a compound Poisson process for the jump component was derived in [1]. To be able to use martingale inequalities (see section III) to derive bounds on the conditional moments, a compensator must be added to the compound Poisson term [10, 18].

The derivation of the conditional moments and of their matrix representation is presented briefly here. A more detailed description of this procedure was discussed in [1]. The resulting matrix representations of the conditional moments for both the compensated and the non-compensated models are equivalent.

### 2.1. SDE WITH JUMPS

The Jump-Diffusion model presented in [1] describes a microgrid operating between a grid-tied and two distinct standalone modes. This model is represented by an $n$-dimensional SDE with jumps of the form

$$\begin{aligned} d\boldsymbol{X}(t) &= \left\{A_i(t)\big(\boldsymbol{X}(t) - \boldsymbol{X}_i(t)\big) + B_i u_i\right\}dt \\ &+ \beta \boldsymbol{X}(t) dW(t) + \sum_{\ell=1}^{d} \big(\boldsymbol{X}(t) - \boldsymbol{X}(t-)\big) dN^{\ell}(t), \end{aligned} \tag{1}$$

for $t \in [0, T]$, with initial value $\boldsymbol{X}_0 = \boldsymbol{X}(0)$. $\boldsymbol{X} = \{\boldsymbol{X}(t),\ t \geq 0\}$ is a vector stochastic process representing the microgrid dynamic states, $W = \{W(t),\ t \geq 0\}$ is a one-dimensional Wiener process with the volatility constant $\beta$, and $N^{\ell},\ \ell = 1, ..., d$, represents the $\ell^{th}$ Poisson process

with intensity $\lambda_\ell$. The other parameters in (1) are the state matrix $A_i$, the state vector at equilibrium, $X_i$, the input matrix, $B_i$, the control vector, $u_i$, all associated with the stochastic operating mode $i$.

The last term in (1) represents a multidimensional compound Poisson process where $\boldsymbol{X}(t) - \boldsymbol{X}(t-)$ is the jump size at time $t$. To enable the use of the martingale inequalities to the solution of (1), a compensator needs to be inserted into the compound Poisson process term. The definition and characteristics of a martingale process are described in section 3.

## 2.2. COMPENSATED SDE WITH JUMPS

A method from [10, 19] to transform (1) into a martingale is presented here. A generic compound Poisson process $Y = \{Y(t),\ t \geq 0\}$ is described as

$$Y(t) = \sum_{k=1}^{N(t)} \xi_k \tag{2}$$

where $\xi_k = X(\tau_k) - X(\tau_k-)$ represents the $k^{th}$ jump size, and $N = \{N(t),\ t \geq 0\}$ represents a Poisson counting process with intensity $\lambda$. Since the jump sizes are independent identically distributed (i.i.d) random variables independent of $N$, the expected value of $Y(t)$ is

$$E[Y(t)] = \lambda t \hat{\xi} \tag{3}$$

where $\hat{\xi} = E[\xi_k]$ is the mean of all jumps of $Y$ that arise until time $t$ [10], and $\hat{\xi} < \infty$.

The combination of $\hat{\xi}$ and the mean of a counting Poisson process, $\lambda t$, results in a quantity $\lambda \hat{\xi} t$ called the *compensator* of the compound Poisson process. Hence, the compensated compound Poisson process is

$$\hat{Y} = \{\hat{Y}(t) = Y(t) - \lambda \hat{\xi} t,\ t \geq 0\} \tag{4}$$

The SDE with jumps (1) can be rewritten as

$$
\begin{aligned}
d\boldsymbol{X}(t) = &\Big[A_i(t)\big(\boldsymbol{X}(t) - \boldsymbol{X}_i(t)\big) + B_i u_i + \sum_{\ell=1}^{d} \lambda_\ell \hat{\xi}\ \Big] dt \\
&+ \beta \boldsymbol{X}(t) dW(t) \\
&+ \sum_{\ell=1}^{d} \Big[\big(\boldsymbol{X}(t) - \boldsymbol{X}(t-)\big) d\hat{N}^\ell(t)\Big]
\end{aligned} \tag{5}
$$

where $d\hat{N}^\ell(t) = dN^\ell(t) - \lambda_\ell\, dt$.

## 2.3. ITÔ FORMULA

The Itô formula is used in stochastic calculus to find the differential of a time-dependent function of a stochastic process. It is needed to calculate differentials of functions of the stochastic process $X(t)$ such as $E[X]$, $E[X^2]$, etc.

For a process $\psi(t) = \psi(t, \boldsymbol{X}(t))$ continuously differentiable in $t$ and twice continuously differentiable in $X$, the Itô formula with respect to the process $\boldsymbol{X}(t)$ in (5) is expressed as

$$
\begin{aligned}
&d\psi(t, \boldsymbol{X}(t)) = \\
&\left(\frac{\partial \psi}{\partial t} + \big[A_i(t)\big(\boldsymbol{X}(t) - \boldsymbol{X}_i(t)\big) + B_i u_i\big]\frac{\partial \psi}{\partial x}\right. \\
&\left. + \sum_{\ell=1}^{d} \lambda_\ell\, \psi(\hat{\xi}) + \frac{1}{2}\beta^2 \frac{\partial^2 \psi}{\partial x^2}\right) dt + \beta \frac{\partial \psi}{\partial x} dW(t) \\
&+ \sum_{\ell=1}^{d} \Big(\psi\big(t, X_t\big) - \psi\big(t, X_{t-}\big)\Big) d\hat{N}^\ell(t)
\end{aligned} \tag{6}
$$

where the mean jump size for the process $\psi(t)$ is

$$
\psi(\hat{\xi}) \triangleq E\Big[\psi\big(t, \boldsymbol{X}(t)\big) - \psi\big(t, \boldsymbol{X}(t-)\big)\Big] \tag{7}
$$

and the last term on the right-hand side of (6)

$$\sum_{\ell=1}^{d}\Big(\psi\big(t,X(t)\big)-\psi\big(t,X(t-)\big)\Big)d\hat{N}^{\ell}(t) \tag{8}$$

is a $d-$dimensional compensated compound Poisson process with the compensator

$$\sum_{\ell=1}^{d}\lambda_{\ell}\psi(\hat{\xi})dt=\sum_{\ell=1}^{d}\lambda_{\ell}E\Big(\psi\big(t,X(t)\big)-\psi\big(t,X(t-)\big)\Big)dt \tag{9}$$

Following [2, 4, 1], we consider $\psi(t)$ to be a polynomial function of the elements of the state vector, $\boldsymbol{X}$, and not explicitly dependent on time

$$\psi^{(m)}(t):=X_1^{m_1}X_2^{m_2}\ ...\ X_n^{m_n} \tag{10}$$

where $m=m_1+m_2+...+m_n$. The parameter $m$ is used as the moment order to describe the conditional moments of the stochastic system.

The Itô formula (6) can be rewritten to explicitly represent the direction of the jumps from one stochastic mode, $i$, to another, $j$

$$\begin{aligned}
&d\psi_i^{(m)}(t,\boldsymbol{X}(t))=\\
&\Bigg(\big[A_i(t)\big(\boldsymbol{X}(t)-\boldsymbol{X}_i(t)\big)+B_iu_i\big]\frac{\partial\psi_i^{(m)}}{\partial x}+\frac{1}{2}\beta^2\frac{\partial^2\psi_i^{(m)}}{\partial x^2}\\
&+\sum_{\substack{j=1\\j\neq i}}^{N}\lambda_{ji}\,E\big[\psi_j^{(m)}\big(t,\boldsymbol{X}(t)\big)\big]\\
&-\sum_{\substack{k=1\\k\neq i}}^{N}\lambda_{ik}E\big[\psi_i^{(m)}\big(t,\boldsymbol{X}(t)\big)\big]\Bigg)dt+\beta\frac{\partial\psi_i^{(m)}}{\partial x}dW(t)\\
&+\sum_{\substack{j=1\\j\neq i}}^{N}\Big(\psi_j^{(m)}\big(t,X(t)\big)-\psi_i^{(m)}\big(t,X(t)\big)\Big)d\hat{N}^{ij}(t)
\end{aligned} \tag{11}$$

## 2.4. DYNKIN'S FORMULA

In stochastic analysis, the Dynkin's formula is a theorem that gives the expectation of a function of a stochastic process. By using it on the Ito formula, it results in the first derivative of the conditional moment.

The application of Dynkin's formula consists in taking the expectation of (11)

$$
\begin{aligned}
& d\mu_i^{(m)}(t) = E\left[d\psi_i^{(m)}(t, \boldsymbol{X}(t))\right] = \\
& E\Bigg[\left[A_i(t)\left(\boldsymbol{X}(t) - \boldsymbol{X}_i(t)\right) + B_i u_i\right]\frac{\partial \psi_i^{(m)}}{\partial x} + \frac{1}{2}\beta^2\frac{\partial^2 \psi_i^{(m)}}{\partial x^2} \\
& + \sum_{\substack{j=1 \\ j\neq i}}^{N} \lambda_{ji}\, E\left[\psi_j^{(m)}\left(t, \boldsymbol{X}(t)\right)\right] - \sum_{\substack{k=1 \\ k\neq i}}^{N} \lambda_{ik} E\left[\psi_i^{(m)}\left(t, \boldsymbol{X}(t)\right)\right]\Bigg] dt \\
& + E\left[\beta\frac{\partial \psi_i^{(m)}}{\partial x} dW(t)\right] \\
& + E\left[\sum_{\substack{j=1 \\ j\neq i}}^{N}\left(\psi_j^{(m)}\left(t, X(t)\right) - \psi_i^{(m)}\left(t, X(t)\right)\right) d\hat{N}^{ij}(t)\right]
\end{aligned}
\tag{12}
$$

In (12), the expectation of the Wiener process $E[dW(t)] = 0$ and the expectation of a compensated Poisson process $E[d\hat{N}(t)] = 0$. Equation (12) reduces to the following system of ODEs representing the evolution of the conditional moments of the stochastic system

$$
\begin{aligned}
\dot{\mu}_i^{(m)}(t) = & \left[A_i(t)\left(\boldsymbol{X}(t) - \boldsymbol{X}_i(t)\right) + B_i u_i\right]\frac{\partial \psi_i^{(m)}}{\partial x} + \frac{1}{2}\beta^2\frac{\partial^2 \psi_i^{(m)}}{\partial x^2} \\
& + \sum_{\substack{j=1 \\ j\neq i}}^{N} \lambda_{ji}\, E\left[\psi_j^{(m)}\left(t, \boldsymbol{X}(t)\right)\right] - \sum_{\substack{k=1 \\ k\neq i}}^{N} \lambda_{ik} E\left[\psi_i^{(m)}\left(t, \boldsymbol{X}(t)\right)\right]
\end{aligned}
\tag{13}
$$

Note that the resulting equation (13) is equivalent to the system of ODEs derived in [1] from a non-compensated compound Poisson process.

## 2.5. MATRIX FORMULATION

Following a procedure described in length in [1], the system of ODEs (13) can be put into matrix form for each order $m$ of the conditional moments. The representation described below is limited to lower order moments [1] up to $m = 2$.

For $m = 0$, the matrix equation is equivalent to the occupational probabilities

$$\dot{\mu}^{(0)} = G^0 \mu^{(0)}(t) \tag{14}$$

For $m = 1$, the matrix equation corresponds to the means of the stochastic system

$$\dot{\mu}^{(1)} = G^1 \mu^{(1)}(t) + H^1 \mu^{(0)}(t) \tag{15}$$

For $m = 2$, the matrix equation corresponds to the uncentered second moments of the stochastic system

$$\dot{\mu}^{(2)} = G^2 \mu^{(2)}(t) + H^2 \mu^{(1)}(t) + J^2 \mu^{(0)}(t) \tag{16}$$

The definitions of matrices $G^1, H^1, G^2, H^2, J^2$ were presented in [1] and are not included here.

**2.5.1. Example 1.** Consider a switching system composed of two dynamic states switching between two stochastic modes $\{1, 2\}$. The example is inspired by the Markov reward model in [20], augmented with a scalar input. The state matrices corresponding to the two modes are

$$A_1 = \begin{bmatrix} -1 & -2 \\ 1 & -3 \end{bmatrix}, A_2 = \begin{bmatrix} 1 & 0 \\ 0 & -4 \end{bmatrix}. \tag{17}$$

The equilibrium state vectors are $X_1 = [10, -3]^T$ and $X_2 = [-10, 8]^T$. The transition rates between the two modes are $\lambda_{12} = 4s^{-1}$ and $\lambda_{21} = 6s^{-1}$. The input matrices are $B_1 = [7, -2]^T$ and $B_2 = [0, 0]^T$ and the scalar input $u = 2$.

Using the model in (13), the evolution of the conditional moments are obtained, for $m = 1$ and $m = 2$

$$G_1 = \begin{bmatrix} -5 & -2 & 0 & 0 \\ 1 & -7 & 0 & 0 \\ 0 & 0 & -5 & 0 \\ 0 & 0 & 0 & -10 \end{bmatrix} \tag{18}$$

$$H_1 = \begin{bmatrix} 18 & 60 \\ -23 & -18 \\ -40 & 10 \\ 32 & 32 \end{bmatrix} \tag{19}$$

$$G_2 = \begin{bmatrix} -5.99 & 0 & -4 & 0 & 0 & 0 \\ 0 & -9.99 & 2 & 0 & 0 & 0 \\ 1 & -2 & -7.99 & 0 & 0 & 0 \\ 0 & 0 & 0 & -3.99 & 0 & 0 \\ 0 & 0 & 0 & 0 & -13.99 & 0 \\ 0 & 0 & 0 & 0 & 0 & -8.99 \end{bmatrix} \tag{20}$$

$$H_2 = \begin{bmatrix} 36 & 0 & 0 & 0 \\ 0 & -46 & 0 & 0 \\ -23 & 18 & 0 & 0 \\ 0 & 0 & 20 & 0 \\ 0 & 0 & 0 & 64 \\ 0 & 0 & 32 & 10 \end{bmatrix} \tag{21}$$

$$J_2 = \begin{bmatrix} 0 & 600 \\ 0 & 54 \\ 0 & -180 \\ 400 & 0 \\ 256 & 0 \\ -320 & 0 \end{bmatrix} \tag{22}$$

Results for first and second moment dynamics are shown in figures (1) and (2). Solutions to (15) and (16) are compared to the average of 10,000 Monte Carlo simulations.

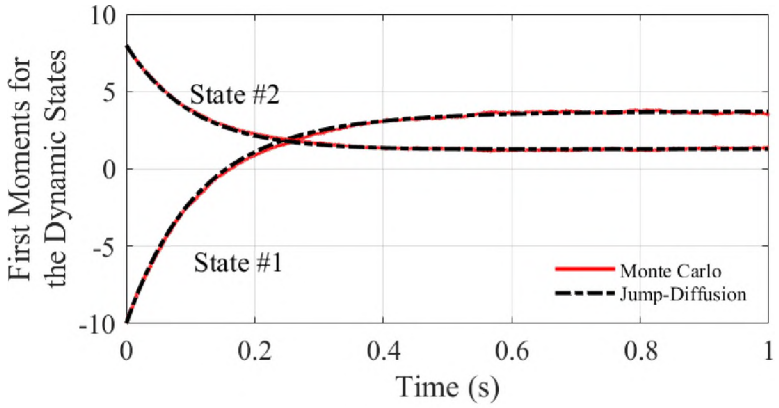


Figure 1. Conditional First Moments of the dynamic states

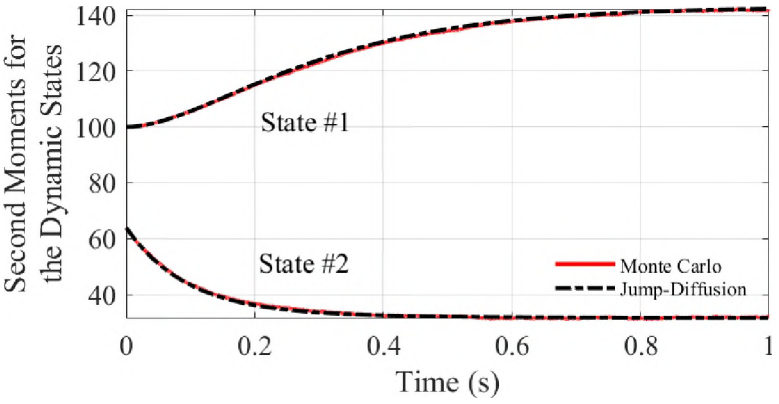


Figure 2. Conditional Second Moments of the dynamic states

# 3. THE BURKHOLDER-DAVIS-GUNDY INEQUALITY FOR MARTINGALES

To derive bounds on the moments of a stochastic system, one relies on powerful inequalities that apply to martingales. Many concepts of the stochastic theory were developed for applications in finance. For instance, the concept of martingale is extremely important in modeling asset price behaviors. It is briefly described here without all the theoretical framework more appropriate for stock prices and hedge ratios than for power system dynamics. The BDG inequality, and some other inequalities that are precursors to it, are presented here without proof, and the reader is encouraged to check the abundant literature on this topic such as [16, 17, 10].

## 3.1. THE MARTINGALE CONCEPT

Martingales are defined with respect to a filtered probability space. A probability space $(\Omega, \mathcal{A}, \mathcal{P})$ consists of a sample space $\Omega$, a $\sigma$-algebra or collection of events $\mathcal{A}$, and a probability measure $\mathcal{P}$ [10, 21]. On this probability space, a filtration is defined as a family of increasing $\sigma$-algebras

$$\mathbb{A} = \{\mathcal{A}_t : \ t \geq 0; \ \mathcal{A}_s \subseteq \mathcal{A}_t, \ 0 \leq s \leq t < \infty\} \tag{23}$$

and the extended space $(\Omega, \mathcal{A}, \mathcal{P}, \mathbb{A})$ is called a *filtered probability space*. $\mathcal{A}_t$ denotes the known information of the system at time $t \geq 0$, and a continuous time stochastic process $X = X(t), t \geq 0$ is said to be $\mathcal{A}_t$-adapted to the filtration $\mathbb{A}$ if $X(t)$ is $\mathcal{A}_t$-measurable $(X(t) \in \mathcal{A}_t)$ for each $t$.

Given a filtered probability space $(\Omega, \mathcal{A}, \mathcal{P}, \mathbb{A})$, an $\mathcal{A}_t$-adapted stochastic process $X = X(t), t \geq 0$ is called a martingale if it satisfies the equation

$$X(s) = E(X(t)|\mathcal{A}_s) \tag{24}$$

for all $s \in [0,t]$ provided $X(t)$ is absolutely integrable

$$E(|X(t)|) < \infty \tag{25}$$

for $t \geq 0$.

Two examples of martingales on a filtered probability space $(\Omega, \mathcal{A}, \mathcal{P}, \mathbb{A})$ are a Wiener process $W = \{W(t), t \geq 0\}$ , and a compensated Poisson process $\hat{N}(t) = N(t) - \lambda t$, where $N(t)$ is a standard Poisson process with intensity $\lambda$.

Another concept relevant to this study is that of *semimartingale*. A process $X = \{X(t), t \geq 0\}$ is called a semimartingale if $X(t)$ can be expressed as a sum of the form

$$X(t) = X(0) + A(t) + M(t) \tag{26}$$

for $t \geq 0$. In (26), $M(t)$ is a martingale, and $A(t)$ is a process of finite total variation. While in general, $A(t)$ could be any stochastic process, in this application it represents an ordinary Riemann-Stieltjes integral of the drift term of an Itô process.

## 3.2. MARTINGALE INEQUALITIES

The inequalities provided below are precursors to the BDG inequality and provide a basis for the derivation of bounds on the $p^{th}$ moments of a stochastic process $X(t)$. They are covered in depth in many stochastic theory books [22, 21, 19, 10].

The maximum martingale inequality is defined for a continuous martingale $X = \{X(t),\ t \geq 0\}$ with finite $p^{th}$ moment as

$$P\left( \sup_{s\in[0,t]} |X(s)| > a \right) \leq \frac{1}{a^p} E(|X(t)|^p) \tag{27}$$

where $a > 0$ and $p > 1$.

Doob's inequality provides the expectation of the maximum of the $p^{th}$ moment

$$E\left(\sup_{s\in[0,t]}|X(s)|^p\right) \leq \left(\frac{p}{p-1}\right)^p E(|X(t)|^p) \tag{28}$$

where $p > 1$. In particular, when $p = 2$, we obtain the expectation of the maximum of the square of the estimate

$$E\left(\sup_{s\in[0,t]}|X(s)|^2\right) \leq 4\, E(|X(t)|^2) \tag{29}$$

Jensen's inequality is defined for a random variable $X(t)$ with finite first moment, and a convex function $g : \mathbb{R} \to \mathbb{R}$

$$g\Big(E(X)\Big) \leq E\Big(g(X)\Big) \tag{30}$$

Lyapunov's inequality is defined as

$$\big(E(|X|^r)\big)^{1/r} \leq \big(E(|X|^s)\big)^{1/r} \tag{31}$$

where $0 < r < s < \infty$.

Finally, Hölder's inequality for $1 < p < \infty$,

$$\left(\sum_{i=1}^{n} a_i\right)^p \leq n^{p-1} \sum_{i=1}^{n} a_i^p \tag{32}$$

## 3.3. BURKHOLDER-DAVIS-GUNDY INEQUALITY

The Burkholder-Davis-Gundy (BDG) inequality relates the maximum of a semi-martingale to its quadratic variation.

For a semimartingale $X = \{X(t),\ t \geq 0\}$ with decomposition (26) and for any $p \geq 1$, the BDG inequality is expressed as

$$E\left[\sup_{s\in[0,t]} |X(s)|^p\right] \leq C_p E\left[\left[X(t), X(t)\right]^{p/2}\right] \tag{33}$$

where the coefficient $C_p$ depends on the value of $p$

$$C_p = \begin{cases} \sqrt{10p} & 1 \leq p < 2 \\ 2 & p = 2 \\ p\sqrt{\frac{e}{2}} & p > 2 \end{cases} \tag{34}$$

In (33), $[X(t), X(t)]$ (also written $[X(t)]$) denotes the scalar quadratic variation process of $X(t)$.

The quadratic variation process $[X] = \{[X]_t, t \geq 0\}$ of a process $X(t)$ is

$$[X]_t = \lim_{h\to 0} [X(t)]_{h,t} \tag{35}$$

Its numeric approximation is given by the sum

$$[X]_{h,t} = \sum_{k=1}^{n_t} (X_{t_k} - X_{t_{k-1}})^2 \tag{36}$$

where $h = t_k - t_{k-1}$ is the time step, and $n_t = \max\{k \in \mathbb{N} : t_k \leq t\}$.

Similarly, the total variation process $|X| = \{|X|_t, t \geq 0\}$ is described by its approximation

$$\sum_{k=1}^{n_t} |X_{t_k} - X_{t_{k-1}}| \tag{37}$$

# 4. STABILITY ANALYSIS OF OF THE JUMP-DIFFUSION MODEL

This section discusses the application of the mean-square stability criterion to the jump diffusion model (5) of a microgrid.

## 4.1. STABILITY CRITERION

The $p-$stability criterion for a stochastic process $X = \{X_t,\ t \geq 0\}$ states that for a bounded (in the $p$th mean) initial value, $|X_0|^p$, the integral solution to the SDE (5) remains bounded.

**4.1.1. Definition 1.** A stochastic process $X = \{X_t,\ t \geq 0\}$ is said to be $p-$stable if for $|X_0|^p < \delta$ there exists $\varepsilon > 0$ such that

$$E\left(|X(t)|^p\right) < \varepsilon \tag{38}$$

for $t > t_0$.

The limit case is called asymptotic $p-$stability and requires that a stochastic process be $p-$stable and that its $p^{th}$-moment vanishes in the long run.

**4.1.2. Definition 2.** A stochastic process $X(t)$ is said to be asymptotically $p-$stable if it is $p-$stable and for $|X_0|^p < \delta$

$$\lim_{t\to\infty} E\left(|X(t)|^p\right) = 0 \tag{39}$$

for $t > t_0$.

This study is concerned with the case of $p = 2$, called *mean-square stability*, which is one of the most popular stability concepts for stochastic processes.

## 4.2. P-STABILITY AND THE BDG INEQUALITY

The analysis of the $p-$stability (38) is equivalent to determining bounds on the solution to the SDE with jumps (5)

$$\begin{aligned}
\boldsymbol{X}(t) &= \boldsymbol{X}(0) \\
&+ \int_0^t \left( A_i(s)\big(\boldsymbol{X}(s) - \boldsymbol{X}_i(s)\big) + B_i u_i + \sum_{\ell=1}^{d} \lambda_\ell \, \hat{\xi} \right) ds \\
&+ \int_0^t \beta \boldsymbol{X}(s) dW(s) \\
&+ \int_0^t \sum_{\ell=1}^{d} \big(\boldsymbol{X}(\tau_k) - \boldsymbol{X}(\tau_k-)\big) d\hat{N}^\ell(s)
\end{aligned} \tag{40}$$

The last integral in (40) is merely a sum over jump times. Using the inequality (32), the expectation of the maximal process of $\boldsymbol{X}(t)$ applied on both sides of (40) yields

$$\begin{aligned}
E\left[ \sup_{s\in[0,T]} |\boldsymbol{X}(s)|^p \right] &\leq 4^{p-1} \Bigg\{ \Big|\boldsymbol{X}(0)\Big|^p \\
&+ E\left[ \sup_{s\in[0,T]} \left| \int_0^T \left( A_i(t)\big(\boldsymbol{X}(t) - \boldsymbol{X}_i(t)\big) + B_i u_i \right.\right.\right. \\
&\left.\left.\left. + \sum_{\ell=1}^{d} \lambda_\ell \, \hat{\xi} \right) dt \right|^p \right] + E\left[ \sup_{s\in[0,T]} \left| \int_0^T \beta \boldsymbol{X}(t) dW(t) \right|^p \right] \\
&+ E\left[ \sup_{s\in[0,T]} \left| \int_0^T \sum_{\ell=1}^{d} \Big( \boldsymbol{X}(t) - \boldsymbol{X}(t-) \Big) d\hat{N}^\ell(t) \right|^p \right] \Bigg\}
\end{aligned} \tag{41}$$

Each component of the second member of (41) is evaluated using the BDG inequality (33) and the quadratic variation of the semimartingale solution to the compensated Poisson stochastic integrale. The quadratic variation of a jump-diffusion stochastic integral is discussed next.

## 4.3. QUADRATIC VARIATION OF A JUMP-DIFFUSION MODEL

The components of a semimartingale $\boldsymbol{X} = \{\boldsymbol{X}(t),\ t \geq 0\}$ (26) can further be decomposed into a continuous and a discontinuous components

$$\boldsymbol{X}(t) = \boldsymbol{X}(0) + A(t) + M^{cont}(t) + M^{disc}(t) \tag{42}$$

. The correspondence with the solution process (40) to the jump-diffusion model (5) shows that the process $M^{cont}(t)$ is equivalent to the stochastic integral with respect to the Wiener process $W(t)$, and the discontinuous process $M^{disc}(t)$ is equivalent to the stochastic integral with respect to the Compensated Poisson process $\hat{N}(t)$. $A^{cont}(t)$ represents a process with finite total variation and corresponds to the Riemann-Stieltjes integral part of an Itô process.

Combining (40) and (42) yields

$$\begin{aligned}
A(t) &= \int_0^t \left( A_i(s)\big(\boldsymbol{X}(s) - \boldsymbol{X}_i(t)\big) + B_i u_i + \sum_{\ell=1}^{d} \lambda_\ell \hat{\xi} \right) ds \\
M^{cont}(t) &= \int_0^t \beta \boldsymbol{X}(s) dW(s) \\
M^{disc}(t) &= \int_0^t \sum_{\ell=1}^{d} \Big( \boldsymbol{X}(s) - \boldsymbol{X}(s-) \Big) d\hat{N}^\ell(s)
\end{aligned} \tag{43}$$

The quadratic variation of the initial value is $[X, X]_0 = |X_0|^2$ and the quadratic variation of a process with finite total variation $[A, A]_t = 0$. Therefore the quadratic variation of a semimartingale of the type (42) is due to contributions from the initial value and from the continuous, $M^{cont}(t)$, and discontinuous, $M_d(t)$, martingale processes.

$$[X, X]_t = |X_0|^2 + [M^{cont}, M^{cont}]_t + [M^{disc}, M^{disc}]_t \tag{44}$$

The continuous part is due to the diffusion term

$$[M^{cont}, M^{cont}]_t = \beta^2 \int_0^t \boldsymbol{X}^2(s)ds \tag{45}$$

The discontinuous part is due to the jump component

$$[M^{disc}, M^{disc}]_t = \int_0^t \sum_{\ell=1}^{d} \Big(\boldsymbol{X}(s) - \boldsymbol{X}(s-)\Big)^2 d\hat{N}^{\ell}(s) \tag{46}$$

With the assumption that these quadratic variation components are integrable, their expectation (with respect to a mode, $i$) can be expressed as

$$\begin{aligned} E\big([X,X]_t\big) =& |X_0|^2 + \beta^2 \int_0^t E\big(\boldsymbol{X}^2(s)\big)ds \\ &+ \int_0^t \sum_{\ell=1}^{d} E\Big(\boldsymbol{X}(s) - \boldsymbol{X}(s-)\Big)^2 \lambda_\ell \, ds \end{aligned} \tag{47}$$

It follows from (47) and the definition of the conditional moments in (13), (14), (15), (16)

$$\beta^2 \int_0^t E\big(\boldsymbol{X}^2(s)\big)ds \quad = \quad \beta^2 \int_0^t \mu^{(}2)(s)ds \tag{48}$$

and

$$\begin{aligned} &\int_0^t \sum_{\ell=1}^{d} E\Big(\boldsymbol{X}(s) - \boldsymbol{X}(s-)\Big)^2 \lambda_\ell \, ds \\ &= \int_0^t \sum_{\ell=1}^{d} E\Big(\boldsymbol{X}^2(s) - 2\boldsymbol{X}(s)\boldsymbol{X}(s-) + \boldsymbol{X}^2(s-)\Big)\lambda_\ell \, ds \\ &= \int_0^t \sum_{\ell=1}^{d} \Big[E\big(\boldsymbol{X}^2(s)\big) - 2E\big(\boldsymbol{X}(s)\big)E\big(\boldsymbol{X}(s-)\big) \\ &\qquad + E\big(\boldsymbol{X}^2(s-)\big)\Big]\lambda_\ell \, ds \\ &= \int_0^t \sum_{\ell=1}^{d} \lambda_\ell \Big(\mu_i^{(2)}(s) - 2\boldsymbol{X}(s-)\mu_i^{(1)}(s) + \boldsymbol{X}^2(s-)\mu_i^{(0)}\Big) \, ds \end{aligned} \tag{49}$$

To have dimension consistency between various terms of (48) and (49) requires a transformation matrix $T_x$, defined in [1, 3],

$$\begin{aligned} \boldsymbol{X}(s-) &\rightarrow T_x \left(\boldsymbol{X}(s-) \otimes I(n)\right) \\ \boldsymbol{X}^2(s-) &\rightarrow T_x \left(\boldsymbol{X}(s-) \otimes \boldsymbol{X}(s-)\right) \end{aligned} \tag{50}$$

where $\otimes$ denotes the Kronecker product, $n$ represents the system order (dimension of the process state vector $\boldsymbol{X}(s)$), and $I(n)$ is the identity matrix of the $n^{th}$ order.

The second conditional moment transformation matrices were derived in [3]. A brief description of these matrices is presented in Table 1.

Table 1. Second conditional moment transformation matrices

| Matrice | Denomination in [3] | Definition | Description |
|---|---|---|---|
| $T_x$ | $W_x$ | $R(W_c + I(N^2))$ | – |
| $T_y$ | $W_y$ | $RW_s$ | – |
| $T_z$ | – | $R(W_s + W_c + I(N^2))$ | – |
| – | $W_m$ | $(W_s + W_c + I(N^2))$ | describes the structure of the second conditional moments and represents how second order moments relate to each other |
| $T_{diag}$ | $W_s$ | – | describes an additional self dependence for moments of the form $\mathbb{E}[X_i(t)X_i(t)\|Q(t) = q$ |
| $T_{cross}$ | $W_c$ | – | describes dependence on an equivalent moment |
| – | $R$ | – | eliminates all redundant moments for $\mu_i^{(2)}(t)$ |

By using the law of total expectation, the quadratic variation $[\boldsymbol{X}, \boldsymbol{X}]_t$ corresponds to the sum of contributions from all stochastic modes. The general expression for an n-state, N-mode stochastic system is

$$\begin{aligned}[\boldsymbol{X}, \boldsymbol{X}]_t = |\boldsymbol{X}_0|^2 + \sum_{i=1}^{N} \beta^2 \int_0^t \mu_i^{(2)} ds \\ + \sum_{\substack{i,j=1 \\ i \neq j}}^{N} \int_0^t \lambda_{ij} \Big( \mu_i^{(2)} - 2T_x\big(\boldsymbol{X_j} \otimes I(n)\big)\mu_i^{(1)} \\ + T_x\big(\boldsymbol{X_j} \otimes \boldsymbol{X_j}\big)\mu_i^{(0)} \Big) ds \end{aligned} \tag{51}$$

**4.3.1. Example 2.** For the two-mode, two-state system from *Example* 1, and using the law of total expectation, the quadratic variation process of $\boldsymbol{X}(t)$ is

$$\begin{aligned}[\boldsymbol{X}, \boldsymbol{X}]_t = |\boldsymbol{X}_0|^2 + \beta^2 \int_0^t \mu_1^{(2)} ds + \beta^2 \int_0^t \mu_2^{(2)} ds \\ + \int_0^t \lambda_{12} \Big( \mu_1^{(2)} - 2T_x\big(\boldsymbol{X_2} \otimes I(2)\big)\mu_1^{(1)} \\ + T_x\big(\boldsymbol{X_2} \otimes \boldsymbol{X_2}\big)\mu_1^{(0)} \Big) ds \\ + \int_0^t \lambda_{21} \Big( \mu_2^{(2)} - 2T_x\big(\boldsymbol{X_1} \otimes I(2)\big)\mu_2^{(1)} \\ + T_x\big(\boldsymbol{X_1} \otimes \boldsymbol{X_1}\big)\mu_2^{(0)} \Big) ds \end{aligned} \tag{52}$$

where $\beta = 0.1$ and $T_x = \begin{bmatrix} 1 & 0 & 0 & 0 \\ 0 & 0 & 0 & 1 \\ 0 & 1 & 1 & 0 \end{bmatrix}$

On the other hand, the maximal process of $\boldsymbol{X}$ is

$$E\left[ \sup_{s \in [0,1]} |X(s)|^p \right] = \sup_{s \in [0,1]} |\mu^{(2)}(s)| \tag{53}$$

Figure 3 shows comparisons of Monte Carlo results for the quadratic variations of the dynamic states (red) to the jump-diffusion model results (black).

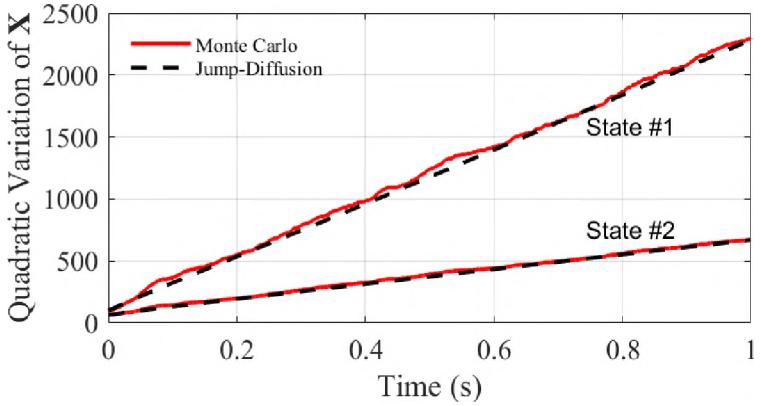


Figure 3. Quadratic variation of the dynamic states. Comparison averaged Monte Carlo vs. jump-diffusion model.

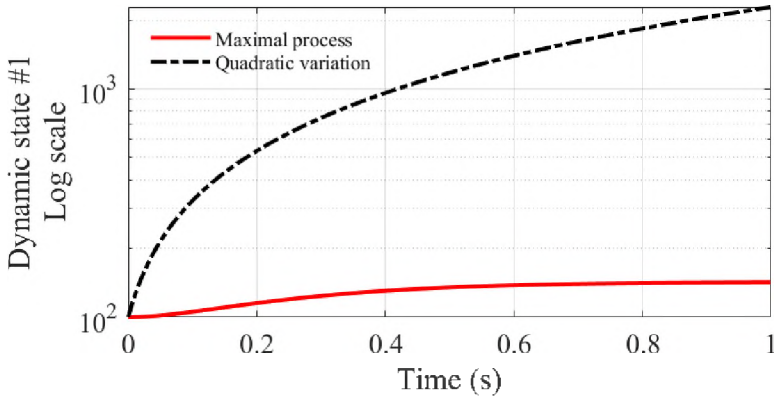


Figure 4. Log plot of the quadratic variation of the dynamic state $x_1$ (52) compared to the maximal process of $x_1$, (53)

The quadratic variation derived in (52) and illustrated in Figure 4 provides an upper bound to the maximal process of the second moment of $\boldsymbol{X}(t)$, solution to (16).

## 5. NUMERICAL APPLICATION

In this section, the case of the IEEE 37-bus microgrid is discussed. The mean square stability criterion is applied to the jump-diffusion model to derive bounds on the statistics of the system. Examples 1 and 2 above have shown that the mean square stability

can be accurately applied to a small microgrid's jump-diffusion model. Averaged Monte Carlo results were shown to converge to the jump-diffusion model results. Per the BDG inequality, the quadratic variation processes of the dynamic states provide upper limits to the maximal processes of the second moments, hence to the second moments themselves. Consequently, the conditions of the mean square stability criterion are met and the model is deemed stable in mean square for small microgrid systems.

The method is now applied to a larger microgrid system. The modified IEEE 37-bus microgrid was described in [4, 1, 23, 24]. With 56 dynamic states and 3 stochastic modes, the switching behavior is more complex. The jump-diffusion model is used to derive the conditional moments which have already been validated through convergence to Monte Carlo results [1]. The quadratic variations processes are then computed for selected dynamic states, associated with inverter #2.

Figures 5 and 6 shows the second conditional moments for the dynamic states (black) and their respective upper bounds (dashed red). The interpretation to make of Figures 5 and 6 is that for a microgrid where system dynamics are driven mostly by random jumps of large magnitude (greater than variations due to drift and diffusion processes), the variations in the dynamic states are bounded in square mean. In other words, the square of the jumps have an upper limit on average. These bounds provide an important information for the stochastic control of a microgrid, here represented by a jump-diffusion model.

## 6. CONCLUSION

This paper presented a method to analyze the stability of a microgrid operating in grid-tied and standalone modes. The system is modeled as a compensated jump-diffusion process to allow for the use of martingale inequalities. The mean square stability is utilized to derive bounds on the statistics of the system. The Burkholder-Davis-Gundy inequality

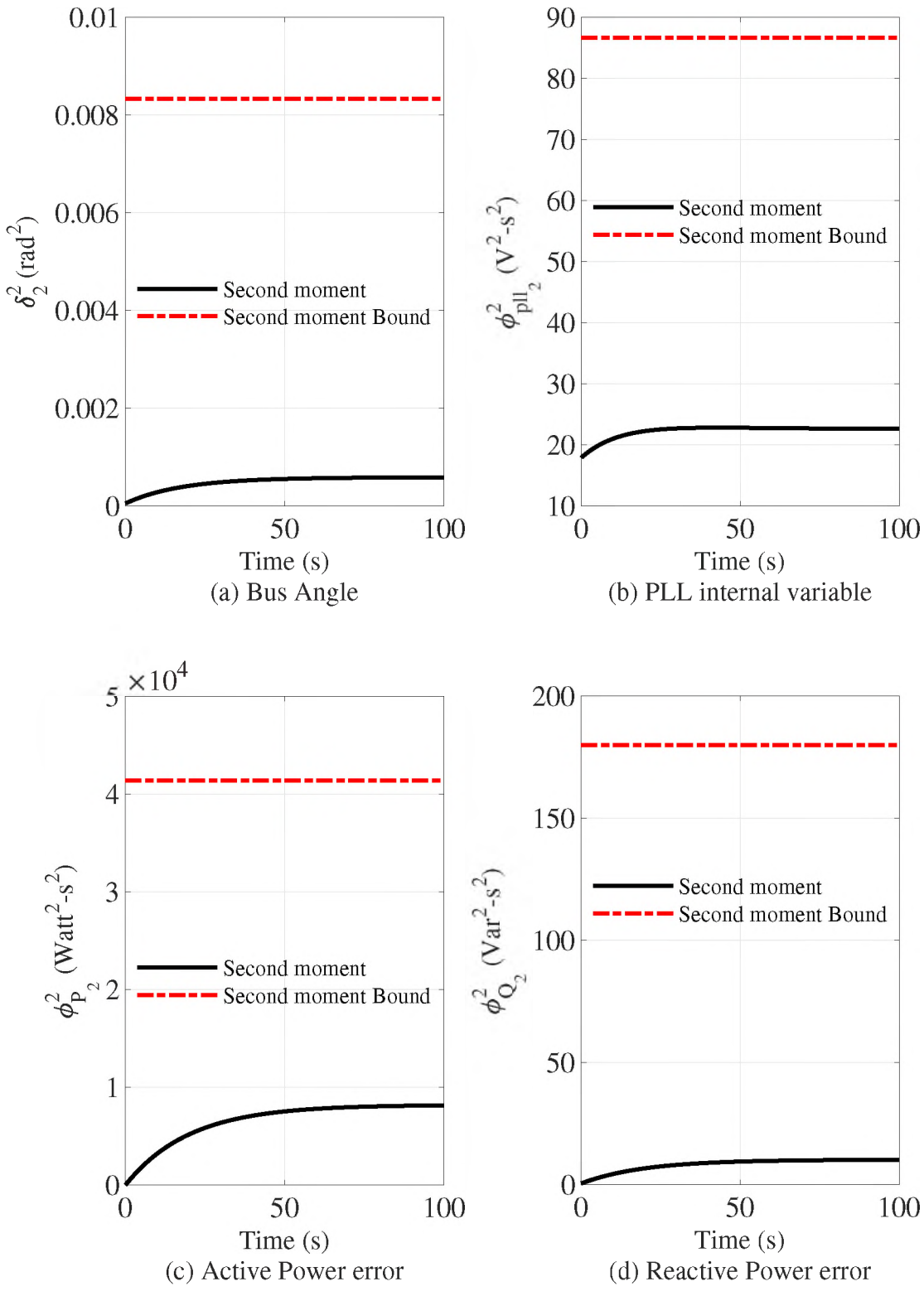


Figure 5. Second Moments of the dynamic states and moment bounds (first 4 states)

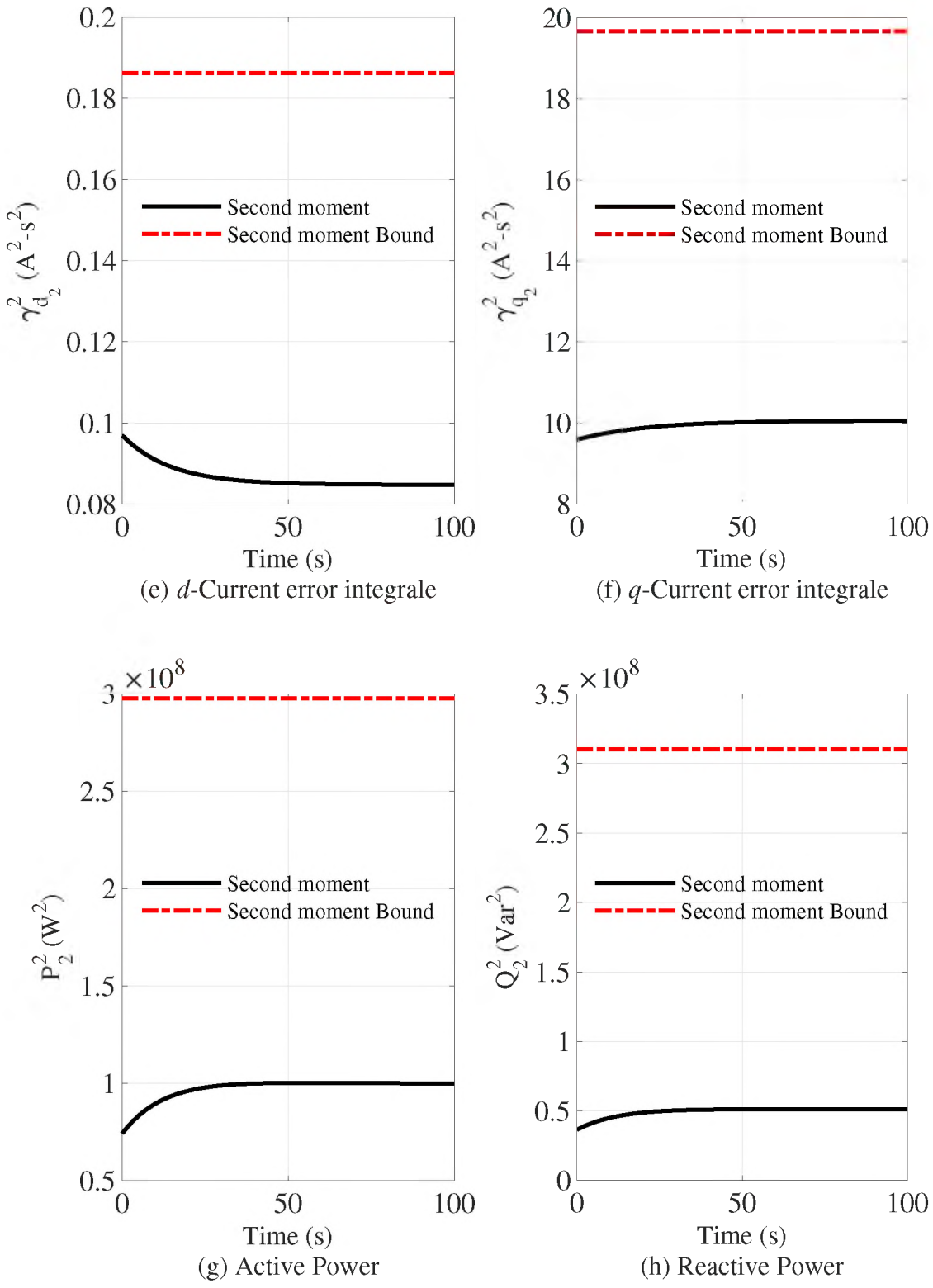


(e) *d*-Current error integrale (f) *q*-Current error integrale

(g) Active Power (h) Reactive Power

Figure 6. Second Moments of the dynamic states and moment bounds (last 4 states)

was used on the second moments of the dynamic an it was demonstrated that the moment solutions to the jump-diffusion process are bounded by their respective quadratic variation processes.

## REFERENCES


[1] G. Mpembele and J. Kimball, "Jump-diffusion modeling of a markov jump linear system with applications in microgrids," *TechRxiv*, Feb 2021.

[2] S. V. Dhople, Y. C. Chen, L. DeVille, and A. D. Dominguez-Garcia, "Analysis of power system dynamics subject to stochastic power injections," *IEEE Transactions on Circuits and Systems I: Regular Papers*, vol. 60, no. 12, pp. 3341–3353, 2013.

[3] J. A. Mueller and J. W. Kimball, "Modeling and analysis of dc microgrids as stochastic hybrid systems," *IEEE Transactions on Power Electronics*, pp. 1–1, 2021.

[4] G. Mpembele and J. Kimball, "Markov jump linear system analysis of a microgrid operating in islanded and grid tied modes," *TechRxiv*, 2020.

[5] A. R. Teel, A. Subbaraman, and A. Sferlazza, "Stability analysis for stochastic hybrid systems: A survey," *Automatica (Oxford)*, vol. 50, no. 10, pp. 2435–2456, 2014.

[6] S. Wu, D. Han, and X. Meng, "p-moment stability of stochastic differential equations with jumps," *Applied mathematics and computation*, vol. 152, no. 2, pp. 505–519, 2004.

[7] H. Wu and J. Sun, "p-moment stability of stochastic differential equations with impulsive jump and markovian switching," *Automatica (Oxford)*, vol. 42, no. 10, pp. 1753–1759, 2006.

[8] Z. Y. Dong, J. H. Zhao, and D. J. Hill, "Numerical simulation for stochastic transient stability assessment," *IEEE Transactions on Power Systems*, vol. 27, no. 4, pp. 1741–1749, 2012.

[9] K. Wang and M. L. Crow, "Numerical simulation of stochastic differential algebraic equations for power system transient stability with random loads," in *2011 IEEE Power and Energy Society General Meeting*, 2011, pp. 1–8.

[10] E. Platen and N. Bruti-Liberati, *Numerical solution of stochastic differential equations with jumps in finance*, ser. Stochastic modelling and applied probability. Springer-Verlag, 2010, vol. 64.

[11] W. S. Pierre and J. W. Kimball, "Minimum dwell times for the stability of switched systems with multiple stable operating points," in *2018 Annual American Control Conference (ACC)*, 2018, pp. 3798–3803.

[12] G. Chesi, P. Colaneri, J. C. Geromel, R. Middleton, and R. Shorten, "Computing upper-bounds of the minimum dwell time of linear switched systems via homogeneous polynomial lyapunov functions," in *Proceedings of the 2010 American Control Conference*, 2010, pp. 2487–2492.

[13] G. Liju and W. Yuqiang, "Exponential stability of impulsive jump linear systems with markov process," *Journal of Systems Engineering and Electronics*, vol. 18, no. 2, pp. 304–310, 2007.

[14] P. Bolzern, P. Colaneri, and G. De Nicolao, "Almost sure stability of markov jump linear systems with deterministic switching," *IEEE Transactions on Automatic Control*, vol. 58, no. 1, pp. 209–214, 2013.

[15] M. Rasheduzzaman, T. Paul, and J. W. Kimball, "Markov jump linear system analysis of microgrid stability," in *2014 American Control Conference*, 2014, pp. 5062–5066.

[16] J.-C. Breton and N. Privault, "Integrability and regularity of the flow of stochastic differential equations with jumps," 2019.

[17] K. Bichteler, *Stochastic Integration with Jumps*, ser. Encyclopedia of Mathematics and its Applications. Cambridge University Press, 2002.

[18] P. E. Protter, *Stochastic Integration and Differential Equations*. Springer-Verlag, 2013.

[19] N. Privault, *Stochastic finance: an introduction with market examples*. Chapman et Hall/CRC, 2014.

[20] S. Dhople, L. DeVille, and A. Dominguez-Garcia, "A stochastic hybrid systems framework for analysis of markov reward models," *Reliability Engineering & System Safety*, vol. 123, pp. 158–170, 2014.

[21] O. L. V. Costa, M. G. Todorov, M. D. Fragoso, and S. O. service), *Continuous-Time Markov Jump Linear Systems*. Berlin, Heidelberg: Springer Berlin Heidelberg, 2013.

[22] F. B. Hanson, *Applied Stochastic Processes and Control for Jump-Diffusions: Modeling, Analysis and Computation*, ser. Advances in Design and Control. Society for Industrial and Applied Mathematics, 2007.

[23] M. Rasheduzzaman, J. Mueller, and J. W. Kimball, "Reduced-order small-signal model of microgrid systems," *IEEE Transactions on Sustainable Energy*, vol. 6, no. 4, pp. 1292–1305, 2015.

[24] L. Luo and S. V. Dhople, "Spatiotemporal model reduction of inverter-based islanded microgrids," *IEEE Transactions on Energy Conversion*, vol. 29, no. 4, pp. 823–832, 2014.

# SECTION

# 2. CONCLUSION

The objective of this dissertation is to develop stochastic models for a microgrid operating in grid-tied and islanded modes. In the first paper, the model of a microgrid is developed in the SHS framework and corresponds to a MJLS for a system switching between different operating modes. The transitions between different operating modes is modeled as CTMC, according to an algorithm developed for the generation of different paths of the underlying Markov process. The method results in a set of ODEs representing the evolution of the conditional moments of the dynamic and algebraic states of the stochastic system. The analytical solutions to these ODEs are more easily computed when they are put into a matrix form and the method is illustrated for the first and second order moments. It is demonstrated that these solutions converge to the averaged Monte Carlo simulation. However, the Monte Carlo simulation shows impulses during the transitions from one stochastic mode to the other. An improvement of these transitions is described and modeled in the second paper.

A stochastic model of a microgrid is presented in the second paper, starting with a stochastic differential equation with jumps. The solution to the SDE corresponds to a jump-diffusion process that involves a drift term, a diffusion term, and a jump component. The drift term represents the traditional power system model in the state space. The diffusion term correspond to a Wiener process with linear coefficient. The jump component is described by a compound Poisson process with the jump sizes modeled appropriately to represent a more realistic switching behavior. The procedure includes the derivation of the conditional moments and their matrix representation, and the analytical solutions are shown to converge to the averaged Monte Carlo simulation with great accuracy.

The third paper discusses the stability of the jump-diffusion model of a microgrid developed in the second paper. The analysis is based on the mean-square stability criterion. First, the jump-diffusion model is converted into a compensated Poisson stochastic integral process. Then, martingales inequalities are applied to the solutions to the jump-diffusion model to derive bounds on the conditional moments of the stochastic system. In particular, the Burkholder-Davis-Gundy inequality relates the maximal process of a stochastic process to its quadratic variation. It is used here to evaluate the mean-square stability criterion on the second order moments of the jump-diffusion model. The methods results in realistic bounds that can be used in a microgrid control system.

The numerical application of all the models described above are based on the modified IEEE 37-bus microgrid. The original system has 225 dynamic states and, in previous studies, was reduced to a $56^{th}$ order system using the singular perturbation technique. The system is considering between two distinct standalone and one grid-tied operating modes. In all cases, the stochastic model is validated through comparison with the averaged Monte Carlo simulation. An important advantage of the stochastic method is that it is far less computational expensive than the Monte Carlo method.

# REFERENCES


[1] Klaus Bichteler. *Stochastic Integration with Jumps*. Encyclopedia of Mathematics and its Applications. Cambridge University Press, 2002.

[2] P. Bolzern, P. Colaneri, and G. De Nicolao. Almost sure stability of markov jump linear systems with deterministic switching. *IEEE Transactions on Automatic Control*, 58(1):209–214, 2013.

[3] Jean-Christophe Breton and Nicolas Privault. Integrability and regularity of the flow of stochastic differential equations with jumps, 2019.

[4] G. Chesi, P. Colaneri, J. C. Geromel, R. Middleton, and R. Shorten. Computing upper-bounds of the minimum dwell time of linear switched systems via homogeneous polynomial lyapunov functions. In *Proceedings of the 2010 American Control Conference*, pages 2487–2492, 2010.

[5] Oswaldo L. V. Costa, Marcos G. Todorov, Marcelo D. Fragoso, and SpringerLink (Online service). *Continuous-Time Markov Jump Linear Systems*. Springer Berlin Heidelberg, Berlin, Heidelberg, 2013. ISBN 9783642341014.

[6] Sairaj V. Dhople, Yu Christine Chen, Lee DeVille, and Alejandro D. Dominguez-Garcia. Analysis of power system dynamics subject to stochastic power injections. *IEEE Transactions on Circuits and Systems I: Regular Papers*, 60(12):3341–3353, 2013. doi: 10.1109/tcsi.2013.2265972.

[7] S.V. Dhople, L. DeVille, and A.D. Dominguez-Garcia. A stochastic hybrid systems framework for analysis of markov reward models. *Reliability Engineering & System Safety*, 123:158–170, 2014. doi: 10.1016/j.ress.2013.10.011.

[8] Z. Y. Dong, J. H. Zhao, and D. J. Hill. Numerical simulation for stochastic transient stability assessment. *IEEE Transactions on Power Systems*, 27(4):1741–1749, 2012.

[9] Daniel T. Gillespie. Exact stochastic simulation of coupled chemical reactions. *The Journal of Physical Chemistry*, 81:2340–2361, 1977. doi: 10.1021/j100540a008.

[10] T. C. Green and M. Prodanović. Control of inverter-based micro-grids. *Electric Power Systems Research*, 77(9):1204–1213, 2007.

[11] Mircea Grigoriu. *Stochastic systems: uncertainty quantification and propagation*. Springer, 2014.

[12] Floyd B Hanson. *Applied Stochastic Processes and Control for Jump-Diffusions: Modeling, Analysis and Computation*. Advances in Design and Control. Society for Industrial and Applied Mathematics, 2007. ISBN 978-0898716337. doi: 10.1137/1.9780898718638.

[13] Joao P. Hespanha. A model for stochastic hybrid systems with application to communication networks. *Nonlinear Analysis: Theory, Methods & Applications*, 62(8): 1353–1383, 2005. doi: 10.1016/j.na.2005.01.112.

[14] J.P. Hespanha. Modelling and analysis of stochastic hybrid systems. *IEE Proceedings - Control Theory and Applications*, 153(5):520–535, 2006. doi: 10.1049/ip-cta:20050088.

[15] P. Hespanha. Modeling and analysis of networked control systems using stochastic hybrid systems. *Annual Reviews in Control*, 38(2):155–170, 2014. doi: 10.1016/j.arcontrol.2014.09.001.

[16] Adam Hirsch, Yael Parag, and Josep Guerrero. Microgrids: A review of technologies, key drivers, and outstanding issues. *Renewable & sustainable energy reviews*, 90: 402–411, 2018.

[17] Nobuyuki Ikeda and Shinzo Watanabe. *Stochastic differential equations and diffusion processes*. North-Holland, 2011.

[18] G. Liju and W. Yuqiang. Exponential stability of impulsive jump linear systems with markov process. *Journal of Systems Engineering and Electronics*, 18(2):304–310, 2007.

[19] Ling Luo and Sairaj V. Dhople. Spatiotemporal model reduction of inverter-based islanded microgrids. *IEEE Transactions on Energy Conversion*, 29(4):823–832, 2014. doi: 10.1109/tec.2014.2348716.

[20] Valerio Mariani, Francesco Vasca, Juan C. Vasquez, and Josep M. Guerrero. Model order reductions for stability analysis of islanded microgrids with droop control. *IEEE Transactions on Industrial Electronics*, 62(7):4344–4354, 2015. doi: 10.1109/tie.2014.2381151.

[21] G. Mpembele and J. Kimball. Analysis of a standalone microgrid stability using generic markov jump linear systems. In *2017 IEEE Power and Energy Conference at Illinois (PECI)*, pages 1–8, Feb 2017. doi: 10.1109/PECI.2017.7935737.

[22] G. Mpembele and J. W. Kimball. A matrix representation of a markov jump linear system applied to a standalone microgrid. In *2018 9th IEEE International Symposium on Power Electronics for Distributed Generation Systems (PEDG)*, pages 1–8, June 2018. doi: 10.1109/PEDG.2018.8447779.

[23] Gilles Mpembele and Jonathan Kimball. Markov jump linear system analysis of a microgrid operating in islanded and grid tied modes. *TechRxiv*, 2020. doi: 10.36227/techrxiv.13370312.v1.

[24] Gilles Mpembele and Jonathan Kimball. Jump-diffusion modeling of a markov jump linear system with applications in microgrids. *TechRxiv*, Feb 2021. doi: 10.36227/techrxiv.13670818.v1.

[25] J. A. Mueller and J. W. Kimball. Modeling and analysis of dc microgrids as stochastic hybrid systems. *IEEE Transactions on Power Electronics*, pages 1–1, 2021. doi: 10.1109/TPEL.2021.3055456.

[26] Jacob A. Mueller, Md. Rasheduzzaman, and Jonathan W. Kimball. A model modification process for grid-connected inverters used in islanded microgrids. *IEEE Transactions on Energy Conversion*, 31(1):240–250, 2016. doi: 10.1109/tec.2015.2476600.

[27] W. S. Pierre and J. W. Kimball. Minimum dwell times for the stability of switched systems with multiple stable operating points. In *2018 Annual American Control Conference (ACC)*, pages 3798–3803, 2018.

[28] Eckhard Platen and Nicola Bruti-Liberati. *Numerical solution of stochastic differential equations with jumps in finance*, volume 64 of *Stochastic modelling and applied probability*. Springer-Verlag, 2010. ISBN 978-3-642-12057-2. doi: 10.1007/978-3-642-13694-8.

[29] Nicolas Privault. *Stochastic finance: an introduction with market examples*. Chapman et Hall/CRC, 2014.

[30] Philip E Protter. *Stochastic Integration and Differential Equations*. Springer-Verlag, 2013.

[31] M. Rasheduzzaman, T. Paul, and J. W. Kimball. Markov jump linear system analysis of microgrid stability. In *2014 American Control Conference*, pages 5062–5066, 2014.

[32] Md Rasheduzzaman, Jacob A. Mueller, and Jonathan W. Kimball. An accurate small-signal model of inverter- dominated islanded microgrids using *dq* reference frame. *IEEE Journal of Emerging and Selected Topics in Power Electronics*, 2(4):1070–1080, 2014. doi: 10.1109/jestpe.2014.2338131.

[33] Md. Rasheduzzaman, Jacob Mueller, and Jonathan W. Kimball. Reduced-order small-signal model of microgrid systems. *IEEE Transactions on Sustainable Energy*, 6(4): 1292–1305, 2015. doi: 10.1109/tste.2015.2433177.

[34] Atle Seierstad. *Stochastic control in discrete and continuous time*. Springer, 2009. ISBN 978-0-387-76616-4. doi: 10.1007/978-0-387-76617-1.

[35] Andrew R. Teel, Anantharaman Subbaraman, and Antonino Sferlazza. Stability analysis for stochastic hybrid systems: A survey. *Automatica (Oxford)*, 50(10):2435–2456, 2014.

[36] A.R. Teel, L. Moreau, and D. Nesic. A unified framework for input-to-state stability in systems with two time scales. *IEEE Transactions on Automatic Control*, 48(9): 1526–1544, 2003. doi: 10.1109/tac.2003.816966.

[37] K. Wang and M. L. Crow. Numerical simulation of stochastic differential algebraic equations for power system transient stability with random loads. In *2011 IEEE Power and Energy Society General Meeting*, pages 1–8, 2011.

[38] Huijun Wu and Jitao Sun. p-moment stability of stochastic differential equations with impulsive jump and markovian switching. *Automatica (Oxford)*, 42(10):1753–1759, 2006.

[39] Shujin Wu, Dong Han, and Xianzhang Meng. p-moment stability of stochastic differential equations with jumps. *Applied mathematics and computation*, 152(2):505–519, 2004.

[40] Yan Xu, Fushuan Wen, Hongwei Zhao, Minghui Chen, Zeng Yang, and Huiyu Shang. Stochastic small signal stability of a power system with uncertainties. *Energies*, 11 (11):2980, 2018. doi: 10.3390/en11112980.

# VITA

Gilles Mpembele was born in the Democratic Republic of Congo, where he received the BS in Electrical Engineering in 1998 from the University of Kinshasa. In 2001, he migrated to the United States and completed the MS in Electrical Engineering from the University of Bridgeport, CT in 2007. He received the PhD degree in Electrical Engineering from Missouri S&T in May 2021. He was employed with the Boeing Company in St Louis, MO, as an Electrical and Electronics Design and Analysis Engineer.

His research interests included renewable energy systems and microgrid deployment worldwide.